Alma Mater Studiorum - Università di Bologna

DOTTORATO DI RICERCA IN SCIENZE BIOCHIMICHE E BIOTECHNOLOGICHE
Ciclo XXVII

Settore Concorsuale di afferenza: 07/E1
Settore Scientifico disciplinare: AGR/07

FINE MAPPING OF *qroot-yield-1.06*, A QTL FOR ROOT, PLANT VIGOR AND YIELD IN MAIZE

Presentata da: Dott.ssa Ana Karine Martinez Ascanio

Coordinatore
Prof. Santi Mario Spampinato

Relatore
Prof. Roberto Tuberosa

Correlatore
Prof. Silvio Salvi

Esame finale anno 2015

"A mis dos hombres, mi adorado esposo Juan Fernando, por su apoyo constante, y a mi chiquitín Juan Martin, por su paciencia y comprensión. Gracias porque juntos logramos afrontar un reto más en nuestras vidas… los amo"

Index

Table Index

Figure Index

Summary

Root-yield-1.06 is a major QTL affecting root architecture and other agronomic traits in maize. *Root-yield-1.06* was previously mapped on bin 1.06 in an experimental population derived from the cross between inbred lines Lo964 and Lo1016 and subsequently validated by the development and testing of near isogenic lines (NILs) differing for the parental chromosome segment at the QTL position. The objective of this study was to fine map *qroot-yield-1.06* by marker-assisted searching for chromosome recombinants in the QTL interval and concurrent root phenotyping in both controlled and field conditions, through successive generations. Additionally, complementary approaches such as QTL meta-analysis and RNA-seq were deployed in order to help prioritizing candidate genes within the QTL target region.

In a first experiment, we aimed to introduce and adapt a root phenotyping protocol enabling highly efficient collection of root architecture data suitable for mapping and cloning purposes. A selected group of maize genotypes grown in the field was utilized as plant materials. We tested and compared a non-invasive method (root electrical capacitance) and an invasive one (shovelomics) for field-based root analysis. Results showed that root electrical capacitance was not a good predictor of total root mass. On the contrary, shovelomics enabled to accurately collect root system architecture information of adult maize plants. Additionally, shovelomics combined with software-assisted root imaging analysis (we tested three different software), proved to be a reliable, informative and relatively highly automated phenotyping protocol.

In a second experiment, QTL interval mapping analysis was conducted using a segregating population at the seedling stage and grown in controlled environment. This experiment enabled to narrow down the QTL supporting interval and to identify and map new markers, which were subsequently utilized in fine mapping using recombinant lines.

In a third experiment, a new large collection of homozygous recombinant nearly isogenic lines (NILs) was developed by screening segregating populations with markers flanking *qroot-yield-1.06*. A first set of lines from this collection was phenotyped based on the adapted shovelomics protocol. QTL analysis based on these data highlighted an interval of 1.3 Mb as completely linked with the target QTL. Based on these results, a larger safer interval of 4.1 Mb was selected for further investigations.

We carried out a QTL meta analysis for root traits in maize by collecting root QTL information from literature, and including *qroot-yield-1.06.* Two metaQTLs (mQTLs) in the *qroot-yield-1.06* interval were identified, flanking the QTL position as obtained based on the analysis of the first set homozygous recombinant NILs.

Trascriptomics analysis based on RNA-seq data of the two contrasting QTL-NILs confirmed alternative haplotypes at chromosome bin 1.06. A 67% of the total number of differentially expressed genes on chromosome 1 mapped to our target QTL interval.

The mapping resolution obtained so far is still too broad for the molecular dissection of *qroot-yield-1.06* into its component(s) and even to shortlist a small number of candidate genes. However, because *qroot-yield-1.06* has now been delimited to a 4.1-Mb interval, and thanks to the availability of additional untested homozygous recombinant NILs, the potentially achievable mapping resolution at *qroot-yield-1.06* is c. 50 kb (approx. the same scale dimension of mean gene density in maize). High genetic and physical resolution combined with reliable phenotypic data on this additional set of NILs, and information of gene expression, should therefore enable us to confidently identify a small selection of candidate genes responsible for the *qroot-yield-1.06*.

1 General Introduction

Nowadays the main limitation in crop productivity is water and nutrient availability. As a consequence, in low-input agricultural systems in most of the developing world, substantial reductions in crop yields are reported, especially if compared with full yield potential (FAO, 2010). On the contrary, in developed world, greater crop yield is usually achieved with an intensive use of fertilizers and irrigation, at the cost of serious environmental problems (Cordell *et al.*, 2009). In both systems, the challenge for crop breeding is to improve crop resource-use efficiency (Lynch and Brown, 2012). As argued by Lynch (2007), improving resource acquisition likely represents the greatest opportunity. Although many traits could be targeted in breeding programs to improve plant's capacity for uptake and fixation of nutrients, root system should be a central component in this effort (Den Herder *et al.*, 2010, Lynch *et al.*, 2007).

Root system is crucially involved in several plant functions such as uptake of water and nutrients, plant anchorage to the soil and interaction with symbiotic organisms (Herder *et al.*, 2010). Several root traits could be potentially selected to improve soil resource acquisition including enhanced symbiosis with microorganisms, rhizosphere modification and root architectural traits (Lynch and Brown, 2012). Root system architecture (RSA), namely the spatial configuration of the root system as a whole is particularly important because it affects the ability of the plant to explore the soil for resource acquisition (Lynch, 1995 and 2007). RSA is plastic and dynamic and many efforts have been conducted to identify root traits (phenes; Pieruschka and Poorter, 2012), or combination of traits (i.e. ideotype Donald, 1968), to optimize crop nutrient acquisition in target environments that will frequent determine yield (White *et al.*, 2013). For instance, Brown *et al.*, (2013) suggested modified root ideotypes for improving P acquisition in barley; Rose *et al.*, (2013) suggested root ideotypes for improving the acquisition of P and Zn in rice and Lynch (2013) described a steep, cheap and deep root ideotype for optimizing water and N acquisition in maize.

As for other species, maize root system provides anchorage and secures the adequate uptake of water and nutrients. Maize root system consists of roots formed during embryogenesis (primary root and the variable number of seminal roots), and roots that are formed in the postembryonic development (shoot borne roots. Feldman,1994). Both embryonic and shoot borne roots usually develop multiple branched lateral roots that are extremely important as they are responsible for the major part of water and nutrient acquisition (Lynch *et al.*, 1995). During the first weeks after germination, the seedling rootstock is basically constituted by the embryonic roots, while later in the development (e.g. starting from approx. 2 weeks), post-embryonic shoot-borne roots start to

form and gradually become the dominant structure of the maize root system. On average, shoot-borne roots are distributed in six whorls of underground crown roots and two to three whorls of aboveground brace roots (Figure 1. From Hochholdinger 2004).

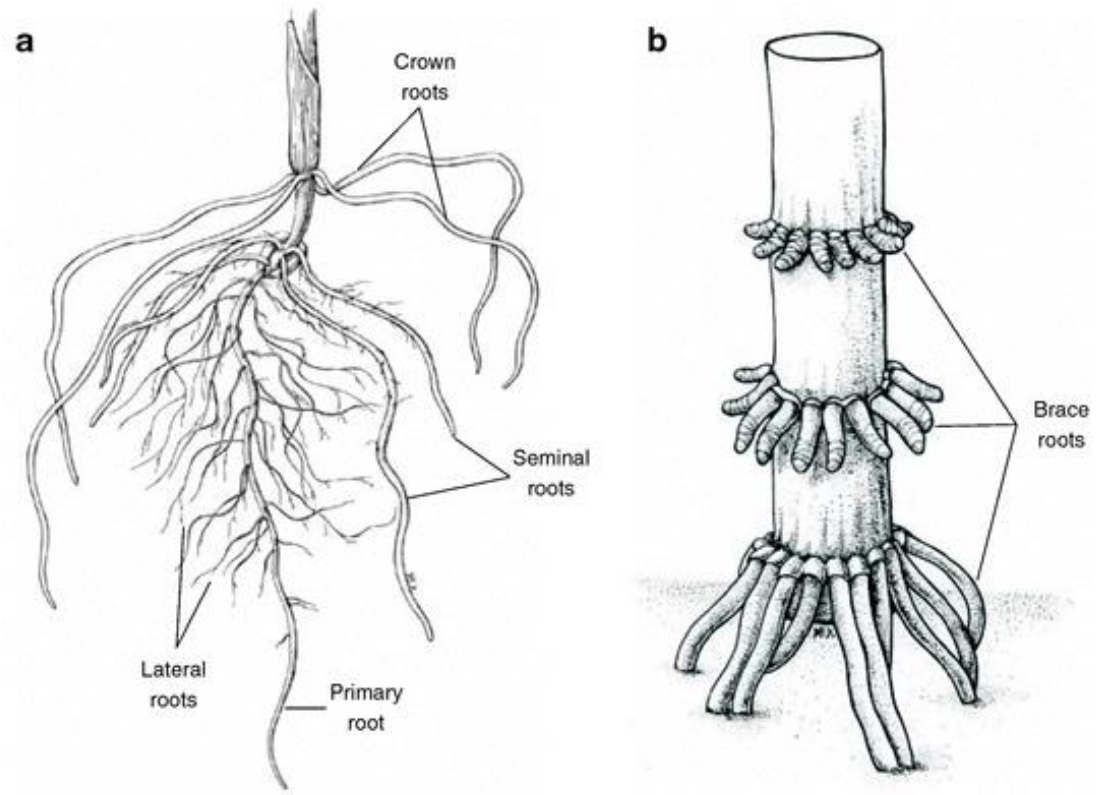

Figure 1. Maize root system. a. Embryonic primary and seminal roots and postembryonic lateral and crown roots. b. Aboveground shoot borne brace roots (From Hochholdinger, 2009).

Despite the recognized importance of maize root system, a thorough genetic analysis has only been initiated in the last decade (Hochholdinger and Feix 2013). The progress in root genetic analysis has been hampered by the inherent reduced accessibility of the root system, by the considerable size and complexity of an adult plant root system and by the extremely high root plasticity, caused by the strong sensitivity to changes in environmental conditions (Hochholdinger *et al.,* 2004). In the attempt to identify genes involved in root formation and development in maize, several mutants have been characterized altering the specific development of shoot-borne roots, lateral roots and root hairs (Jenkins 1930, Wen and Schnable 1994, Hetz *et al.,* 1996, Woll *et al.,* 2005). However, only very few mutants have already been cloned: Rtcs (Taramino *et al.,* 2007), Rth1 (Wen *et al.,* 2005), Rth3 (Hochholdinger *et al.,* 2008) and rum1 (von Behrens *et al.,* 2011). The cloning of these genes provided valuable information to understand genetic networks involved in the formation of

the complex maize root system. However, large differences in RSA are present among maize germplasm, which is mostly under polygenic control as witnessed by several quantitative trait loci (QTL) mapping investigations (Tuberosa *et al.*, 2003; Hund *et al.*, 2011).

Identification of QTLs for root traits in maize has been limited and studies have been mainly conducted at early growth stage (Tuberosa *et al.*, 2002, Hund *et al.*, 2004; Zhu *et al.*, 2006; Trachsel *et al.*, 2009; Ruta *et al.*, 2010a,b; Zhu *et al.*, 2005, Burton *et al.*, 2014, Burton *et al.*, 2015). Few QTL studies addressed the genetic control of root trait variation in adult maize plants likely because of the practical difficulties to evaluate larger plants in a considerable number (Lebreton *et al.*, 1995, Guingo *et al.*, 1998, Mano *et al.*, 2005, Liu et al 2008, Cai et al 2012, Ku et al 2012). One interesting QTL for root architecture is *root-ABA-1*, which was mapped on bin 2.04 (Guiliani *et al.*, 2005). First described by Lebreton *et al.*, (1995) affecting roots traits and ABA concentration in the background Polj17xF-2, the same region was shown to affect root architecture, root lodging, leaf ABA concentration and grain yield in the cross Os420xIABO078 (Tuberosa *et al.*, 1998, Landi *et al.*, 2001). Another important QTL is *root-yield-1.06* which was mapped on bin 1.06 in the background of Lo964xLo1016. First described by Tuberosa *et al.*, (2002), this QTL affects root traits of plants growing in hydroponics, however its effect was also confirmed in adults plants grown in the field (Landi *et al.*, 2002). The effects of these QTLs on bins 2.04 and 1.06 on root traits and grain yield have been evaluated more accurately with the development of near isogenic lines (NILs) differing for the parental chromosome segment at these QTLs (Landi *et al.*, 2005, Landi *et al.*, 2010).

Development and characterization of NILs is one of the most common approaches for QTL validation and fine mapping towards the identification of a causal gene. By homogenizing the genetic background, a better estimation of the QTL effect on the phenotype can be obtained, thanks to the absence of other segregating QTLs (Salvi and Tuberosa, 2005). The use of NILs for root QTL alleles has been reported in breeding approaches (Steele et al 2013), in detailed physiological studies (Henry *et al.*, 2015, Mu *et al.*, 2015), and in studies evaluating the effect of the QTL in target environments (Landi *et al.*, 2005, Borrel *et al.*, 2014, Suji et al, 2012). NILs have been successfully helped in positional cloning major root QTLs in rice as PHOSPHORUS UPTAKE 1 (PUP1) and DEEPER ROOTING 1 (DRO1) (Uga *et al.*, 2013).

Positional cloning based on increasingly accurate fine mapping, and association mapping (also known as genome wide association, GWA) (Hall *et al.*, 2010) have been reported as the main strategies for QTL cloning (Salvi and Tuberosa 2007, Salvi and Tuberosa 2015). Fine mapping can

accurately identify candidate genes for the QTL but can be time and resource- consuming while GWA may suffer of several weaknesses such as unpredictable linkage disequilibrium, population structure and others. Complementary approaches, which could help in QTL cloning are QTL meta-analysis and expression analysis of genes within the candidate region (Norton *et al.,* 2008). Meta-analysis, a method proposed by Goffinet and Gerber (2000) and improved by Veyrieras *et al.,* (2007), allows combining QTL results from independent studies into a single result. This can be obtained using software packages such as BioMercator (Arcade *et al.,* 2004, Sosnowski *et al.,* 2012), which enables large set of previously generated QTL data to be grouped in meta QTLs (mQTLs). As result, in most cases, confidence intervals (CI) of the resulting mQTLs are shorter than CI of corresponding QTLs (Arcade *et al.,* 2004). This reduction of the CI could help to prioritize candidate genes to be included in further studies (Veyrieras *et al.,* 2007). An additional reduction of the number of candidate genes can then be achieved carrying out transcriptional profiling between contrasting QTL genotypes, which provide a list of genes differentially expressed. Currently, RNA sequencing (RNA-seq) technology is becoming the standard method that allows the entire transcriptome to be inspected in a high-throughput and quantitative manner (Wang *et al.,* 2009).

Even with the recent advances in genomic technologies and the availability of the maize genome sequence (Schnable *et al.,* 2009), none of the hundreds of maize root QTLs so far reported has been cloned. Phenotyping for root traits in large populations remains a bottleneck in root genetic analysis including investigations aimed at QTL cloning (Zhu *et al.,* 2011). High throughput root phenotyping is particularly challenging because of the complexity of the root system and the multiple interaction with environmental variables (Lynch and Brown 2012). A possible shortcut is moving root phenotyping to controlled environment conditions. Many protocols have been developed combining plant growth systems in controlled conditions, root imaging and software-based image-analysis tools (Iyer-Pascuzzi *et al.,* 2010, Grift *et al.,* 2011, Nagel *et al.,* 2012, Lobet and Draye, 2013). The main concern with these artificial systems is usually weak or at the best-unknown correlation with field conditions (Lynch and Brown 2012). Ideally, the solution of this conundrum is the development of efficient and reliable high-throughput phenotyping protocols in the field. The use of non-invasive techniques is continuously advancing (Fioriani and Schurr 2013), however, root system architecture has commonly been evaluated in the field in a destructive manner. For instance, 'shovelomics', is a method that utilizes a visual estimation of excavated root clumps to assess different root architecture parameters (Trachsel *et al.,* 2011). Recently, the development of software for root images analysis from field grown adult maize plants obtained by

shovelomics allowed to scale up in terms of throughput and reliability (Bucksch *et al.*, 2014, Colombi *et al.*, 2015).

In the present study, we report the progress about fine mapping of *root-yield-1.06*, a major QTL for root, plant vigor and yield in maize. The main goal was to carry out a standard fine mapping of the target QTL and contemporarily provide an adequate description of root phenotype. In addition, we used QTL meta-analysis and transcriptomics to gain information on the presence of possible candidate genes at the target region. Specific objectives of this research were:

i) To implement a protocol for rapid and reliable root phenotyping applicable to maize adult plants in the field.
ii) To narrow down the *qroot-yield-1.06* interval.
iii) To carry out QTL meta-analysis to synthetize information on root QTLs
iv) To carry out a comparative transcriptomics analysis of *qroot-yield-1.06* NILs

1.1 References

Arcade, A., Labourdette, A., Falque, M., Mangin, B., Chardon, F., Charcosset, A., & Joets, J. (2004). BioMercator: integrating genetic maps and QTL towards discovery of candidate genes. *Bioinformatics*, *20*(14), 2324-2326.

Borrell, A. K., Mullet, J. E., George-Jaeggli, B., van Oosterom, E. J., Hammer, G. L., Klein, P. E., & Jordan, D. R. (2014). Drought adaptation of stay-green sorghum is associated with canopy development, leaf anatomy, root growth, and water uptake. Journal of experimental botany, eru232.

Brown, L. K., George, T. S., Dupuy, L. X., & White, P. J. (2013). A conceptual model of root hair ideotypes for future agricultural environments: what combination of traits should be targeted to cope with limited P availability?. *Annals of botany*, *112*(2), 317-330.

Bucksch, A., Burridge, J., York, L. M., Das, A., Nord, E., Weitz, J. S., & Lynch, J. P. (2014). Image-based high-throughput field phenotyping of crop roots. *Plant physiology*, *166*(2), 470-486.

Burton, A. L., Johnson, J., Foerster, J., Hanlon, M. T., Kaeppler, S. M., Lynch, J. P., & Brown, K. M. (2015). QTL mapping and phenotypic variation of root anatomical traits in maize (Zea mays L.). *Theor Appl Genet*, *128*(1), 93-106. doi: 10.1007/s00122-014-2414-8

Burton, A. L., Johnson, J. M., Foerster, J. M., Hirsch, C. N., Buell, C. R., Hanlon, M. T., . . . Lynch, J. P. (2014). QTL mapping and phenotypic variation for root architectural traits in maize (Zea mays L.). *Theoretical and Applied Genetics, 127*(11), 2293-2311. doi: 10.1007/s00122-014-2353-4

Cai, H., Chen, F., Mi, G., Zhang, F., Maurer, H. P., Liu, W., . . . Yuan, L. (2012). Mapping QTLs for root system architecture of maize (Zea mays L.) in the field at different developmental stages. *Theoretical and Applied Genetics, 125*(6).

Colombi, T., Kirchgessner, N., Le Marié, C. A., York, L. M., Lynch, J. P., & Hund, A. (2015). Next generation shovelomics: set up a tent and REST. Plant and Soil, 1-20.

Cordell, D., Drangert, J. O., & White, S. (2009). The story of phosphorus: global food security and food for thought. *Global environmental change*, *19*(2), 292-305.
Den Herder, G., Van Isterdael, G., Beeckman, T., & De Smet, I. (2010). The roots of a new green revolution. Trends in plant science, 15(11), 600-607.
Donald, C. M. T. (1968). The breeding of crop ideotypes. Euphytica, 17(3), 385-403.
FAO 2010 Current world fertilizer trends and outlook to 2014. Rome, Italy: Food and Agriculture Organization of the United Nations.
Feldman, L. (1994). The maize root. In *The maize handbook* (pp. 29-37). Springer New York.
Fiorani, F., & Schurr, U. (2013). Future scenarios for plant phenotyping. *Annual review of plant biology*, *64*, 267-291.
Giuliani, S., Sanguineti, M. C., Tuberosa, R., Bellotti, M., Salvi, S., & Landi, P. (2005). Root-ABA1, a major constitutive QTL, affects maize root architecture and leaf ABA concentration at different water regimes. *Journal of Experimental Botany, 56*(422). doi: 10.1093/jxb/eri303
Goffinet, B., & Gerber, S. (2000). Quantitative trait loci: a meta-analysis. *Genetics*, *155*(1), 463-473.
Grift, T. E., Novais, J., & Bohn, M. (2011). High-throughput phenotyping technology for maize roots. *Biosystems Engineering*, *110*(1), 40-48.
Guingo, E., Hebert, Y., & Charcosset, A. (1998). Genetic analysis of root traits in maize. *Agronomie*, *18*(3).
Hall, D., Tegström, C., & Ingvarsson, P. K. (2010). Using association mapping to dissect the genetic basis of complex traits in plants. *Briefings in functional genomics*, 9:157-165
Henry, A., Swamy, B. M., Dixit, S., Torres, R. D., Batoto, T. C., Manalili, M., ... & Kumar, A. (2015). Physiological mechanisms contributing to the QTL-combination effects on improved performance of IR64 rice NILs under drought. *Journal of experimental botany*, eru506.
Hetz, W., Hochholdinger, F., Schwall, M., & Feix, G. (1996). Isolation and characterization of rtcs, a maize mutant deficient in the formation of nodal roots. *Plant Journal, 10*(5), 845-857.
Hochholdinger, F., Woll, K., Sauer, M., & Dembinsky, D. (2004). Genetic dissection of root formation in maize (Zea mays) reveals root-type specific developmental programmes. *Annals of Botany*, *93*(4), 359-368.
Hochholdinger, F., Wen, T. J., Zimmermann, R., Chimot-Marolle, P., Da Costa e Silva, O., Bruce, W., ... & Schnable, P. S. (2008). The maize (Zea mays L.) roothairless3 gene encodes a putative GPI-anchored, monocot-specific, COBRA-like protein that significantly affects grain yield. *The Plant Journal*, *54*(5), 888-898.
Hochholdinger, F. (2009). The maize root system: morphology, anatomy, and genetics. In Handbook of maize: Its biology (pp. 145-160). Springer New York.
Hochholdinger F. & Feix G. (2013). Genetic analysis of maize root development, in Eshel, A., & Beeckman, T. (Eds.). Plant roots: the hidden half. CRC Press.
Hund, A., Fracheboud, Y., Soldati, A., Frascaroli, E., Salvi, S., & Stamp, P. (2004). QTL controlling root and shoot traits of maize seedlings under cold stress. *Theoretical and applied genetics*, *109*(3), 618-629.
Jenkins, M. (1930). Heritable characters of maize. XXXIV. Rootless. . *J Hered, 21*, 79-80.
Iyer-Pascuzzi, A. S., Symonova, O., Mileyko, Y., Hao, Y., Belcher, H., Harer, J., ... & Benfey, P. N. (2010). Imaging and analysis platform for automatic phenotyping and trait ranking of plant root systems. *Plant Physiology*, *152*(3), 1148-1157.
Ku, L. X., Sun, Z. H., Wang, C. L., Zhang, J., Zhao, R. F., Liu, H. Y., . . . Chen, Y. H. (2012). QTL mapping and epistasis analysis of brace root traits in maize. *Molecular Breeding, 30*(2).
Landi, P., Sanguineti, M. C., Conti, S., & Tuberosa, R. (2001). Direct and correlated responses to divergent selection for leaf abscisic acid concentration in two maize populations. *Crop Science*, *41*(2), 335-344.
Landi, P., Sanguineti, M. C., Darrah, L. L., Giuliani, M. M., Salvi, S., Conti, S., & Tuberosa, R. (2002). Detection of QTLs for vertical root pulling resistance in maize and overlap with QTLs

for root traits in hydroponics and for grain yield under different water regimes. *Maydica, 47*(3-4).

Landi, P., Sanguineti, M. C., Salvi, S., Giuliani, S., Bellotti, M., Maccaferri, M., . . . Tuberosa, R. (2005). Validation and characterization of a major QTL affecting leaf ABA concentration in maize. *Molecular Breeding, 15*(3), 291-303. doi: 10.1007/s11032-004-7604-7

Landi, P., Giuliani, S., Salvi, S., Ferri, M., Tuberosa, R., & Sanguineti, M. C. (2010). Characterization of root-yield-1.06, a major constitutive QTL for root and agronomic traits in maize across water regimes. *Journal of Experimental Botany, 61*(13), 3553-3562.

Lebreton, C., Lazić-Jančić, V., Steed, A., Pekić, S., & Quarrie, S. A. (1995). Identification of QTL for drought responses in maize and their use in testing causal relationships between traits. *Journal of Experimental Botany*, *46*(7), 853-865.

Liu, J., Li, J., Chen, F., Zhang, F., Ren, T., Zhuang, Z., & Mi, G. (2008). Mapping QTLs for root traits under different nitrate levels at the seedling stage in maize (Zea mays L.). *Plant and Soil*, *305*(1-2).

Lobet, G., & Draye, X. (2013). Novel scanning procedure enabling the vectorization of entire rhizotron-grown root systems. *Plant methods*, *9*(1), 1-11.

Lynch, J. (1995). Root architecture and plant productivity. *Plant physiology*, *109*(1), 7.

Lynch, J. P. (2007). Turner review no. 14. Roots of the second green revolution. *Australian Journal of Botany, 55*(5), 493-512.

Lynch, J. P., & Brown, K. M. (2012). New roots for agriculture: exploiting the root phenome. *Philosophical Transactions of the Royal Society B: Biological Sciences*, *367*(1595), 1598-1604.

Lynch, J. P. (2013). Steep, cheap and deep: an ideotype to optimize water and N acquisition by maize root systems. *Annals of botany*, *112*(2), 347-357.

Mano, Y., Omori, F., Muraki, M., & Takamizo, T. (2005). QTL mapping of adventitious root formation under flooding conditions in tropical maize (Zea mays L.) seedlings. *Breeding Science, 55*(3).

Mu, X., Chen, F., Wu, Q., Chen, Q., Wang, J., Yuan, L., & Mi, G. (2015). Genetic improvement of root growth increases maize yield via enhanced post-silking nitrogen uptake. European Journal of Agronomy, 63, 55-61.

Nagel, K. A., Putz, A., Gilmer, F., Heinz, K., Fischbach, A., Pfeifer, J., ... & Schurr, U. (2012). GROWSCREEN-Rhizo is a novel phenotyping robot enabling simultaneous measurements of root and shoot growth for plants grown in soil-filled rhizotrons. *Functional Plant Biology*, *39*(11), 891-904.

Norton, G. J., Aitkenhead, M. J., Khowaja, F. S., Whalley, W. R., & Price, A. H. (2008). A bioinformatic and transcriptomic approach to identifying positional candidate genes without fine mapping: an example using rice root-growth QTLs. *Genomics*, *92*(5), 344-352.

Pieruschka, R., & Poorter, H. (2012). Phenotyping plants: genes, phenes and machines. *Functional Plant Biology*, *39*(11), 813-820.

Rose, T. J., Impa, S. M., Rose, M. T., Pariasca-Tanaka, J., Mori, A., Heuer, S., ... & Wissuwa, M. (2013). Enhancing phosphorus and zinc acquisition efficiency in rice: a critical review of root traits and their potential utility in rice breeding. *Annals of botany*, *112*(2), 331-345.

Ruta, N., Liedgens, M., Fracheboud, Y., Stamp, P., & Hund, A. (2010a). QTLs for the elongation of axile and lateral roots of maize in response to low water potential. *Theoretical and Applied Genetics, 120*(3). doi: 10.1007/s00122-009-1180-5

Ruta, N., Stamp, P., Liedgens, M., Fracheboud, Y., & Hund, A. (2010b). Collocations of QTLs for Seedling Traits and Yield Components of Tropical Maize under Water Stress Conditions. *Crop Science, 50*(4), 1385-1392. doi: 10.2135/cropsci2009.01.0036

Salvi, S., & Tuberosa, R. (2005). To clone or not to clone plant QTLs: present and future challenges. *Trends in Plant Science, 10*(6), 297-304. doi: 10.1016/j.tplants.2005.04.008

Salvi, S., & Tuberosa, R. (2007). Cloning QTLs in plants. In *Genomics-assisted crop improvement* (pp. 207-225). Springer Netherlands.

Salvi, S., & Tuberosa, R. (2015). The crop QTLome comes of age. Curr Opin Biotechnol, 32C, 179-185.

Schnable, P. S., Ware, D., Fulton, R. S., Stein, J. C., Wei, F., Pasternak, S., ... & Cordes, M. (2009). The B73 maize genome: complexity, diversity, and dynamics. *science*, *326*(5956), 1112-1115.

Steele KA, Price AH, Witcombe JR, Shrestha R, Singh BN, Gibbons JM, Virk DS.QTLs associated with root traits increase yield in upland rice when transferred through marker-assisted selection. Theor Appl Genet. 2013 Jan; 126(1):101-8. Epub 2012 Sep 12.

Sosnowski, O., Charcosset, A., & Joets, J. (2012). BioMercator V3: an upgrade of genetic map compilation and quantitative trait loci meta-analysis algorithms. *Bioinformatics*, *28*(15), 2082-2083.

Suji, K. K., Prince, K. S. J., Mankhar, P. S., Kanagaraj, P., Poornima, R., Amutha, K., ... & Babu, R. C. (2012). Evaluation of rice (Oryza sativa L.) near iso-genic lines with root QTLs for plant production and root traits in rainfed target populations of environment. *Field Crops Research*, *137*, 89-96.

Taramino, G., Sauer, M., Stauffer, J. L., Multani, D., Niu, X., Sakai, H., & Hochholdinger, F. (2007). The maize (Zea mays L.) RTCS gene encodes a LOB domain protein that is a key regulator of embryonic seminal and post-embryonic shoot-borne root initiation. *The Plant Journal*, *50*(4), 649-659.

Trachsel, S., Messmer, R., Stamp, P., & Hund, A. (2009). Mapping of QTLs for lateral and axile root growth of tropical maize. *Theoretical and Applied Genetics*, *119*(8).

Trachsel, S., Kaeppler, S. M., Brown, K. M., & Lynch, J. P. (2011). Shovelomics: high throughput phenotyping of maize (Zea mays L.) root architecture in the field. *Plant and Soil*, *341*(1-2), 75-87.

Tuberosa, R., Sanguineti, M. C., Landi, P., Salvi, S., Casarini, E., & Conti, S. (1998). RFLP mapping of quantitative trait loci controlling abscisic acid concentration in leaves of drought-stressed maize (Zea mays L.). *Theoretical and Applied Genetics*, *97*(5-6), 744-755.

Tuberosa, R., Sanguineti, M. C., Landi, P., Michela Giuliani, M., Salvi, S., & Conti, S. (2002). Identification of QTLs for root characteristics in maize grown in hydroponics and analysis of their overlap with QTLs for grain yield in the field at two water regimes. *Plant Molecular Biology*, *48*(5).

Tuberosa, R., Salvi, S., Sanguineti, M. C., Maccaferri, M., Giuliani, S., & Landi, P. (2003). Searching for quantitative trait loci controlling root traits in maize: a critical appraisal. In *Roots: The Dynamic Interface between Plants and the Earth* (pp. 35-54). Springer Netherlands.

Tuberosa, R., Salvi, S., Giuliani, S., Sanguineti, M. C., Frascaroli, E., Conti, S., & Landi, P. (2011). Genomics of root architecture and functions in maize. In Root genomics (pp. 179-204). Springer Berlin Heidelberg.

Uga, Y., Sugimoto, K., Ogawa, S., Rane, J., Ishitani, M., Hara, N., ... & Yano, M. (2013). Control of root system architecture by DEEPER ROOTING 1 increases rice yield under drought conditions. *Nature Genetics*, *45*(9), 1097-1102.

Veyrieras, J. B., Goffinet, B., & Charcosset, A. (2007). MetaQTL: a package of new computational methods for the meta-analysis of QTL mapping experiments. *BMC bioinformatics*, *8*(1), 49.

von Behrens, I., Komatsu, M., Zhang, Y., Berendzen, K. W., Niu, X., Sakai, H., ... & Hochholdinger, F. (2011). Rootless with undetectable meristem 1 encodes a monocot-specific AUX/IAA protein that controls embryonic seminal and post-embryonic lateral root initiation in maize. *The Plant Journal*, *66*(2), 341-353.

Wang, Z., Gerstein, M., & Snyder, M. (2009). RNA-Seq: a revolutionary tool for transcriptomics. *Nature Reviews Genetics*, *10*(1), 57-63.

Wen, T. J., & Schnable, P. S. (1994). Analyses of mutants of 3 genes that influence root hair development in zea-mays (gramineae) suggest that root hairs are dispensable. *American Journal of Botany*, *81*(7), 833-842.

Wen, T. J., Hochholdinger, F., Sauer, M., Bruce, W., & Schnable, P. S. (2005). The roothairless1

gene of maize encodes a homolog of sec3, which is involved in polar exocytosis. *Plant physiology*, *138*(3), 1637-1643.
White, P. J., George, T. S., Gregory, P. J., Bengough, A. G., Hallett, P. D., & McKenzie, B. M. (2013). Matching roots to their environment. Annals of botany, 112(2), 207-222.
Woll, K., Borsuk, L. A., Stransky, H., Nettleton, D., Schnable, P. S., & Hochholdinger, F. (2005). Isolation, characterization, and pericycle-specific transcriptome analyses of the novel maize lateral and seminal root initiation mutant rum1. *Plant Physiology*, *139*(3), 1255-1267. doi: 10.1104/pp.105.067330
Zhu J, Kaeppler SM, Lynch JP (2005b) Mapping of QTLs for lateral root branching and length in maize (Zea mays L.) under differen- tial phosphorus supply. Theoret Appl Genet 111:688–695
Zhu, J., Mickelson, S. M., Kaeppler, S. M., & Lynch, J. P. (2006). Detection of quantitative trait loci for seminal root traits in maize (Zea mays L.) seedlings grown under differential phosphorus levels. *Theoretical and Applied Genetics*, *113*(1).
Zhu, J., Ingram, P. A., Benfey, P. N., & Elich, T. (2011). From lab to field, new approaches to phenotyping root system architecture. *Current opinion in plant biology*, *14*(3), 310-317.

2 Implementing Protocols for Root Phenotyping

2.1 Introduction

Nowadays, with the possibility to have high-density genotypic information using high-throughput genotyping and next-generation sequencing (NGS), phenotyping is indicated as the new bottleneck in genetic studies (Fiorani and Schurr 2013; Furbank *et al.*, 2011; Cobb *et al.*, 2013; Lynch and Brown 2012). The understanding of plant genomes structure and function rapidly evolves but the difficulties in phenotyping delays the actual deployment of genomic knowledge to advance crop breeding. The phenome (i.e. the phenotype as a whole. Houle *et al.*, 2010), is dynamic and integrates a complex set of data at all levels of development, in response to environmental conditions (Cobb *et al.*, 2013). Therefore, technologies enabling high-throughput phenotyping in a high dimension, the so-called phenomics (Houle *et al.*, 2010), is everyday more required for a more precise description and comprehension of genotype-phenotype relationships.

High-throughput phenotyping also means the possibility to evaluate large populations with the minimum possible effort and time. This concept results more challenging when the root system architecture is the target because of its complexity and its sensitivity to multiple interactions with environmental variables (Lynch and Brown 2012). One approach to visualize or characterize roots in the soil is the non-invasive type of techniques (See Fioriani and Schurr 2013, for a detailed review). These methods are not ready yet, although they are in continuous development. Main constraints are the high costs and the required highly specialized expertise.

On the other side, high-throughput root phenotyping protocols encompass a combination of specialized techniques for growing plant in controlled environments, and subsequently for isolating, imaging and analyzing roots, often with the help of specialized software tools (Clark *et al.*, 2013). The majority of these protocols use artificial media that facilitate the root observation, like gel (Iyer-Pascuzzi *et al*, 2010, Clark *et al.*, 2011), hydroponics with nutrient solutions (Sanguineti *et al.*, 2006), aeroponics (de Dorlodot *et al.*, 2007), and growth pouches or paper-like supports (Hund *et al.*, 2009). Others use special containers for root growth in soil (Nagel *et al.*, 2012, Le Marié *et al.*, 2014). All of them are successfully coupled with image acquisition and software-based analysis (Iyer-Pascuzzi *et al.*, 2010, Grift *et al.*, 2011, Nagel *et al.*, 2012, Lobet and Draye, 2013). Of course, a main concern raised by these methods is the feeble similarity with real field conditions (Lynch and Brown 2012).

In maize, a crop with a large and complex root system, these concerns are especially problematic. In addition, maize can generally only be grown for a limited duration in controlled conditions, therefore studies mainly focus to embryonic or early adult root system. On the contrary, field protocols are laborious and destructive and information about phenotypic variation for root architecture in the field and its genetic control remain scarce. In maize, vertical root pulling resistance (VRPR) has been one of the most frequently investigated traits in the field. VRPR is the peak force required to uproot a plant and was repeatedly correlated with several root architectural traits such as root mass, dry weight and others (Kevern and Hallauer 1983; Landi *et al.*, 2002). A more detailed description of root architectural traits of an adult maize plant in the field was obtained with the development of the high-throughput method known as shovelomics (Trachsel *et al.*, 2011). Shovelomics allows a rapid visualization of excavated and washed root crowns giving a visual scoring of the numbers, angles and branching density of brace and crown roots. Recently, specialized software, DIRT (Bucksch *et al.*, 2014) and REST (Colombi *et al.*, 2015), have been developed to analyze crown root images obtained from this protocol addressing the limitations of manual data collection and enhancing the statistical power of the method.

The present study was conducted on a selected group of maize genotypes and aimed at:

1. Testing and comparing a non-invasive method (root electrical capacitance) and an invasive one (shovelomics) for field based root analysis in maize;

2. Improving a field root phenotyping protocol combined with image-based analysis enabling a collection of quantity and quality data suitable for selection in breeding programs and for mapping and cloning purposes, in our case for *qroot-yield-1.06*.

2.2 Materials and methods

2.2.1 Plant material

Five pairs of QTL-Near Isogenic Lines (NILs): IABO (+/+) and (-/-), OS (+/+) and (-/-) for the root QTL qroot-ABA1 (Landi *et al.*, 2007); NIL120 (-/-) and NIL129 (+/+), NIL157 (-/-) and NIL158 (+/+) for the root QTL qroot-yield-1.06 (Landi *et al.*, 2010); N28 and C22-4 for the QTL Vegetative to generative transition 1 (Vgt1) (Salvi *et al.*, 2002). and additional maize inbreeds (Lo1016, B73, Mo17, Va26, A632, 189-7-1-2, 94-6-1-6) for a total of 17 genotypes, were utilized in this experiment.

2.2.2 Field experiment

The field experiment was carried out in 2012 at Cadriano (close to Bologna, Po Valley, Northern Italy; 11° 24' E, 44° 33' N) on a loam soil (clay, 18%; sand, 37%; silt, 45%). Trials were hand-sown at the end of April and phenotyped for root traits in mid August. Row width was 0.90 m and distance between plants was 23 cm for a plant density of 4,83 plants m^{-2}. Weeds were manually removed as necessary. Genotypes were randomly assigned to plots using a randomized complete block design with three replications. One plot consisted of one 3 m row containing 13 plants.

Two different approaches were used to asses root architecture in the field: a non-destructive analysis based on analysis of field electrical capacitance nearby the sampled plant, which was previously shown to correlate with root mass (van Beem *et al.,* 1998) and the destructive digging-based approach called 'shovelomics' (Trachsel *et al.,* 2011) coupled with collection and analysis of digital images using specialized software.

Field electrical capacitance. To ensure soil humidity around the roots, field was irrigated to field capacity 24 h prior to capacitance readings. Four plants at flowering stage, fully bordered, were selected for each plot based on plant height and general appearance. Root electrical capacitance was measured at 1 kHz with a Capacitor BK 890C (BK precision, Yorba Linda, CA, USA) using the auto mode. Electrical contact with the plant was established connecting the negative electrode to the maize stem via a battery clam at 15 cm above the ground. The positive electrode was connected via a battery clamp to a copper rod 60 cm in length inserted in the soil at 12 cm from the stem base to a depth of 15 cm (Figure 2).

Figure 2. Root electrical capacitance measurement in the field using a portable capacitance meter (BK Precision 890C). The positive electrode is attached to a copper ground rod and the negative electrode is attached to the maize stem at 15cm above the ground.

Shovelomics. In the same experiment where root capacitance was collected we also analyzed root architecture by implementing a typical shovelomics (Trachsel *et al.*, 2011) protocol as detailed below. Roots were excavated by removing a soil cylinder of approximately 40 cm using a standard shovel, briefly shaken, soaked in water with detergent and finally cleaned removing the remaining soil particles using water a low pressure. Following this treatment, roots were digitally photographed (Figure 3A). Visual scores were given to each experimental unit by examining four representative plants from the same plot. Visual scores were used to evaluate brace roots number (BO) and branching density of the crown (BB) using a scale from 1 (low root numbers and low branching) to 5 (higher numbers and higher branching). Root clumps were stored and preserved at 4 °C to conserve their three-dimensional structure and subsequently for measuring and counting the number of whorls occupied with brace roots (BW), number of roots in the first whorl (that touching the soil) (BO1) and angles (respect to the soil level) of brace roots in the first whorl (BA) (Figure 3B). Root clumps were dried for five days in the oven at 105 °C for measuring the dry weight (DW). Statistical data analysis was done using the computer program for statistical analysis PLABSTAT version 3A, free available online (Utz, 2001).

Figure 3. Steps of the shovelomics protocol (Trachsel *et al.*, 2011) as implemented in this study. 1- Plot preparation. 2- Root excavation. 3- Soaking on water with a mild detergent. 4- Removal of soil particles from the root clumps by vigorous rinsing with water at low pressure. 5- Digital imaging (previous to digital image acquisition improvement) . 6- Details of traits visually scored.

2.2.3 Image analysis

Images were evaluated using two different software tools designed for analysis of root system images: GiA Roots (Galkovskyi *et al.,* 2012) and DIRT- Digital Imaging of Root Traits (Bucksch *et al.,* 2014). GiA Roots can be free-downloaded from the website (http://giaroots.biology.gatech.edu/). For DIRT, an online application at (http://www.dirt.biology.gatech.edu/) was needed to access to a beta version ("computation is only accessible within the Georgia Tech network until security and policy issues are solved").

Both software assume by default that bright pixels are that of the background and dark pixels are that of the root, thus, images were previously edited using standard image editors (Adobe® Photoshop®) to clean the background and avoid possible mistakes in the forward analysis.
In the case of GiA Roots, cleaned images were loaded and each image was manual cropped and adjusted to the correct scale given the corresponding value of pixels for 1 cm. For the analysis, all of the 20 root analysis features provided by the software were selected take full advantage of GiA Roots. Following GiA Roots manual, the feature "Number of connected components" was used to assess the quality of image pre-processing. Root network should have one component then, images with 'number of connected components' higher than 1 were processed again by adjusting the parameters of "adaptive image thresholding".

For image analysis using DIRT, data were loaded to the website and analyzed for the 30 phenotypic traits checked by default. At the end of the process a .CSV file with the results is available for downloading and following analysis. Statistical data analysis was done using PLABSTAT version 3A (Utz, 2001).

2.2.4 Improving digital imaging acquisition

Analysis of root digital images may provide information about numerous additional traits in respect to visual scoring, thus strongly improving root phenotyping protocols. However, low-quality digital images strongly impair downstream analysis. Therefore, during the experiment, effort was given in continuously improving images quality. A new protocol was adopted following the recommendations of Bucksch's paper (Bucksch *et al.,* 2014 and Bucksch, personal communication). Briefly, in the protocol reported for imaging, the root crown is placed on a black board together with optional elements as: excised roots, a circle and a marker, placed arbitrarily.

Next, root system is photographed using high-end consumer digital cameras, fixed on a tripod and trying to maintain relatively constant diffuse lighting.

This protocol was applied for the image acquisition and analysis of the experiment concerning the shovelomics-based root phenotyping of 46 homozygous recombinant lines at *qroot-yield-1.06* (F4 families) (See Chapter 3).

2.3 RESULTS

2.3.1 Electrical root capacitance

The measurement of root capacitance with a portable capacitor has been reported as a non-destructive method to easily assesses differences in root mass between genotypes, thanks to the high correlation observed between root capacitance and fresh root mass, in experiments carried out in the greenhouse and in the field (Messmer *et al.*, 2011). In our experiment, measurements of the electrical capacitance of the roots were not significantly correlated with dry weight (coefficient of correlation r = 0.173). Figure 4 shows the low value of the coefficient of determination (R^2 = 0.022) when capacitance vs. DW is plotted.

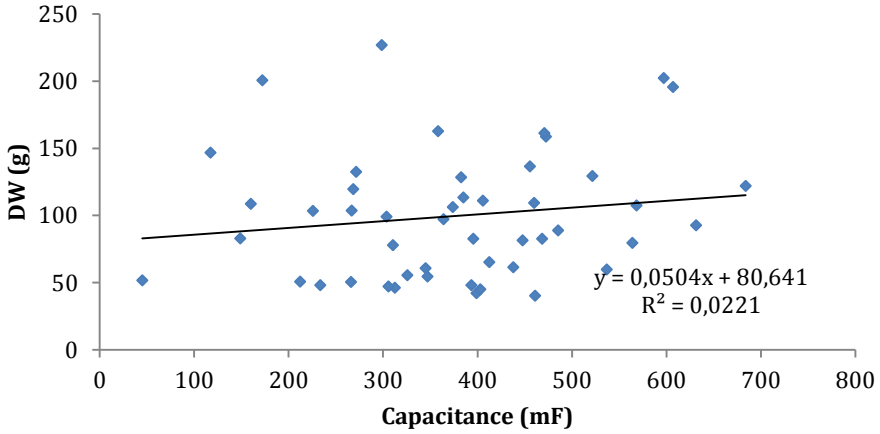

Figure 4. Relationship between maize dry weight and capacitance taken 120 d after planting under field conditions.

2.3.2 Shovelomics

On average, the time required for uprooting and evaluation of an individual root crown, in our condition, was c. 20 min. In more detail, the time required for excavation and visual evaluation was c. 5 min, similarly to what previously reported (Trachsel *et al.*, 2011). Soaking and rinsing took

additional 15 min, and this time was highly dependent on the branching density of the genotype. All together, this uprooting and washing protocol was successful in permitting, a good visual inspection of the main root architecture traits (Figure 5).

Figure 5. Digital images of root apparatus as obtained following the shovelomics protocol. In the figure, contrasting NILs for root QTLs: Top, NILs for *qroot-ABA-1* (Os--, Os++) and bottom, NILs for *qroot-yield-1.06* (NIL120 (--), NIL129 (++)).

Considerable variability was observed among genotypes with the largest coefficient of variation (C.V.) for dry weight (48.5%). The visual scoring for the number of brace roots (BO) (39.3%) and the branching density of the crown (BB) (30%), and the number of whorls occupied with brace roots (30%) had intermediate variability. The lowest variability was observed for the angle of brace roots on the first whorl (17.1%) and the number of brace roots in the first whorl (BO1) (6.1%).

Mean values, analysis of variance and the heritability of the different traits measured doing shovelomics, for the 17 genotypes are summarized in Table 1. ANOVA evidenced significant variation among genotypes for all traits except for the number of brace roots in the first whorl (BO1). Additionally, a low value of heritability (36.9) is reported for BO1, in contrast with the high values ranged from 84.1 to 94.9 for the other traits. A high correlation value was found between DW and BB (0.81) and also between the count (BW) and the visual scoring (BO) of the brace roots (0.88).

Regarding *qroot-yield-1.06* (see Chapter 3) both pairs of NILS were significantly different for most of the root traits evaluated. NILs homozygous for the minus (-) allele (120 and 157) were characterized by a wider root angle, minor branching density and smaller number of brace roots and, in consequence, a smaller dry weight. Correspondingly, for NILs (++) (129 and 158) the root architecture was significantly different with shallower roots angles, higher branching density and a bigger number of brace roots.

Table 1. Analysis of variance for traits of the root crown, in 17 genotypes. Significance level (p), mean values, Least significance difference at 5% level (LSD5), standard error (SE) and heritability (h2) are displayed for the following traits: Dry weight in g (DW), number of whorls occupied with brace roots (BW), number of roots in the first whorl (that touching the soil) (BO1) and angle (respect to the soil level) of brace roots in the first whorl (BA), visual scorings for brace roots number (BO) and branching density of the crown (BB). ** denotes significance at p-level of 0.01.

Genotypes	**DW**	**BW**	**BO1**	**BA**	**BO**	**BB**
Iabo (+/+)	99,5	2,3	18,6	43,5	2,7	3,5
Iabo (-/-)	140,8	1,8	20,4	53,9	2,2	3,4
OS (+/+)	102,4	1,9	20,3	40,7	1,3	3,3
OS (-/-)	47,4	2,0	17,6	57,3	1,7	2,5
NIL129 (+/+)	190,8	2,1	16,8	55,0	2,7	4,3
NIL120 (-/-)	80,3	1,6	16,5	37,8	1,7	2,2
NIL158 (+/+)	156,1	2,0	18,4	61,3	2,3	4,2
NIL157 (-/-)	55,8	1,3	17,7	45,8	1,8	1,3
Va26	107,7	2,7	16,2	68,2	1,7	3,0
N28	111,5	2,9	17,8	40,1	4,0	4,5
Lo1016	63,9	1,9	18,3	63,0	2,0	1,8
C22-4	115,2	2,6	17,7	48,1	2,5	3,7
B73	88,3	3,3	18,3	63,0	4,0	3,8
Mo17	59,3	1,8	18,1	45,8	2,0	3,3
A632	47,3	2,3	19,2	57,9	2,8	1,7
189-7-1-2	132,0	4,1	17,8	60,2	5,0	3,3
94-6-1-6	77,8	2,0	16,3	67,0	2,0	2,8
Significance (p-level)	**	**	NS	**	**	**
LSD5	46,4	0,5	2,8	11,5	0,8	0,8
SE	25,6	0,2	0,8	3,5	0,3	0,3
h^2**(%)**	84,1	92,7	36,9	84,3	92,9	90,7

2.3.3 Image analysis

All twenty features included in the GIA Roots software were evaluated: Average root width (Width), Bushiness (Bush), Number of connected components (Ncon), Network Depth (Ndepth), Aspect ratio (AspR), Network length distribution (Ldist), Major Ellipse Axis (MajA), Maximum number of roots (MaxR), Network width (Nwidth), Median number of roots (MedR), Minor Ellipse Axis (MinA), Network Area (NwA), Network Convex Area (ConvA), Network perimeter (Perim), Network solidity (NS), Specific root length (SRL), Nsurf (Network surface area), Network length (Nlen), Netwok volume (Nvol) and Network width to depth ratio. The ANOVA (data no shown) evidenced significant variation among genotypes for 18 out of 20 traits. A significant difference for Ncon suggests that were not expected because values must be one for all samples. Values greater than one mean that the root structure was not analyzed as a unique element maybe due to the image quality.

Spearman's correlation coefficients among features obtained with GiA Roots and visual scoring for branching density (BB) for the 17 genotypes evaluated, are reported in Table 2. BB was found highly (> 0.70) correlated with MaxR, MedR, Perim, Nsurf and Nlen.

Table 2. Spearman's correlation coefficients among features obtained with GiA Roots and visual scoring for branching density (BB) for 17 genotypes. Traits displayed are: Average root width (Width), Bushiness (Bush), Network Depth (Ndepth), Aspect ratio (AspR), Network length distribution (Ldist), Major Ellipse Axis (MajA), Maximum number of roots (MaxR), Network width (Nwidth), Median number of roots (MedR), Minor Ellipse Axis (MinA), Network Area (NwA), Network Convex Area (ConvA), Network perimeter (Perim), Network solidity (NS), Specific root length (SRL), Nsurf (Network surface area), Network length (Nlen), Netwok volume (Nvol) and Network width to depth ratio.* and ** denote significances at p-levels of 0.05 and 0.01.

	Width	**Bush**	**Ndepth**	**AspR**	**Ldist**	**MajA**	**MaxR**	**Nwidth**	**MedR**	**MinA**
BB	-0.462	-0.087	0.262	-0.048	-0.027	0.452	0.788**	0.248	0.816**	0.340

	NwA	**ConvA**	**Perim**	**NS**	**SRL**	**Nsurf**	**Nlen**	**Nvol**	**NW/D**
BB	0.685**	0.418	0.823**	0.488*	0.482*	0.709**	0.823**	0.395	0.100

Image quality was found particularly important to enable root analysis with the software DIRT. A notable amount of time was invested in improving image quality before sending them to DIRT. However, 16 % of the images could not be analyzed by DIRT because the process failed.

The output file also include several parameters describing architectural traits of dicot and monocot root system based on the computation of root length, density, angles, diameters and spatial root architecture. In this study, 26 different traits were selected according to previously reported in Bucksch *et al.*, (2014) for the analysis of monocots crown root images. Traits are listed on Table 3.

Table 3. Crown root traits evaluated using DIRT (Bucksch *et al.*, 2014).

Name	**Definition**
No. RTPs	Number of root-tip paths
Median/mean T	Median and mean tip diameters of all tips
DD90max	Maximal tip diameter in the last 10% of the image
Median/max width	Median/maximum of the calculated width in the width height diagram
D10 to D90	Accumulated width over the depth at x%. The change in width accumulation denotes a change of the root-top angle
DS10 to DS90	Slop of the graph of D values.
Spatial root distribution (as separate x an Y)	Displacement of the center of mass between the bounding box of the RTP skeleton and the RTP skeleton excluding the central path.

Relative phenotypic variation (RPV) was calculated to compare the potential of differentiation using shovelomics and image-based traits. RPV is defined as: 'the ratio between the variance of the

trait of all roots of the data set (V_d) and the average trait variance per genotype (V_{avg})' (Bucksch *et al.*, 2014). Accordingly with DIRT paper, an RPV value, significantly > 1 suggests that the trait is useful for differentiating genotypes. In Figure 6 is shown the RPV values for the different traits measured for the maize root crown. Visual scorings (BB and BO) show the greater values. This could be explained by the fact the visual scorings were given for the bulk of 4 plants of each replicate reducing the trait variance per genotype. In average, GiA Roots traits show higher RPV values (1.14-2) respect to DIRT traits (0.93-1.3). Width, SRL and NW/D could be highlighted as traits with a good differentiation potential.

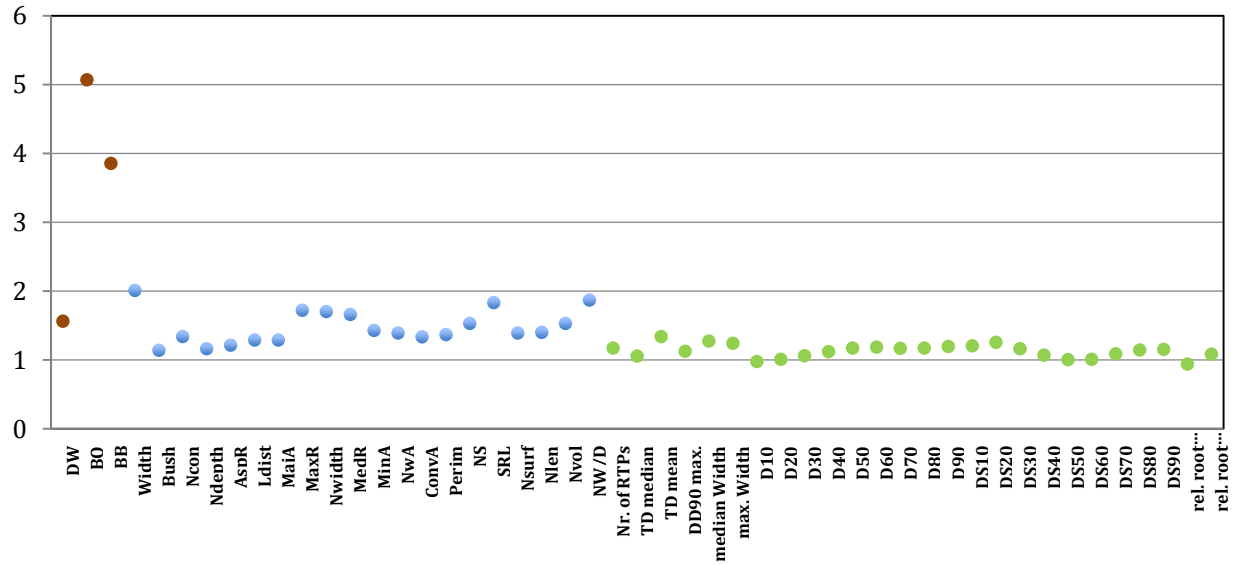

Figure 6. RPV analysis of the crown root measurements using shovelomics (red dots), and image-based traits: GiA Roots (blue dots) and DIRT (green dots).

Inter-genotype variation can also be observed in Figure 7, in which normalized values of manual and image-based traits are plotted, for the 17 genotypes. NILs pairs, Os--/Os++ and NIL120 (--)/NIL129 (++) for the qroot-ABA-1 and *qroot-yield*-1.06, respectively, are graphed with lines for an easy visualization of contrasting phenotypes shown in Figure 5. Error bars correspond to the standard error of the mean and indicate the precision of the population mean. The set of traits optimal to distinguish the four genotypes shown in the Figure 4, are those in which the error bars not overlapped. According with this criterion, GiA Roots provided a larger set of traits optimal for phenotype differentiation when compared to DIRT. However, it must be mentioned that DIRT is highly dependent on image quality, and not all the images used in this experiment were of high quality (and many required heavy quality editing).

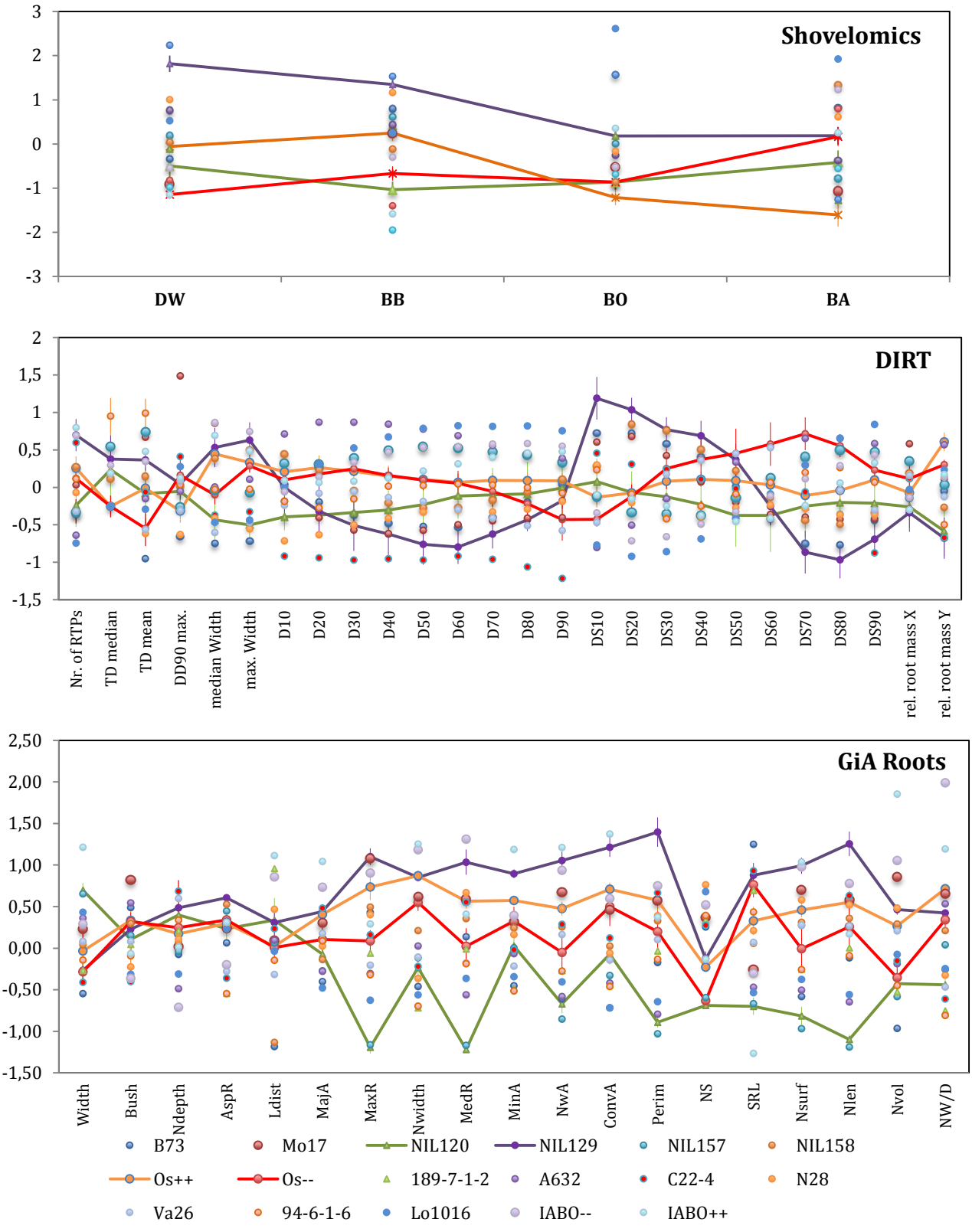

Figure 7. Phenotype differentiation of the 17 genotypes, based on shovelomics and imaging analysis with DIRT and GiA Roots. Dots represent the normalized mean trait values for each genotype for shovelomics traits (Top): Dry weight (DW), visual scorings for brace roots number (BO) and branching density of the crown (BB), and brace root angle (BA); DIRT features (middle): Maximum width (MaxW), accumulated width over the depth at 10% (D10) and 20% (D20); and GiA Roots features (bottom): Maximum number of roots (MaxR), network perimeter (Perim) and specific root length (SRL). Lines represent the four genotypes shown in Figure 4. The error bars indicate the Standard Error of the Mean.

2.3.4 Improving digital imaging acquisition

The improved digital imaging set for shovelomics consisted of a structure with a board and a perpendicular tube in which the camera was fixed at about 40 cm above the board. As background, it was used a black cloth, easily cleaned with a brush to remove soil particles and root fragments. The root clump was placed on the board and next, were placed a white circle of known diameter (scale marker) and a rectangular label with the experimental identification in barcodes (Figure 8). The scale marker is used for the correction of camera tilting and transforming image coordinates into metric units (Bucksch *et al.*, 2014). Finally, the group of elements was enclosed in a 'white box' constructed with polystyrene to have homogenous light conditions. The study was performed with a Nikon COOLPIX P310 digital camera with a focal length of 4,3mm and a maximal aperture of 2.8. Images were taken at a resolution of 3264x2448 pixels using the self-timer device.

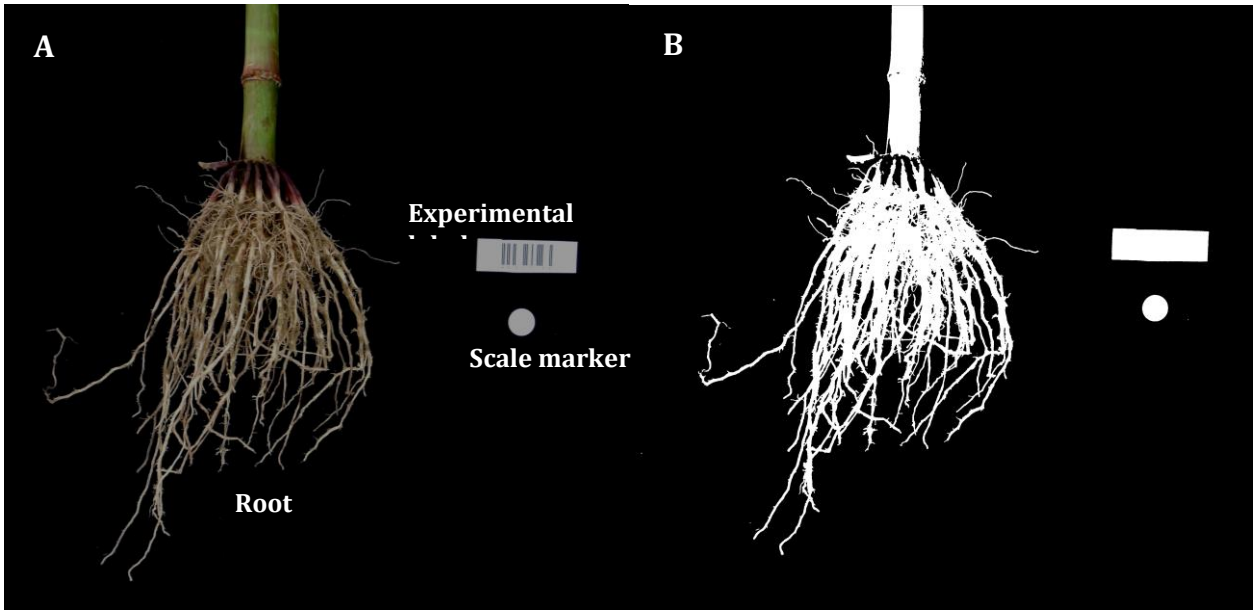

Figure 8. A. Image board including the root crown, the experimental label and the scale marker. B. Binary image.

The new protocol used significantly improved the image quality allowing a good segmentation into foreground (white pixels) and background (black pixels) in the binary image (Figure 8B). Consequently, no image edition was needed before downstream analysis with specialized software and only five images, out of 180, were discarded from the data set. The inclusion of the scale marker helps to control the image quality and to convert pixel values in cm values. Additionally, accordingly with DIRT paper, the label marker, included for DIRT analysis, should help to name automatically the photos by recognizing the barcodes. However, we were unable to have this system

work properly. The reasons could have been the size of the label or the image settings, which in turn required too long expositions (2-4 s).

With this set of high quality images, the software REST (Colombi *et al.*, 2015) was also tested with good results (data shown in chapter 3). In this case, scale marker was useful but label marker must be discarded. One of the traits that was easily visualized with this software was the root crown angle. However, software was quite sensitive to the presence of roots out of the crown which were not previously organized ('comb'), miscalculating the topsoil angle, as is shown in Figure 9A. Nevertheless, this mistake in the image acquisition was easily solved with an image editor, removing those single roots. The left angle of the figure 7A calculated as 19.4 °C was corrected after the image edition to 57.9 °C.

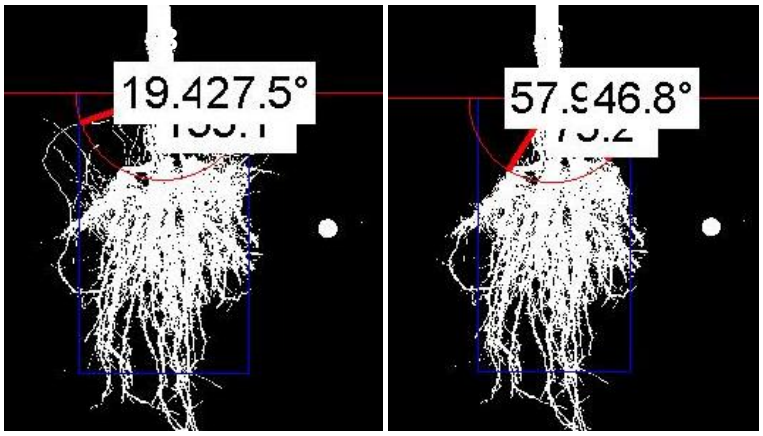

Figure 9. REST display of root angle measurements. A- Root angle values of an original image miscalculated because of the presence of roots out of the crown. B- Recalculated values of the root angles after image edition.

2.4 Discussion and conclusions

Electrical root capacitance was initially reported as an in-situ, non-destructive and not labor-intensive method to estimate root mass (Dalton, 1995). The introduction of lightweight, hand held capacitance meters and the significant correlation between root mass and capacitance, made this technique eligible for field root phenotyping (van Beem, 1998). Several studies have reported capacitance as a good predictor of root mass and capacitance itself was used for genetic mapping studies (Choulopek *et al.*, 2006). However, many biological and technical limitations were pointed as well. Dalton (1995) reported a strong dependence of the measurement on soil water content and sensitivity of results to the placement of the plant shoot negative electrode. This was successively confirmed in the study of van Beem *et al.*, (1998). In addition, root dry matter content seems to

affect the preferential pathway of the electrical current changing the root capacitance response (Aulen and Shipley 2012).

In the present study, capacitance was not significantly correlated with root dry mass. According with the previously mentioned observations, one possible explanation could be the changes on soil moisture occurred during the time sampling was carried out, which in our case was from early morning to mid-day. A second source of noise could be the position of the shoot electrode that was fixed at 15 cm above soil level because of the large quantity of brace roots present in some genotypes in the first 2-3 whorls. As more shoot tissue is included, the effective capacitance could decrease while the effective resistance increase (Dalton 1995). On the other side, shovelomics, even if much more labor intense, allows to physically (i.e. directly) visualize the main traits describing root architecture. The time required for the whole process from excavation to analysis was longer (2-4 times) respect to what was previously reported by Trachsel *et al.,* (2011) for a sand and silt-loam soils. In particular, significantly more time than expected was required for soaking and removing the soil particles attached to the roots. Genotypes with larger and more branched roots obviously required more time for cleaning.

For the analysis, the number of traits was reduced in order to speed out the method assuming that angles and branching are consistent between brace and crown roots; and to increase the accuracy, angles were measured and not visually scored, as suggested by Trachsel *et al.,* (2011). All traits, with the exception of the number of brace roots on the first whorl, show high heritabilities (i.e. >84%). However, the method was greatly dependent on the researcher imposing limitations in terms of objectivity and throughput. Then, one of the main purposes of this study was to extend the analysis of maize root system from traits as 'visual scoring' and 'dry weight' to traits more objective and informative (i.e. traits form image software analysis). Image-based analyses with specialized software allowed the automatic testing of many root architectural traits in a high-throughput way. Nevertheless, a really informative analysis is strongly dependent upon the quality of the root images collected (Bucksh *et al.,* 2014).

The set of images used in this study enables to compare the performance of two of the software reported for the analysis of root images. DIRT trait data, contrary to what was reported by Bucksh *et al.,* (2014), appeared less likely to be useful in differentiating genotypes, as inferred by the inferior RPV values, compared to standard manually collected shovelomics traits. However, for GiA Roots, even RPV values were also inferior than for shovelomics, a set of traits resulted optimal

for phenotype differentiation. Curiously, while GiA Roots was validated on a set of rice seedling root images grown on gel (Iyer-Pascuzzi *et al.,* 2010), this software resulted also useful for root analysis in maize adult plants.

GiA Roots and DIRT utilize the thresholding method to segment images into a foreground and background. The algorithms used are highly dependent on the provided image quality. The advantage of GiA Roots when compared to DIRT is that users can manually optimize default thresholding parameters to suit specific needs (Galkovsky *et al.*, 2012). This possibility resulted quite convenient for image quality improvement of the set of images acquired in the field experiment in summer 2012.

As mentioned before, many phenotyping platforms have been developed based on artificial (i.e. non field) environments for root growing, for the most allowing to evaluate early growth stages only. The results presented in this study show that an automatized root phenotyping protocol can be adopted to enable a level of phenotypic investigation suitable for genetic mapping and physiological studies. Additional improvement to the here-described protocol is possible. A representative nodal root sample should be included in the image board in order to detail the fine root structure, because digital cameras cannot resolve large occlusion of the root system, as reported by Bucksch *et al.*, (2014).

2.5 References

Aulen, M., & Shipley, B. (2012). Non-destructive estimation of root mass using electrical capacitance on ten herbaceous species. *Plant and soi*l, 355(1-2), 41-49.

Bucksch, A., Burridge, J., York, L. M., Das, A., Nord, E., Weitz, J. S., & Lynch, J. P. (2014). Image-based high-throughput field phenotyping of crop roots. *Plant physiology*, 166(2), 470-486.

Cobb, J. N., DeClerck, G., Greenberg, A., Clark, R., & McCouch, S. (2013). Next-generation phenotyping: requirements and strategies for enhancing our understanding of genotype–phenotype relationships and its relevance to crop improvement. Theoretical and Applied Genetics, 126(4), 867-887.

Chloupek, O., Forster, B. P., & Thomas, W. T. (2006). The effect of semi-dwarf genes on root system size in field-grown barley. *Theoretical and Applied Genetic*s, 112(5), 779-786.

Clark, R. T., Famoso, A. N., Zhao, K., Shaff, J. E., Craft, E. J., Bustamante, C. D., ... & Kochian, L. V. (2013). High-throughput two-dimensional root system phenotyping platform facilitates genetic analysis of root growth and development. *Plant, cell & environment*, 36(2), 454-466.

Colombi, T., Kirchgessner, N., Le Marié, C. A., York, L. M., Lynch, J. P., & Hund, A. (2015). Next generation shovelomics: set up a tent and REST. *Plant and Soi*l, 1-20.

Dalton, F. N. (1995). In-situ root extent measurements by electrical capacitance methods. *Plant and soil*, 173(1), 157-165.

Fiorani, F., & Schurr, U. (2013). Future scenarios for plant phenotyping. *Annual review of plant biology*, 64, 267-291.

de Dorlodot S, Forster B, Pagès L, Price A, Tuberosa R, Draye X (2007) Root system architecture: opportunities and constraints for genetic improvement of crops. Trends Plant Sci 12: 474–481

Furbank, R. T., & Tester, M. (2011). Phenomics–technologies to relieve the phenotyping bottleneck. *Trends in plant science*, 16(12), 635-644.

Galkovskyi, T., Mileyko, Y., Bucksch, A., Moore, B., Symonova, O., Price, C. A., ... & Weitz, J. S. (2012). GiA Roots: software for the high throughput analysis of plant root system architecture. BMC plant biology, 12(1), 116.Grift, T. E., Novais, J., & Bohn, M. (2011). High-throughput phenotyping technology for maize roots. *Biosystems Engineering*, 110(1), 40-48.

Houle, D., Govindaraju, D. R., & Omholt, S. (2010). Phenomics: the next challenge. *Nature Reviews Genetics*, 11(12), 855-866.

Hund, A., Trachsel, S., & Stamp, P. (2009). Growth of axile and lateral roots of maize: I development of a phenotying platform. *Plant and Soil*, 325(1-2), 335-349.

Iyer-Pascuzzi, A. S., Symonova, O., Mileyko, Y., Hao, Y., Belcher, H., Harer, J., ... & Benfey, P. N. (2010). Imaging and analysis platform for automatic phenotyping and trait ranking of plant root systems. *Plant Physiology*, 152(3), 1148-1157.

Kevern, T. C., & Hallauer, A. R. (1983). Relation of verital root-pull resistance and flowering in maize. *Crop Science*, *23*(2), 357-363.

Landi, P., Sanguineti, M. C., Darrah, L. L., Giuliani, M. M., Salvi, S., Conti, S., & Tuberosa, R. (2002). Detection of QTLs for vertical root pulling resistance in maize and overlap with QTLs for root traits in hydroponics and for grain yield under different water regimes. *Maydica*, 47(3-4).

Landi, P., Sanguineti, M. C., Liu, C., Li, Y., Wang, T. Y., Giuliani, S., ... & Tuberosa, R. (2007). Root-ABA1 QTL affects root lodging, grain yield, and other agronomic traits in maize grown under well-watered and water-stressed conditions. *Journal of experimental botany*, 58(2), 319-326.

Landi, P., Giuliani, S., Salvi, S., Ferri, M., Tuberosa, R., & Sanguineti, M. C. (2010). Characterization of root-yield-1.06, a major constitutive QTL for root and agronomic traits in maize across water regimes. *Journal of Experimental Botany*, 61(13), 3553-3562.

Le Marié, C., Kirchgessner, N., Marschall, D., Walter, A., & Hund, A. (2014). Rhizoslides: paper-based growth system for non-destructive, high throughput phenotyping of root development by means of image analysis. *Plant methods*, 10(1), 13.

Lobet, G., & Draye, X. (2013). Novel scanning procedure enabling the vectorization of entire rhizotron-grown root systems. *Plant methods*, 9(1), 1-11.

Lynch, J. P., & Brown, K. M. (2012). New roots for agriculture: exploiting the root phenome. *Philosophical Transactions of the Royal Society B: Biological Sciences*, 367(1595), 1598-1604.

Messmer, R., Fracheboud, Y., Bänziger, M., Stamp, P., & Ribaut, J. M. (2011). Drought stress and tropical maize: QTLs for leaf greenness, plant senescence, and root capacitance. *Field Crops Research*, 124(1), 93-103.

Nagel, K. A., Putz, A., Gilmer, F., Heinz, K., Fischbach, A., Pfeifer, J., ... & Schurr, U. (2012). GROWSCREEN-Rhizo is a novel phenotyping robot enabling simultaneous measurements of root and shoot growth for plants grown in soil-filled rhizotrons. *Functional Plant Biology*, 39(11), 891-904.

Salvi, S., Tuberosa, R., Chiapparino, E., Maccaferri, M., Veillet, S., van Beuningen, L., ... & Phillips, R. L. (2002). Toward positional cloning of Vgt1, a QTL controlling the transition from the vegetative to the reproductive phase in maize. *Plant Molecular Biology*, 48(5-6), 601-613.

Sanguineti, M. C., Duvick, D. N., Smith, S., Landi, P., & Tuberosa, R. (2006). Effects of long-term selection on seedling traits and ABA accumulation in commercial maize hybrids. *Maydica*, 51(2), 329.

Trachsel, S., Kaeppler, S. M., Brown, K. M., & Lynch, J. P. (2011). Shovelomics: high throughput phenotyping of maize (Zea mays L.) root architecture in the field. *Plant and Soil*, 341(1-2), 75-87.

Utz, H. F. (2001). PLABSTAT: a computer program for statistical analysis of plant breeding experiments. Institute for Plant Breeding, Seed Science and Population Genetics, University of Hohenheim, Stuttgart.

van Beem, J., Smith, M. E., & Zobel, R. W. (1998). Estimating root mass in maize using a portable capacitance meter. *Agronomy Journal*, 90(4), 566-570.

3 Narrowing down *qroot-yield*-1.06 interval

3.1 Introduction

Many economically important traits have a complex genetic control as they influenced by many and often interacting genes; in addition they are often strongly affected by environmental conditions (Collard *et al.,* 2005). Quantitative trait loci (QTLs) are the genomic regions where functionally different alleles or haplotypes segregate and cause significant effect on a quantitative trait. QTL mapping entails the detection and localization of QTLs via an association between the genotype of mapped markers and phenotype. Nowadays, QTL mapping is a standard procedure and many research papers have been published reporting original data in the main crop species (Salvi and Tuberosa, 2015).

Despite the large quantity of QTL studies, only a handful has reported the cloning of QTLs (Salvi and Tuberosa 2005), the majority via positional cloning. Positional cloning basically consists of increasing the QTL mapping resolution with the aim to assign the QTL to the smallest possible genetic interval (QTL fine genetic mapping). This is usually obtained by means of larger population sizes and a greater number of markers (Collard *et al.,* 205); eventually the genetic region is linked to a corresponding interval on the DNA sequence (QTL physical mapping) (Salvi and Tuberosa 2005). While positional cloning remains the main way to identify a gene that underlies a quantitative trait, many highly reliable gene-phenotype association have been recently accumulating based on genome wide association studies (Tian *et al.,* 2011; Olukolu *et al.,* 2014; Wallace *et al.,* 2014)

Positional cloning in maize has been considered as not easily achievable because of its large genome and redundancy (Tuberosa and Salvi 2009). However, with the recent release of the maize genome sequence (Schnable *et al.,* 2009) and the availability of high-density polymorphic markers (Ganal *et al.,* 2011) positional cloning is rapidly becoming routine (Gallavotti and Whipple 2015). So far, QTLs cloned in maize are *Tb1* (Doebley *et al.,* 1997) for plant architecture, *Tga1* for glume architecture (Wang *et al.,* 2005), *Vgt1* for flowering time (Salvi *et al.,* 2007), and more recently, *qPH3.1* for plant height (Teng *et al.,* 2013) and *qLA4-1* for leaf angle (Zhang *et al.,* 2014).

In the case of root traits in maize, two major QTLs *Root-ABA1* (Tuberosa *et al.,* 1998) and *root-yield-1.06* (Landi *et al.,* 2002, Tuberosa *et al.,* 2002) have been described affecting root architecture

and a number of agronomic traits. *Root-yield-1.06* was mapped on bin 1.06 in the background of the cross of the contrasting lines for the root morphology, Lo964 and Lo1016 (Sanguineti *et al.*, 1998). Lo964 is characterized by a root system dominated by the primary root; Lo1016 develops a root system with uniform root types. The QTL was shown influencing root traits of seedlings grown in hydroponics (Tuberosa *et al.,* 2002) and of adult plants grown in the field (Landi *et al.,* 2002), and also was reported influencing grain yield under both well-watered and water-stressed conditions.
For both QTLs, near isogenic lines have been already produced and evaluated per se and in testcross combinations (Landi *et al.,* 2005, Landi *et al.,* 2010). Isogenization of QTLs is fundamental for fine mapping purposes because target QTL becomes the major genetic source of variation, in the absence of other segregating QTLs (Salvi and Tuberosa 2005). Development of NILs and QTL fine mapping have been successfully applied to positional cloning major QTLs in rice as PHOSPHORU S UPTAKE 1 (PUP1) and DEEPER ROOTING 1 (DRO1) (Uga *et al.,* 2013).

The main goal of this study was to fine map *qroot-yield-1.06* to a cM-size interval using two different approaches:

1) QTL analysis of an F2 population in the greenhouse;

2) Searching for recombinants in the *qroot-yield-1.06* interval by means of QTL mapping and marker-assisted selection in search of local recombination events, through successive generations.

3.2 Materials and methods

3.2.1 Plant material

The starting materials of this project were the Near Isogenic Lines (NILs) previously developed and characterized (Landi *et al.*, 2010). Briefly, pairs of NILs were developed from F3:4 families of the cross Lo964xLo1016 by several cycles of marker-assisted selection using SSR markers (umc1601 and umc1709, which are 29 cM apart on chr. 1 based on the reference maize map 'Genetic', (http://www.maizegdb.org) flanking *qroot-yield*-1.06. At F6:7 generation, homozygous plants for the parental allele combination were selected and self-pollinated. Two pairs of NILs (as F7:8) were obtained. NILs are homozygous for either the plus allele (+), which is the one increasing root values and originally provided by Lo1016 (Landi *et al.*, 2002, Tuberosa *et al.,* 2002); or the minus allele (-)

allele provided by Lo964. In this work, NILs pairs are named NIL120 (--)/NIL129 (++) and NIL157 (--)/NIL158 (++), family #1 and family #4, respectively, according to Landi *et al.,* (2010). Thorough NILs genotyping was obtained by Illumina MaizeSNP50 BeadChip, that confirmed the presence of alternative haplotypes at chromosome bin 1.06, while the rest of their genomes resulted identical and homozygous.

Field experiments were carried out at the Unibo experimental field in Cadriano, Italy, and the other, on November using a private service of winter nursery (WN) in Buin, Chile.

3.2.2 Greenhouse experiment

F2 seeds derived from the cross NIL157xNIL158 were surface-sterilized and pre-germinated in Petri dishes for 48 h in the dark. Homogeneous seedlings were transferred into pots (10x10x14 cm) containing peat and sand (1:1) and were grown under controlled conditions in the greenhouse (day: 16 h, 26–28 °C, with supplemental light 500 μE m^{-2} s^{-1} photosynthetic photon flux density; night: 16 °C). At the third-leaf stage, leaf tissue was collected for a total of 263 F2 plants and the parental NILs, and sent to KWS SAAT AG (Einbeck, Germany) for DNA extraction and molecular genotyping with an in-house12K SNP-chip, which is a subset of the MaizeSNP50 Beadchip (Illumina Inc., San Diego, CA).

In order to choose the best stage for root phenotyping of the F2 population, a parallel experiment including parental NILs (NIL157 and NIL158) and their F1 was carried out. From 21 to 42 days after planting (DAP) we periodically (every week) uprooted 6 plants for each of the three genotypes, which were phenotyped for the following traits: number of seminal roots (SR), total number of crown roots (TNCr), angle of crown roots, shoot diameter and dry weight (DW). Phenotypic data underwent analysis of variance to check when the phenotypic expression of the QTL was significantly different among contrasting genotypes. The F2 the population underwent root phenotyping at 42 DAP, approximately corresponding to 7-leaf stage. Plants were phenotyped for SR, TNCr angle of crown roots and DW. Additionally, a visual score (VS) for root branching according to a scale from 1- less branching to 5- higher branching was given, and the root system of each plant was scanned using a P3600 A3PRO Scanner (Mustek). Digital images were analyzed using ImageJ 1.46r software (Rasband) to quantify the relation between number of pixels corresponding to the roots and the total number of pixels of the image acquired. QTL analysis was done using MapQTL®6 software (van Ooijen *et al.,* 2009).

3.2.3 DNA-marker analysis

Throughout this study, molecular genotyping was generally carried out starting from fresh leaf-tissue collected from field plots. A piece of leaf of c. 100 mg was collected. DNA extraction was done using the CTAB protocol adapted to 96-well plates. Briefly, aluminum grinding powder (TED Pella, INC., CA, USA) was added to the samples, which were ground using a TissueLyser (QIAGEN). One volume of CTAB buffer (Doyle and Doyle, 1987) was added and samples were incubated for 1h at 65 °C. Then, 1 vol. of chloroform was added and samples were mixed by gentle inversion. Supernatant was recovered after centrifugation at maximum speed and mixed with 0.5 vol of isopropanol. DNA pellet was recovered by centrifugation, washed with ethanol 70% and diluted in distilled water. Finally, DNA quality was controlled in a 1% agarose gel.

Initially (WN 2012-13 and summer 2013) marker-assisted selection (MAS) for the identification of plants carrying recombinant chromosomes at the target QTL region was carried out using reported SSR markers (umc1601 and umc1709) flanking the *qroot-yield*-1.06 interval (Landi *et al.*, 2010). High resolution Melting (HRM) protocol was standardized to test both markers, using the MeltDoctor^{TM} HRM Master Mix (Applied Biosystems, CA, USA).

Subsequently, a set of SNP markers from the 12K SNP-chip were selected according to the results of the QTL analysis of the greenhouse experiment. The new set included 14 markers covering a region of 17 cM and was used for MAS of the plant materials produced in the WN 2013-2014. In summer 2014, five additional SNP markers inside the same interval of 17 cM were included for a total of 19 markers for the MAS (Table 4).

Table 4. List of SNPs selected from the 12K SNP-chip and used for the marker-assisted selection in the winter nursery 2013-14. In bold, additional markers used in summer 2014.

Marker name	MapDisto[1] (cM)	B73 RefGen_v2[2] (bp)
PZE-101129304	3,8	164954939
SYN10174	5,4	170849266
PZE-101133216	6,2	172284467
PZE-101133651	6,7	172918316
PZE-101134093	7,1	173313597
PZE-101134142	7,3	173423575
PZE-101135508	8,6	175292737
SYN2406	**9,0**	**176095459**
PZE-101136791	**9,4**	**176941113**
SYN9635	9,6	177052727

Marker name	MapDisto[1] (cM)	B73 RefGen_v2[2] (bp)
PZE-101138198	**10,5**	**179341109**
SYN13130	14,7	180836644
PZE-101140981	**15,7**	**182103926**
SYN8998	17,4	183451693
0192831_0351	17,7	183802036
SYN1741	18,4	183848635
PZE-101143985	**18,8**	**187189842**
PUT-163a-13178383-177	20,2	188083114
SYN37120	21,4	189088258

[1] position on the genetic map constructed for the *qroot-yield-1.06* interval based on the analysis of the F2 population with a 12K SNP-chip (Figure 14)
[2] position on the maize reference physical map B73 RefGen_v2 (http://www.maizegdb.org).

3.2.4 F4 families characterization

In summer 2014, 46 homozygous recombinants families (F4 families) were characterized in a field-replicated experiment at Cadriano. Genotypes were randomly assigned to plots using a randomized complete block design with two replications. One replication was hand-sown at the end of May, and the second one, five days later. Row width was 0.90 m and distance between plants was 25 cm. One plot consisted of one 2.75 m row containing 12 plants.

Genotyping was carried out with a set of 19 SNPs covering an interval of 17 cM (Table 4, Figure 14). Root phenotyping was obtained, when possible, for three homogenous plants per plot, using the improved protocol mentioned in chapter 1, in which shovelomics is combined with root imaging analysis. Additionally, plant height (PH) was measured in the plants selected.
Marker-trait association evaluation was done using the non-parametric test Kruskal-Wallis using MapQTL®6 software (van Ooijen 2004).

3.3 Results

3.3.1 Greenhouse experiment

The aim of this experiment was to speed up the fine mapping of the *qroot-yield*-1.06. Preliminary results (data not shown) showed significant differences in root architecture between the minus NIL and its corresponding plus NIL at 40 days after planting (DAP). However, based on the parallel experiment of root phenotyping on NILs parent lines and corresponding F1, the phenotypic expression of the *qroot-yield-1.06* was not detectable at an early stage of development for any of the

four evaluated traits, throughout the four sampling dates (21 (data not shown), 28, 35 and 42 DAP). Mean values for DW, angle, SR and TNCr, and analysis of variance are shown in Table 5.

Table 5. Analysis of variance of the root crown traits measured in a F_2 population (NIL157xNIL158) grown in the greenhouse. Significance level (p) and mean values are displayed for the following traits: Dry weight in g (DW), angle respect to the soil level, seminal roots number (SR) and total number of crown roots, at three sampling times (28, 35 and 42 days after planting (DAP)).

	28DAP				35DAP				42DAP			
Genotype	**DW**	**Angle**	**SR**	**TN Cr**	**DW**	**Angle**	**SR**	**TN Cr**	**DW**	**Angle**	**SR[1]**	**TN Cr**
NIL120	426,2	50,6	2,50	9,7	606,5	50,8	1,33	11,7	741,7	47,8		12,6
NIL129	454,2	57,5	2,67	10,7	695,0	57,8	3,00	11,2	875,0	51,4		12,0
NIL157	364,5	48,6	3,25	10,3	737,0	60,0	3,00	11,7	935,0	52,8		13,0
NIL158	373,0	55,8	2,83	10,2	691,2	51,7	3,17	10,8	925,0	54,7		12,7
F_1 157x158	506,3	59,2	2,75	9,5	370,2	52,8	2,25	11,5	482,5	57,5		12,5
Significance (0.05)	NS	NS	NS	NS	NS	NS	NS	NS	NS	NS	-	NS

[1] Data not taken at this time

Two hundred and sixty-three F_2 plants of the cross 157x158 were genotyped with a 12K SNP-chip. A total of 88 polymorphic markers were detected in the *qroot-yield*-1.06 interval. A new genetic map for the QTL interval was constructed using MapDisto (Lorieux 2012) (Figure 14).

QTL analysis was carried out using two approaches. In the first approach, contrasting phenotypes were visualized in the F_2 population between plants characterized as homozygous for the Lo964 and Lo1016 original contrasting alleles (Figure 10), according to the SNP genotyping. Based on this analysis, *qroot-yield-1.06* did not seem to influence the seedling-based traits measured (DW, Angle, Root visual score and Number of pixels. Figure 10), at P <0.05.

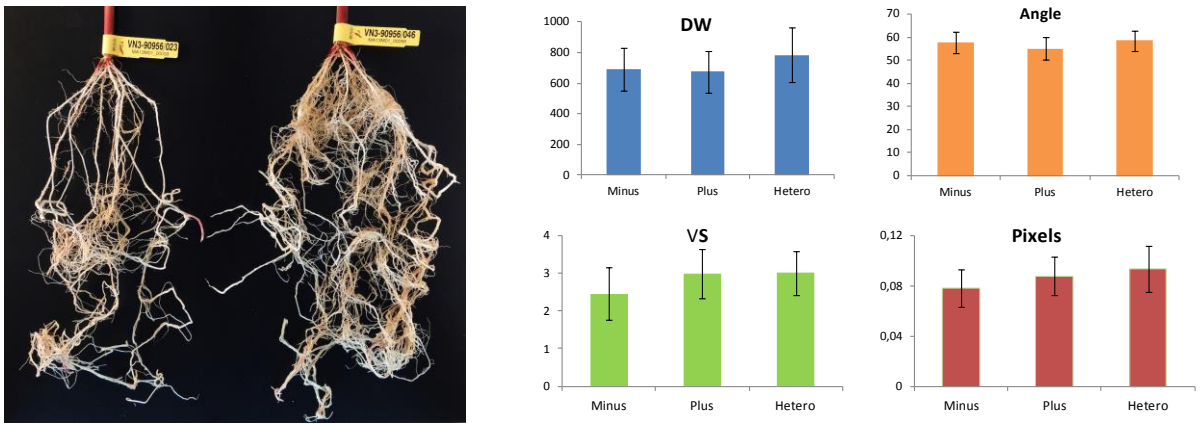

Figure 10. Phenotypic characterization of the F_2 population (NIL157xNIL158) in the greenhouse. The image shows a pair of contrasting phenotypes coming from homozygous plants for the minus allele (left) and the plus allele (right). Graphs in the right are showing the mean values of four different traits evaluated, for minus and plus homozygous, and heterozygous plants. DW- dry weight, VS- visual scoring from 1 to 5, evaluating the general root branch density.

In a second approach, a formal QTL analysis based on interval mapping was carried out for all traits. An acceptable LOD profile was obtained only for Visual score. A new narrower interval of the QTL was detected covering 14 cM between SNP markers PZE-10113651 to SYN37120 (Figure 11). A set of markers covering the new interval was selected for MAS in the following experiments in the field.

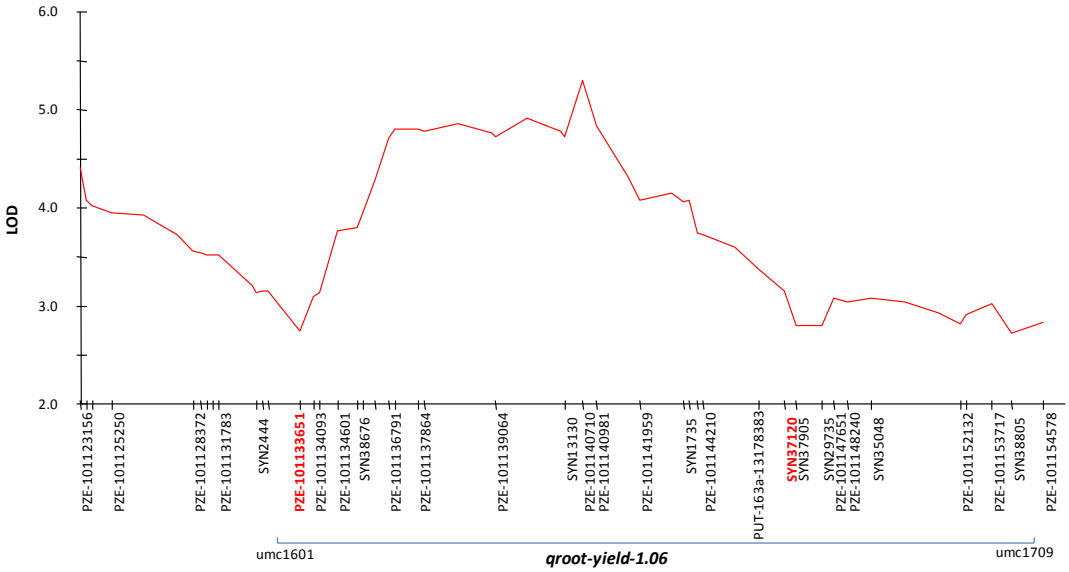

Figure 11. LOD profile obtained based on QTL interval mapping for root Visual score collected in the greenhouse experiment. In red, SNP markers flanking the new interval.

3.3.2 Field experiment

Figure 12 summarizes the field activities from 2012 to 2014 and future activities for 2015. In summer 2012, F_2 populations were developed by self-pollination of F_1 plants of the cross NIL120xNIL129. One thousand F_2 seeds were sent to the WN service in Chile. From there, leaf samples were collected and sent back to UNIBO for MAS using the SSR flanking markers of the *qroot-yield-1.06* (umc1601 and umc1709), aimed at the identification of the plants carrying recombinant chromosomes at the target QTL. A total of 539 leaf samples were analyzed and 214 recombinants plants, heterozygous at one flanking marker and homozygous at the other flanking marker, were identified. This information was transferred back to Chile were corresponding plants were self-pollinated.

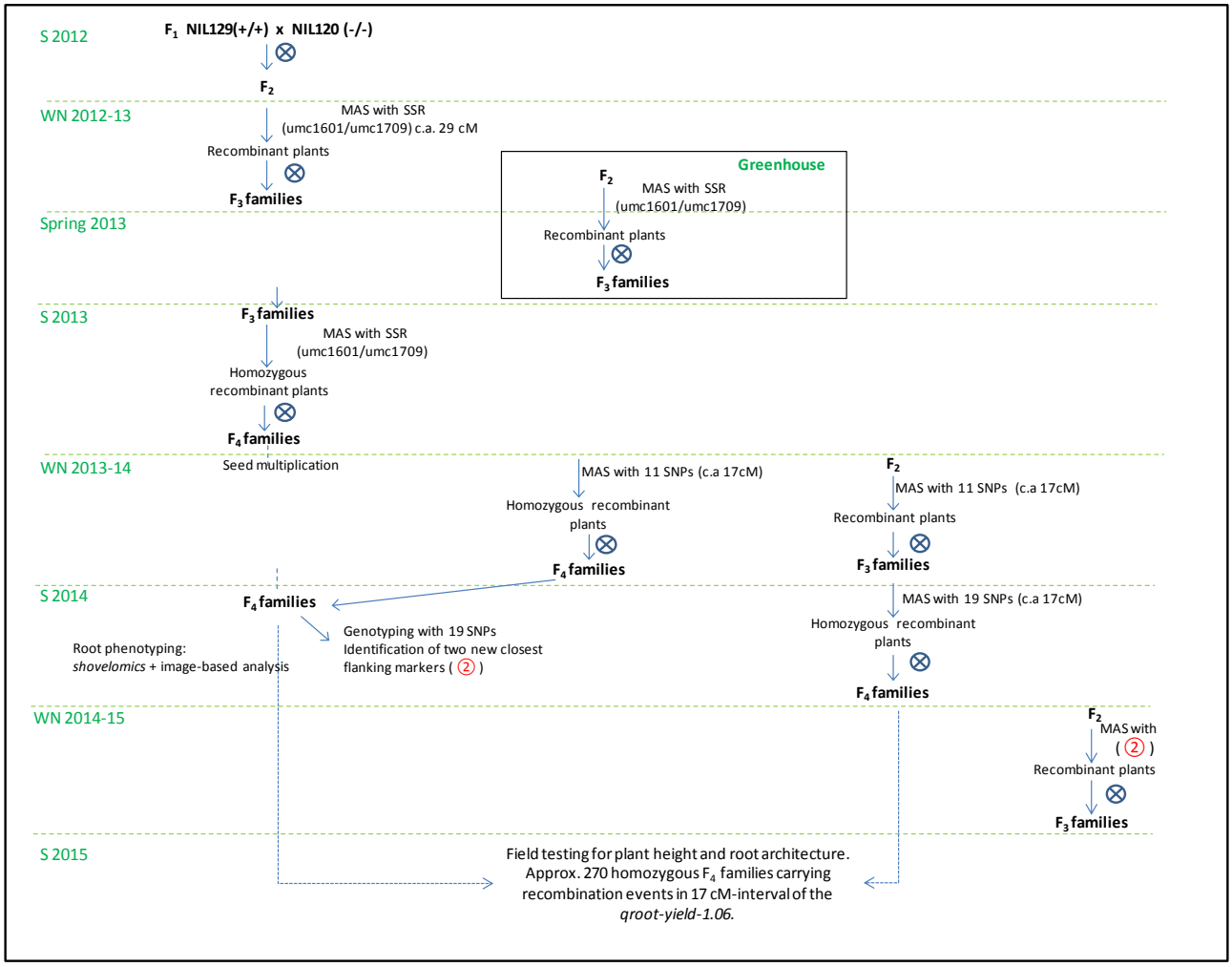

Figure 12. Summary of the field activities from 2012 to 2014 realized to narrow-down the *qroot-yield*-1.06 interval. S- summer, WN- winter nursery, MAS- marker assisted selection.

As a result of this effort, one hundred and fifty-three F_3 families were planted in 2013 in the summer nursery at UNIBO. Fifteen plants per family were genotyped using the SSR flanking markers. A total of 43 plants corresponding to 29 F_3 families, carrying recombinant homozygous events were root phenotyped by shovelomics and characterized with additional SSR markers along the QTL interval (Figure 13). New four polymorphic SSRs were evaluated: umc1988, umc2234, bnlg1057 and bnlg1615, at 126.2, 132.2, 137.1 and 139.4 cM, according to the maize 'Genetic' map and at 11, 15.6, 19.7 and 21.7 cM, according to the new genetic map constructed for the region (Figure 14).

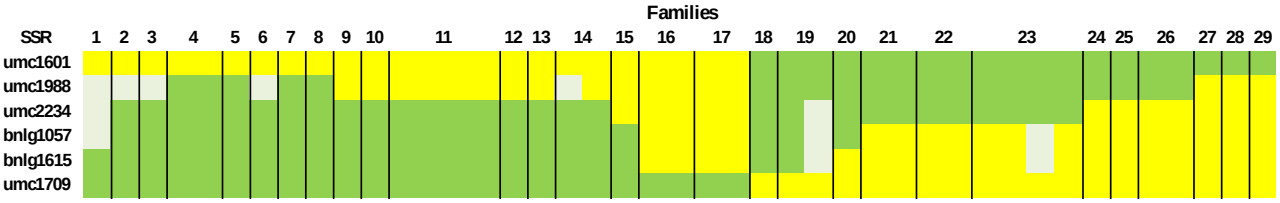

Figure 13. Genotypic profile of 29 homozygous recombinant families using SSR markers along the *qroot-yield-1.06* interval. In yellow, minus allele (Lo964); in green, plus allele (Lo1016); and in gray, heterozygous.

Marker/trait association analysis by Kruskal-Wallis for visual scoring for the crown root density, obtained from shovelomics revealed that the segregating *qroot-yield-1.06* was tightly linked to the marker umc1988 ($P < 0.05$) and marker umc2234 ($P < 0.1$. This association was confirmed for the following traits based on GiA Roots image analysis: Network length (Nlen), maximum number of roots (MaxR) and network perimeter (Perim) (Table 6).

Table 6. Kruskal-Wallis analysis for the visual score of the root crown density (VS) and GiA Roots traits: network length (Nlen), perimeter (Perim) and maximum number of roots (MaxR), in the F3 families. Mean values for each genotypic class are reported: a- minus (Lo964), b- plus (lo1016), h- heterozygous. Sig. – level of significance ***= 0.01, **=0.05 and *= 0.1.

		VS				Nlen				Perim				MaxR			
Locus	**Pos. (cM)**	**Sig.**	**a**	**h**	**b**	**Sig.**	**a**	**h**	**b**	**Sig.**	**a**	**h**	**b**	**Sig.**	**a**	**h**	**b**
umc1601	118,4	**	2.8	3.6	-	-	1001		1129	-	1800		2013	**	38		43
umc1988	126,2	**	2.7	3.6	2.8	***	897	1262	1139	***	1619	2267	2027	***	36	44	43
umc2234	132,2	*	2.7	3.4	2.5	-	1071	936	1061	-	1939	1710	1888	-	39	36	41
bnlg1057	137,1	-	3.2	3.1	3.0	-	1118	917	1028	-	2011	1662	1830	-	42	39	39
bnlg1615	139,4	-	3.3	3.0	3.5	-	1110	804	1036	-	1992	1448	1850	-	42	41	39
umc1709	147	**	3.6	2.8	-	-	1129		1001	-	2013		1800	**	43		38

For 35 families, in which the recombinant events were not found in homozygosis, recombinants plants were self-pollinated during the 2013 summer nursery and seed was sent to the WN 2013-14 in Chile for a second round of MAS. By doing this, 14 additional F4 families were recovered and evaluated in summer 2014 (see details below).

At the same time, effort was given to identify additional recombination events at the target QTL. 3,000 F2 seeds from the cross NIL120xNIL129 were sent to the WN 2013-14. On these plants, MAS was conducted with a set of 14 SNPs markers covering c. 17 cM (Figure 14) and three hundred and five recombinants plants were selected and self-pollinated. F_3 families produced were

planted in the 2014 summer nursery at UNIBO and were genotyped with a set of 19 SNPs, distributed along the same region of 17 cM. Two hundred and twenty-five homozygous recombinants were identified and self-pollinated. These additional F4 families will be evaluated in summer 2015 in field trials for root phenotyping to contribute to fine mapping *qroot-yield*-1.06

Supplemental material was obtained from a small F_2 population of the cross NIL120xNIL129 evaluated in the greenhouse (spring 2013). After MAS in the next generations, seven F4 families were selected and included in the field trial conducted in the summer 2014.

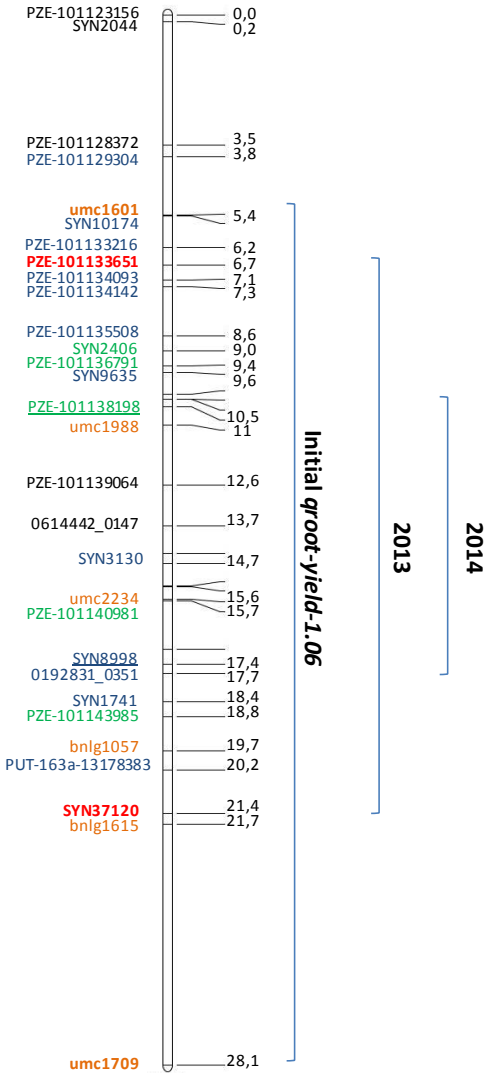

Figure 14. Genetic map for the *qroot-yield-1.06* interval and fine-mapping progress. The map was constructed based on 88 SNP polymorphic markers detected on the analysis of an F2 population (NIL157xNIL158) with a 12K SNP-chip. In orange SSR markers including original flanking markers umc1601 and umc1709; in red, SNP markers flanking the new interval narrowed-down with the results of 2013; In blue, set of SNPs markers used in MAS in WN 2013-14; and in green, additional SNP markers added to the previous set, used in MAS in summer 2014. Underlined SNP markers are the flanking markers for the new interval after 2014 results.

3.3.3 Analysis of F4 families during 2014 summer nursery

Forty-six F4 families were genotyped with 19 SNPs markers covering an interval of 17 cM of the *qroot-yield-1.06* (Table 4, Figure 14). For 14 families, the recombinant chromosome was not fixed (i.e. was still heterozygous) and therefore, were excluded from this preliminary analysis. Conversely, 32 families showed homozygous recombinant chromosomes and were included in this analysis.

First observations of the F4 families in the field, at 50 DAP, showed appreciable differences in PH between families. A similar difference for PH was observed between minus and plus NILs in the same year, in a small experiment grown nearby the F4 families plots. NILs carrying the (+) allele (i.e. Lo1016) were shown to be taller than NILs with the (-) allele (i.e. Lo964) at *qroot-yield-1.06*, with this difference more clear in the earlier growth stages (Figure 15). This result confirmed a previous observation of a potential effect of this chromosome region on PH (Landi *et al.*, 2010).

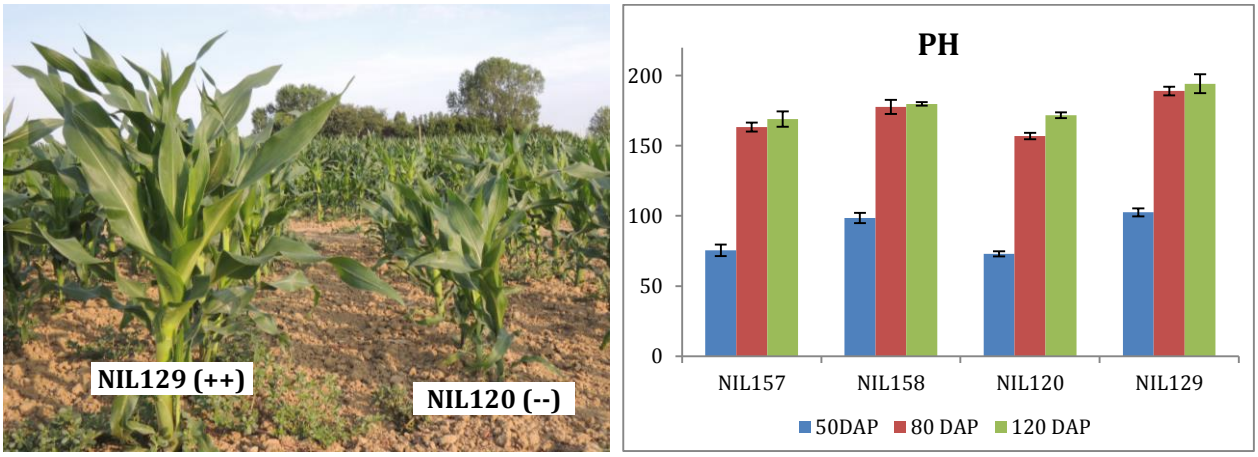

Figure 15. Plant height differences for the *qroot-yield-1.06* contrasting NILs. On the left, the pair of NILs(120 and 129) photographed at 50 days after planting (DAP) in summer 2014. On the right, mean PH values for both pairs of NILs evaluated at 50, 80 and 120 DAP.

At the flowering stage, plant root apparatus were digged out to undergo shovelomics, including image-based trait analysis with three different software: GiA Roots (Galkovskyi *et al.*, 2012), DIRT (Bucksch *et al.*, 2014) and REST (Colombi *et al.*, 2015). Traits were selected for successive analysis according to their values of RPV (Relative Phenotypic Variation), as described in Chapter 2. The greater values were obtained for: D20 to D60 in DIRT, MaxR, Nlen and Perim for GiA Roots, and Area and Total projected structure length (TPSL), for REST.

Kruskal-Wallis analysis was done for PH and DW and the selected root image-based traits (Table 7). Highly significant ($P < 0.0005$) values of the test statistic (K*) were detected for most of the traits, mainly in the interval from PZE-101138198 and 0192831-0351. For PH, the same markers resulted associated but with a lower significance ($P < 0.05$).

Table 7. Kruskal-Wallis analysis for the F4 families. It is reported the Kruskal-Wallis test statistic K*and the level of significance for the traits: Perimeter (Perim), Maximum number of roots (MaxR), network length (Nlen), D20, Area, total projected structure length (TPSL), dry weight (DW) and plant height (PH).

			GiA Roots						DIRT		REST				shovelomics			
			Perim		MaxR		Nlen		D20		Area		TPSL		DW		PH	
#	Position[1]	Locus	K*	Sig.[2]	K*	Sig.	K*	Sig.	K*	Sig.	K*	Sig.	K*	Sig.	K*	Sig.	K*	Sig.
1	3,8	PZE-101129304	1,2	-	1,5	-	1,4	-	0,1	-	2,4	-	1,8	-	1,3	-	0,3	-
2	5,4	SYN10174	1,6	-	2,4	-	1,8	-	0,3	-	3,0	-	2,4	-	1,9	-	0,1	-
3	6,2	PZE-101133216	1,7	-	2,5	-	2,0	-	0,6	-	3,1	-	2,4	-	1,8	-	0,2	-
4	6,7	PZE-101133651	2,4	-	3,7	-	2,5	-	0,5	-	4,3	-	3,6	-	3,8	-	0,7	-
5	7,1	PZE-101134093	2,4	-	3,7	-	2,5	-	0,5	-	4,3	-	3,6	-	3,8	-	0,7	-
6	7,3	PZE-101134142	2,4	-	3,7	-	2,5	-	0,5	-	4,3	-	3,6	-	3,8	-	0,7	-
7	8,6	PZE-101135508	6,9	-	8,4	-	7,2	-	2,9	-	9,3	-	8,5	-	8,5	-	1,7	-
8	9,0	SYN2406	8,1	-	9,6	-	8,3	-	2,7	-	10,0	-	9,5	-	11,0	*	2,4	-
9	9,4	PZE-101136791	10,5	-	10,9	*	10,5	-	4,6	-	11,1	*	10,5	-	11,1	*	2,3	-
10	9,6	SYN9635	10,5	-	10,9	*	10,5	-	4,6	-	11,1	*	10,5	-	11,1	*	2,3	-
11	10,2	PZE-101138198	12,1	**	11,7	*	12,1	**	6,8	-	12,7	**	12,4	**	12,4	**	2,6	-
12	14,8	SYN13130	18,2	**	18,9	**	18,2	**	11,8	*	18,2	**	18,2	**	16,9	**	4,1	+
13	15,7	PZE-101140981	22,5	**	22,1	**	22,5	**	15,0	**	21,8	**	22,1	**	21,8	**	6,5	+
14	17,4	SYN8998	17,4	**	18,0	**	17,0	**	10,3	-	13,7	**	17,0	**	18,4	**	4,5	+
15	17,7	0192831-0351	17,4	**	18,0	**	17,0	**	10,3	-	13,7	**	17,0	**	17,7	**	4,5	+
16	18,4	SYN1741	10,5	-	10,5	-	10,5	-	6,8	-	8,6	-	10,0	-	12,1	*	1,7	-
17	18,8	PZE-101143985	7,2	-	7,2	-	7,2	-	6,6	-	6,6	-	7,7	-	9,8	-	0,5	-
18	20,7	PUT-163a-13178383	2,4	-	2,6	-	2,4	-	4,0	-	2,2	-	2,7	-	4,2	-	0,0	-
19	21,5	SYN37120	1,4	-	2,1	-	1,4	-	6,4	-	0,9	-	1,1	-	2,7	-	0,7	-

[1] Position in cM reported according to map on Figure 14.
[2] Significance levels: ** 0,0005 * 0,001 + 0,05

Figure 16 shows the genotypic profile of the F4 families and the mean values for some of the traits evaluated. Data analysis indicated the markers SYN13130 and PZE-101140981 (at 14.7 and 15.7 cM respectively, within the 28, 1 cM interval illustrated in Figure 10, as linked with *qroot-yield-1.06*. This genetic interval corresponds to 180,8 - 182,1 Mb physical interval on the maize B73 genome sequence (B73 RefGen _v2) (Andorf *et al.*, 2010). Traits confirming these genetic and physical intervals were shovelomics-based DW, root image-based traits such as Perim, MaxR and Nlen for GiA Roots; Area and TPSL for REST; and D20 for DIRT (Table 7, Figure 16). In contrast to previous observations (Landi *et al.*, 2010), the target *qroot-yield-1.06* showed only a mild effect on PH in this analysis.

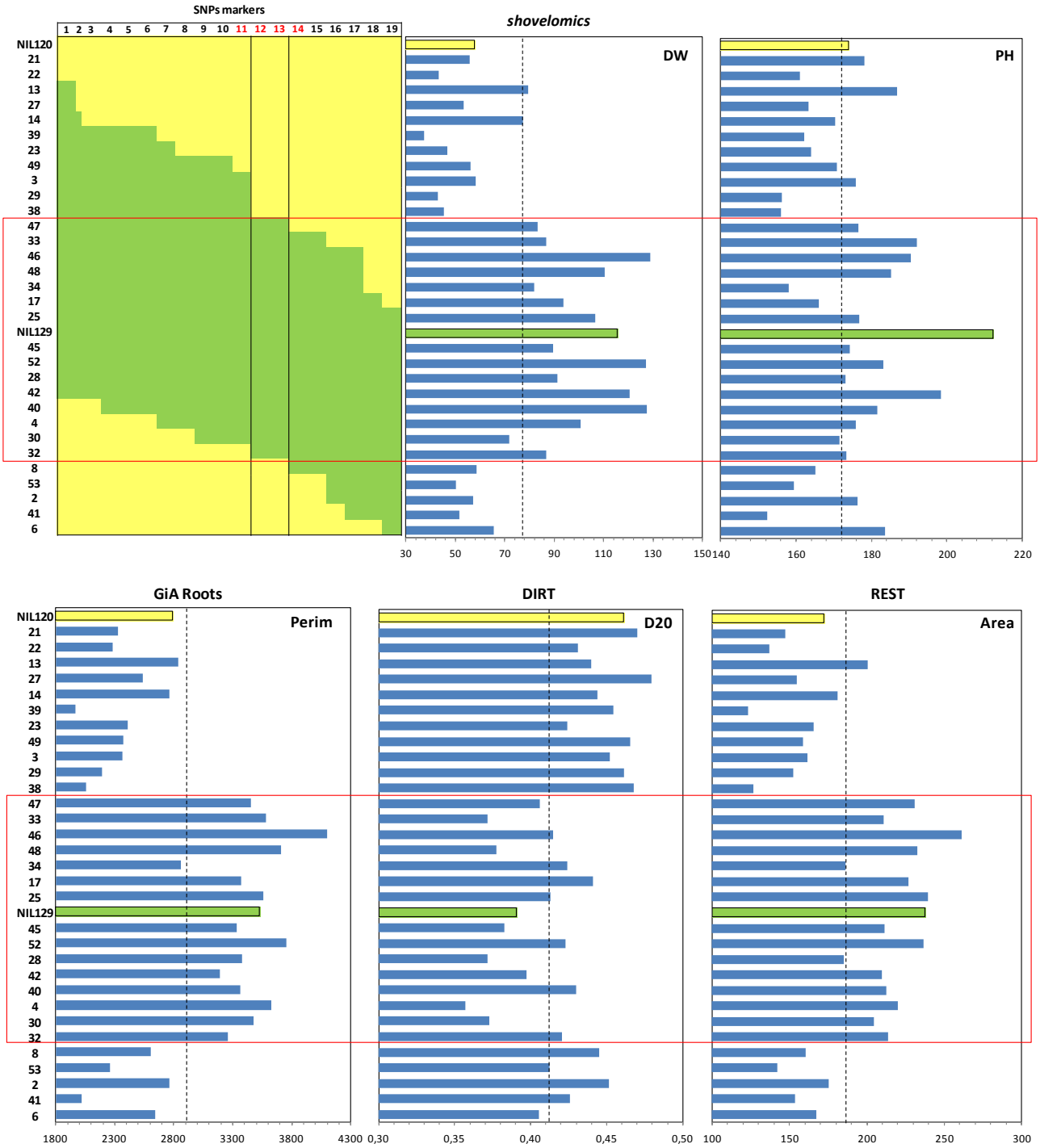

Figure 16. Genotypic and phenotypic characterization of the F4 families and parental NILs, NIL120 and NIL129. The graph at the upper left part shows the results of the genotyping with a set of 19 SNPs (see table 5 for loci names). In yellow, the minus allele and in green, the plus allele. Histograms to the right and in the bottom show mean values of F4 families, NIL120 (yellow bar) and NIL129 (green bar), for the traits: dry weight (DW), plant height (PH), perimeter (Perim), D20, and Area. Dashed lines show the general mean value. Red rectangle encloses families carrying the *qroot-yield-1.06*.

For future MAS, a new marker interval from PZE-101138198 (10.5 cM) to 0192831-0351 (17.4 cM), corresponding to physical positions (B73 RefGen_v2) from 179.3 Mb to 183.4 Mb (4.1 Mb) was selected. Accordingly with results presented in Table 7 and Figure 16, this interval should include *qroot-yield-1.06* even if its position will be close to the borders of the target interval. Inside this interval, there are also included SSRs markers umc1988 (11 cM) and umc2234 (15.6) (Figure 14), which were associated with the expression of the *qroot-yield*-1.06 (Table 6).

In summer 2015, 249 homozygous recombinants lines between markers PZE-101129304 and markers SYN37120 will be evaluated (See supplemental material for genotypes of lines). Among these lines, the ones carrying recombination events within PZE-101138198 and 0192831-0351 (the interval most likely carrying *qroot-yield-1.06*) are currently 83, providing an expected average genetic resolution of one recombination every 49 Kb. In addition, 108 new recombinants selected in the WN 2014-15 using flanking markers of the 4.1 Mb *qroot-yield-1.06* interval will be evaluated for searching homozygous recombinants.

3.4 Discussion and conclusions

QTL analysis commonly produces relatively large confidence intervals spanning 10-30 cM, which may include several hundred genes. Therefore, strong increase in mapping resolution after a first QTL discovery phase is required for QTL positional cloning purposes (Salvi and Tuberosa 2005). This step of fine mapping requires the production of enough recombination events, resolved with high-density molecular markers within the target QTL region, coupled with accurate phenotypic evaluation (Yang *et al.*, 2012).

The phenotypic effect of the major QTL *root-yield-1.06,* on root architecture and other agronomical important traits, was initially described by Tuberosa *et al.,*. (2002). In that study, several easily measurable traits at an early growth stage of plants grown were collected in hydroponics. This effect was also confirmed in adult plants grown in the field as vertical root pulling resistance (Landi *et al.,* 2002). According to these results and in view of the large quantity of plants required for fine mapping purposes, phenotyping in controlled conditions at an early stage of development seemed to be a good option. However, based on the results obtained in the greenhouse experiment, segregation at *qroot-yield-1.06* could not be associated with any seedling-based traits. The use of small pots (10x10x14cm) could mislead relative differences between NILs. Pot size could facilitate the handle

of a bigger number of plants but many biological constraints appear due to scarce resource availability that could be reflected in reducing root growth (Poorter *et al.,* 2012)

At the same time, field grown plants are controlled by very large interactions between root and soil, extremely variable among experiments, that imply that the observed effect of a given QTL in one experiment may not be repeatable in a different one (Mai *et al.,* 2014). This is a general problem of QTL studies, and of breeding practices trying to capitalize on QTL information. As already recognized, a quantitative trait phenotype in one individual is typically the result of non-linear responses to a large number of factors, of genetic and environmental origin (Salvi and Tuberosa 2015). In the present study, shovelomics (Trachsel *et al.,* 2011) combined with image-based analysis with specialized software (Bucksch *et al.,* 2014, Galkovskyi *et al.,* 2012, Colombi *et al.,* 2015), as explained in chapter 2, and marker saturation, allowed to identify recombinants lines at the target QTL region and a new putative region of 1 cM was correlated with the *qroot-yield-1.06* phenotypic expression.

Besides differences in root architecture, Landi *et al.,* (2010) reported that NILs (+/+) and (-/-) for *qroot-yield-1.06* were significantly different for several traits including PH, with higher values for NILs (+/+) that suggested that additive effect always was provided by Lo1016 (Landi *et al.,* 2010). The consistent association reported among additive effects of *qroot-yield-1.06* for root, PH, and agronomic traits suggested that they are concurrently controlled by the same gene/s (Landi *et al.,* 2010). In the present study, PH was measured in 31 homozygous recombinant families (F4 families) and only a mild phenotypic effect was associated to *qroot-yield-1.06.* Even if the possibility that association among additive effects were due to linkage was discarded with previous results (Landi *et al.,* 2010), only the fine mapping and cloning of the *qroot-yield-1.06* will resolve if QTL cluster results from a pleiotropic gene or from multiple linked genes.

In this study, progress toward the positional cloning of *qroot-yield-1.06* was reported. The mapping resolution obtained so far is still too limited for identifying the gene or even to shortlist a small number of candidate genes. However, the reduction of the *qroot-yield-1.06* interval to 4.1 Mb, and the availability of 83 NILs carrying recombinants events in this interval, provide a potential map resolution around the QTL of ca. 49 kb, which corresponds to the average gene density per kilobase in maize (i.e. one gene every 43.5 kb) (Haberer *et al.,* 2005). Such resolution seems sufficient to identify at least one marker tightly linked to and physically placed on the same BAC/YAC clone. For instance, potential map resolution of ca. 120 kb reported for the fine mapping of *Vgt1* (Salvi *et*

al., 2002) allow the successful positional cloning of *Vgt1* (Salvi *et al.,* 2007).

In next chapters we will discuss how tools as QTL meta-analysis and transcriptomics could help to identify possible candidate genes in the narrowed interval obtained after fine-mapping approach.

3.5 References

Andorf, C. M., Lawrence, C. J., Harper, L. C., Schaeffer, M. L., Campbell, D. A., & Sen, T. Z. (2010). The Locus Lookup tool at MaizeGDB: identification of genomic regions in maize by integrating sequence information with physical and genetic maps. *Bioinformatic*s, 26(3), 434-436.

Bortiri, E., Jackson, D., & Hake, S. (2006). Advances in maize genomics: the emergence of positional cloning. *Current opinion in plant biology*, 9(2), 164-171.

Bucksch, A., Burridge, J., York, L. M., Das, A., Nord, E., Weitz, J. S., & Lynch, J. P. (2014). Image-based high-throughput field phenotyping of crop roots. *Plant physiology*, 166(2), 470-486.

Civardi, L., Xia, Y., Edwards, K. J., Schnable, P. S., & Nikolau, B. J. (1994). The relationship between genetic and physical distances in the cloned a1-sh2 interval of the Zea mays L. genome. *Proceedings of the National Academy of Sciences*, *91*(17), 8268-8272.

Collard, B. C. Y., Jahufer, M. Z. Z., Brouwer, J. B., & Pang, E. C. K. (2005). An introduction to markers, quantitative trait loci (QTL) mapping and marker-assisted selection for crop improvement: the basic concepts. *Euphytica*, 142(1-2), 169-196.

Doebley, J., Stec, A., & Hubbard, L. (1997). The evolution of apical dominance in maize.

DoyleJJ, D. J. (1987). A rapid DNA isolation procedure for small quantities of fresh leaf tissue. *Phytochemical Bulletin*, 19, 11-15.

Galkovskyi, T., Mileyko, Y., Bucksch, A., Moore, B., Symonova, O., Price, C. A., ... & Weitz, J. S. (2012). GiA Roots: software for the high throughput analysis of plant root system architecture. *BMC plant biology*, *12*(1), 116.

Gallavotti, A., & Whipple, C. J. (2015). Positional cloning in maize (Zea mays subsp. mays, Poaceae). *Applications in plant sciences*, 3(1).

Ganal, M. W., Durstewitz, G., Polley, A., Bérard, A., Buckler, E. S., Charcosset, A., ... & Falque, M. (2011). A large maize (Zea mays L.) SNP genotyping array: development and germplasm genotyping, and genetic mapping to compare with the B73 reference genome. *PloS one*, 6(12), e28334.

Haberer, G., Young, S., Bharti, A. K., Gundlach, H., Raymond, C., Fuks, G., … Messing, J. (2005). Structure and Architecture of the Maize Genome. Plant Physiology, 139(4), 1612–1624. doi:10.1104/pp.105.068718

Landi, P., Sanguineti, M. C., Darrah, L. L., Giuhani, M. M., Salvi, S., Conti, S., & Tuberosa, R. (2002). Detection of QTLs for vertical root pulling resistance in maize and overlap with QTLs for root traits in hydroponics and for grain yield under different water regimes. *Maydica*, *47*(3-4), 233-243.

Landi, P., Sanguineti, M. C., Salvi, S., Giuliani, S., Bellotti, M., Maccaferri, M., . . . Tuberosa, R. (2005). Validation and characterization of a major QTL affecting leaf ABA concentration in maize. *Molecular Breeding*, 15(3), 291-303.

Landi, P., Giuliani, S., Salvi, S., Ferri, M., Tuberosa, R., & Sanguineti, M. C. (2010). Characterization of root-yield-1.06, a major constitutive QTL for root and agronomic traits in maize across water regimes. *Journal of Experimental Botany*, 61(13), 3553-3562.

Lawrence, C. J., Dong, Q., Polacco, M. L., Seigfried, T. E., & Brendel, V. (2004). MaizeGDB, the community database for maize genetics and genomics. *Nucleic acids research*, 32(suppl 1), D393-D397.

Lorieux, M. (2012). MapDisto: fast and efficient computation of genetic linkage maps. *Molecular breeding*, 30(2), 1231-1235.

Mai, C. D., Phung, N. T., To, H. T., Gonin, M., Hoang, G. T., Nguyen, K. L., ... & Gantet, P. (2014). Genes controlling root development in rice. *Rice*, 7(1), 30.

Olukolu, B. A., Wang, G. F., Vontimitta, V., Venkata, B. P., Marla, S., Ji, J., ... & Johal, G. (2014). A genome-wide association study of the maize hypersensitive defense response identifies genes that cluster in related pathways. *PLoS genetics*, *10*(8), e1004562.

Poorter, H., Bühler, J., van Dusschoten, D., Climent, J., & Postma, J. A. (2012). Pot size matters: a meta-analysis of the effects of rooting volume on plant growth. *Functional Plant Biology*, 39(11), 839-850.

Rasband, W. S., Image, J., & US National Institutes of Health. Bethesda, Maryland, USA, 1997–2009.

Salvi, S., & Tuberosa, R. (2005). To clone or not to clone plant QTLs: present and future challenges. *Trends in Plant Science*, *10*(6), 297-304. doi: 10.1016/j.tplants.2005.04.008

Salvi, S., & Tuberosa, R. (2015). The crop QTLome comes of age. *Curr Opin Biotechnol*, 32C, 179-185.

Salvi, S., Sponza, G., Morgante, M., Tomes, D., Niu, X., Fengler, K. A., ... & Tuberosa, R. (2007). Conserved noncoding genomic sequences associated with a flowering-time quantitative trait locus in maize. *Proceedings of the National Academy of Sciences*, 104(27), 11376-11381.

Sanguinetti, M. C., Giuliani, M. M., Govi, G., Tuberosa, R., & Landi, P. (1998). Root and shoot traits of maize inbred lines grown in the field and in hydroponic culture and their relationships with root lodging [Zea mays L.-Italy]. *Maydica* (Italy).

Schnable, P. S., Ware, D., Fulton, R. S., Stein, J. C., Wei, F., Pasternak, S., ... & Cordes, M. (2009). The B73 maize genome: complexity, diversity, and dynamics. *Science*, 326(5956), 1112-1115.

Teng, F., Zhai, L., Liu, R., Bai, W., Wang, L., Huo, D., ... & Zhang, Z. (2013). ZmGA3ox2, a candidate gene for a major QTL, qPH3. 1, for plant height in maize. *The Plant Journal*, 73(3), 405-416.

Tian, F., Bradbury, P. J., Brown, P. J., Hung, H., Sun, Q., Flint-Garcia, S., ... & Buckler, E. S. (2011). Genome-wide association study of leaf architecture in the maize nested association mapping population. *Nature genetics*, *43*(2), 159-162.

Tuberosa, R., Sanguineti, M. C., Landi, P., Salvi, S., Casarini, E., & Conti, S. (1998). RFLP mapping of quantitative trait loci controlling abscisic acid concentration in leaves of drought-stressed maize (Zea mays L.). *Theoretical and Applied Genetics*, 97(5-6), 744-755.

Tuberosa, R., & Salvi, S. (2009). QTL for agronomic traits in maize production. In Handbook of Maize: Its Biology (pp. 501-541). Springer New York.

Tuberosa, R., Sanguineti, M. C., Landi, P., Michela Giuliani, M., Salvi, S., & Conti, S. (2002). Identification of QTLs for root characteristics in maize grown in hydroponics and analysis of their overlap with QTLs for grain yield in the field at two water regimes. *Plant Molecular Biology*, 48(5).

Uga, Y., Sugimoto, K., Ogawa, S., Rane, J., Ishitani, M., Hara, N., ... & Yano, M. (2013). Control of root system architecture by DEEPER ROOTING 1 increases rice yield under drought conditions. *Nature Genetics*, 45(9), 1097-1102.

Van Ooijen, J. W., & Kyazma, B. V. (2009). MapQTL 6. Software for the mapping of quantitative trait loci in experimental populations of diploid species. Kyazma BV: Wageningen, Netherlands.

Wallace, J. G., Bradbury, P. J., Zhang, N., Gibon, Y., Stitt, M., & Buckler, E. S. (2014). Association Mapping across Numerous Traits Reveals Patterns of Functional Variation in Maize. *PLoS genetics*, *10*(12), e1004845.

Wang, H., Nussbaum-Wagler, T., Li, B., Zhao, Q., Vigouroux, Y., Faller, M., ... & Doebley, J. F. (2005). The origin of the naked grains of maize. Nature, 436(7051), 714-719.

Yang, Q., Zhang, D., & Xu, M. (2012). A Sequential Quantitative Trait Locus Fine-Mapping Strategy Using Recombinant-Derived ProgenyF. *Journal of integrative plant biology*, 54(4), 228-237.

Zhang, J., Ku, L. X., Han, Z. P., Guo, S. L., Liu, H. J., Zhang, Z. Z., ... & Chen, Y. H. (2014). The ZmCLA4 gene in the qLA4-1 QTL controls leaf angle in maize (Zea mays L.). *Journal of experimental botany*, eru271.

4 QTL meta-analysis for maize root traits

4.1 Introduction

With the large quantity of quantitative trait loci (QTL) that have been mapped for many traits in the main crop species, QTL meta-analysis has been suggested as one of the most important approaches to help interpreting the plethora of QTL information (Salvi and Tuberosa 2015). QTL meta-analysis is a statistical approach which combines QTL results from independent analyses in a single output (Goffinet and Gerber 2000). The method implies the construction of a consensus map from independent QTL maps and, if available, the organism reference map, the projection of QTLs onto the consensus map and finally the estimation of meta- (or consensus-) QTLs. The results of a QTL meta-analysis study include genetic positions of meta-QTLs on the consensus map and the length of their confidence interval (CI). An important result is that in most cases, the CI of the resulting metaQTLs (mQTL) are shorter than CI of corresponding QTLs (Arcade *et al.*, 2004). This reduction of the CI could help to prioritize candidate genes to be included in further studies (Veyrieras *et al.*, 2007).

The synthesis power of QTL meta-analysis and its ability to at least theoretically shorten QTL intervals has now made QTL meta-analysis very popular (Salvi and Tuberosa 2015). In addition, the development and improvement of specialized software, such as BioMercator (Arcade *et al.*, 2004, Sosnowski *et al.*, 2012) made meta-analysis a task achievable in a few steps. In maize, QTL meta-analyses have been carried out for flowering time (Chardon *et al.*, 2004), leaf architecture (Ku *et al.*, 2011), grain yield components (Li *et al.*, 2011), grain moisture (Sala, Andrade, and Cerono 2012), ear rot resistance (Xiang *et al.*, 2012), and yield (Wang *et al.*, 2013). Hao *et al.*, (2010) used meta-analysis to highlight important constitutive and adaptive QTLs and to find specific genes potentially involved in drought tolerance networks. Additionally, mQTLs associated with grain yield under both well-watered and water-stressed environments were identified (Semagn *et al.*, 2013). Similar studies have been reported in rice (Courtois *et al.*, 2009, Khowaja *et al.*, 2009); and Barley (Li *et al.*, 2013).

For root traits in maize, Tuberosa *et al.*, (2003) presented the first meta-analysis in which QTLs of four mapping populations were collocated using a bin map by using anchor markers. Later, Hund *et al.*, (2011) summarized literature on QTLs related to root length and reported a consensus map in which root QTLs were clustered to identify loci for selecting efficient root systems. Several loci detected in three or more populations, in different environments or at different developmental stages

and co-located with QTL related to grain yield were considered for QTL validation or cloning. Another specific meta-analysis was carried out by (Landi *et al.*, 2010) to verify the collocation of the major root QTL, *qroot-yield-1.06*, with QTLs for different traits mapped in the same background. The results of this study indicated that the QTL effects on root morphology and pulling resistance, stay-green, plant height, drought-tolerance index, and grain yield, which were mapped on bin 1.06 in the Lo964xLo1016 population, could correspond to a single segregating locus.

The aims of the present study are i) to summarize literature on root QTLs in maize, ii) to synthetize maize root QTL information using meta-analysis, iii) to confirm the previous mQTL detected on bin 1.06 including *qroot-yield-1.06* and iv) identify possible candidate genes in this region.

4.2 Material and methods

4.2.1 Bibliographic review an data collection

The previous work of Hund *et al.*, (2011), of a consensus map for root length in maize was taken as a point of reference to start the literature search of the present study. Web search engines as Web of knowledge and Google Scholar were used to obtain information on scientific papers reporting information on QTLs for root traits. All reported QTLs for root architecture traits including length, diameter, weight, etc. were collected without having any special criterion. In addition, previously characterized root QTLs, *seminal root 1* mapped on the B73 × Gaspé Flint population and *Root-ABA1* mapped on Os420 × IABO78 population (Giuliani *et al.*, 2005) were included.

Database was constructed including a total of 20 studies reporting root QTLs, corresponding to 12 mapping populations (Table 8). A QTL 'experiment' was defined as a QTL analysis of one population evaluated for a given trait in a given environment (Chardon *et al.*, 2004). In the case multiple environments or treatments were evaluated, data were collected only for one environment or for QTLs detected across repeated field experiments. For the same studies, plant height and grain yield were also collected for Chr1. The goal was to confirm previously reported meta-analysis results on bin 1.06, including the target *qroot-yield-1.06*.

The genetic and physical map positions of know maize root mutants were also collected from the Maize Genetics and Genomics Database (MaizeGDB) (Andorf *et al.*, 2010) and from specific studies as follows: *rtcs*-rootless, concerning crown and seminal roots (Hetz *et al.*, 1996); *rt1*-

rootless1 (Jenkins 1930); *rum1*-rootless with undetectable meristems1 (Woll *et al.*, 2005); *rth*- root hair defective 1 and 3 (Wen and Schnable 1994).

For each study and experiment, information was collected on parents of the cross, type of cross or population, number of progenies, analyzed traits. For each QTL, information was collected on QTL name, LOD score, proportion of phenotypic variance explained (PVE), QTL position on the authors' linkage map and QTL supporting or confidence interval (CI). For each QTL CI, we relied on values reported in the original studies. When unavailable, CI values were estimated based on the formulas provided in (Darvasi and Soller 1997):
$CI = 530/NR^2$, where N is the population size and R^2 the proportion of the phenotypic variance explained by the QTL.

Root traits were described as proposed by Hund *et al.*, (2011) using the combination of abbreviations for root traits, root types, branching orders and in some cases the number of whorl evaluated (Table 9). For instance, NoCr6Ax means number of axile crowns in whorl six.

Table 8. QTL studies reporting root architecture traits. Tr# - Number of treatments. Rp.# - Number of replications per treatment.

Cross Name[1]	Cross Type[2]	Media and Treatment[3]	Stage[4]	Tr. #	Rp. #	Traits[5]	QTLs/ trait[6]	Pop. Size	Reference
(IoxF2)x F252	F5:6 RIL	Field	R1-2	1	2	NoCr6Ax, NoCr7Ax, NoCr8Ax, DCr7Ax, AnCr7Ax	2	100	Guingo *et al.*,. 1998
F271 x F288	F7 RIL	Field	R6	1	1	AnCrAx7, DCr7Ax, NoCr6Ax, NoCr7Ax, NoCr8Ax	1,8	132	Barrière *et al.*,. 2001
Lo964 x Lo1016	F2:3	Hydroponics	V2	1	4	LPrAx, DPrAx, DWPrAx, DWSe	8	171	Tuberosa *et al.*,. 2002
	F2:3	Field	R2	1	3	RPF	10	118	Landi *et al.*,. 2002
	F2:4	Pot	V1	1	2	LPrAx, DPrAx, LPrLat, DPrLat, NoSeAx, LSeAxDSeAx, LSeLat, DSeLat	2,3	168	Hund *et al.*,. 2004
B73x Mo17	RIL	Pot P /mycorrhiza	6 wks	3	2	VolRt	1	167	Kaeppler *et al.*,. 2000
	F10 RIL	Paper phosphorus	V1-2	2	3	LPrLat, NoPrLat	6,5	160	Zhu *et al.*,. 2005a
	RIL	Paper phosphorus		2	4	LRh	5	169	Zhu *et al.*,. 2005b
	F10 RIL	Paper phosphorus	V1-2	2	3	LSeAx, NoSeAx	4,5	162	Zhu *et al.*,. 2006
Z3 x 87-1	F8 RIL	Hydroponics nitrogen	6-leaf tip	2	3	Lax, LAxi, Llat, MaxLAx, NoAx	2,2	94	Liu *et al.*,. 2008
Mi29× Z. nicaraguensis	BC2F1	Pot	6-leaf tip	1	1	AER	3	214	Mano and Omori 2008
CML444 x	F7 RIL	Paper	V1-2	1	6	Klat, ERAx, LPrAx, NoAx	3	236	Trachsel *et al.*,.

Cross Name[1]	Cross Type[2]	Media and Treatment[3]	Stage[4]	Tr. #	Rp. #	Traits[5]	QTLs/ trait[6]	Pop. Size	Reference
SC-Malawi									2009
	F7 RIL	Field drought	R1-2	3	2	RCT	11	236	Messmer 2011
Ac7643 x Ac7729/TZSRW	RIL	Paper water potential	V1-2	2	6	LRt, NoCrAx, NoSeAx	3,5	208	Ruta *et al.*,. 2010a
	RIL	Paper water potential	V1-2	2	6	Klat, ERAx, kLat, kLat/ERAx, Lax, Llat/Lax	2	208	Ruta *et al.*,. 2010b
Ye478 x Wu312	BC4F3	Field	R2	1	1	RPF	2,3	187	Liu *et al.*,. 2011
	RIL	FIeld	R2	1	1	RPF	2,8	218	
Ye478 x Wu312	BC4F3	Field	V, R1, R6	1	2	SuRt, DW, LRt, NoAX, Lax	5,6	187	Cai *et al.*,. 2012
Huangzao 4 x CML288	IF2	Field	R3	1	3	TNoBr, ENoBr	3,5	278	Ku *et al.*,. 2012
	RIL	Field	R2	1	3	TNoBr, ENoBr	5		
HZ32x K12	F2:3	Pot/ waterlogging	V2-V4	2	3	DWRt, LRt	10	247	Osman *et al.*,. 2013
	BC2F2:3	Pot/ waterlogging	V2-V4	2	3	DWRt, FWRt	4	180	Zhang *et al.*,. 2013

[1] Contributing parent is underlined; [2] Recombinant Inbred Line (RIL); [3] Growth media under controlled conditions; [4] Vegetative stages (Vn) Reproductive stages (Rn); [5] For traits abbreviations see table 7; [6] Average number of QTLs per trait.

Table 9. Nomenclature and abbreviations modified from Hund *et al.,* (2011).

Traits	Abbreviation
Diameter	D
Angle	An
Number	No
Dry weight	DW
Fresh Weight	FW
Elongation rate	ER
Length	L
Rate constant of elongation	*k*
Total surface area	TSA
Volume	Vol
Aerenchyma	AER
Vertical root pulling resistance (VRPR)	RPF
Root capacitance	RCT
Root type	
Primary	Pr
Seminal	Se
Crown	Cr
Crown axile number in whorl *n*	NoCr*n*Ax
Brace roots	Br
Root hair	Rh
Branching order	
Axile (main root)	Ax
Lateral (branch root)	Lat
Total	Rt

4.2.2 Map projection

Because not all original maps were available on public database, maps were projected to the maize reference map 'Genetic' (Lawrence *et al.,* 2005) by means of a homothetic function (Chardon *et al.,* 2004), using shared common markers. Maps were used to construct a consensus map with all QTLs projected, using BioMercator v. 4.1 (Sosnowski *et al.,* 2012) as described by (Arcade *et al.,* 2004). Each genetic map was loaded in a text file and corresponding QTLs described by the chromosomal position, confidence interval, LOD score and PVE, were loaded in a second text file.

4.2.3 Meta-analysis and QTL overview

Meta-analysis was carried out using BioMercator v. 4.1 (Sosnowski *et al.*, 2012) that includes the methods and code reported by Veyrieras *et al.*, (2007) allowing a full chromosome analysis. In a first step, meta-analysis determines the best model, for each chromosome, based on the following criteria: Akaike information criterion (AIC), AICc, AIC3, Bayesian information criterion (PIC) and average weight of evidence (AWE). The best QTL model was chosen when the lowest value was present in at least three of the five criteria. In the second step, QTL meta-analysis was carried out according to the QTL model chosen. Information on mQTLs positions and 95% CIs were collected for each chromosome.

The statistic 'overview' was calculated according to described by Chardon *et al.,* (2004), to quantify the contribution of a given region to trait variation. The statistic is obtained by computing the average probability that a segment, between position x (in cM) and x+1 position, comprises a QTL in an experiment. This statistic was plotted along the reference map to observe regions in which QTL density shows a marked peak.

4.2.4 Graphical synthesis

A graphical summary of QTLs, metaQTLs and overview statistic was obtained using Circos (Krzywinski *et al.,* 2009). Circos enables to plot concentric circles reporting interconnected layers of information. Two different representations were done, one projecting data to the physical map B73 RefGen_v2, and the other, using as reference the maize genetic map 'Genetic' (Lawrence *et al.,* 2005). In the former, gene frequency (number of genes/2 Mb) calculated from raw data downloaded from MaizeGDB (Lawrence *et al.,* 2005), SNP density (number of SNPs per 5Mb) (Ganal *et al.,* 2011) and the projected position and CI of single QTLs and MQTLs were plotted. The

other graph includes positions and CI in cM of single QTLs, MQTLs and described root mutants, and the 'overview' statistic.

4.3 Results

4.3.1 Characteristics of the QTL experiments

Size of mapping populations considered for meta-analysis ranged from 94 to 278 individuals. Comprised traits are listed in Table 9. In the study we included results from experiments characterized by nutrient (nitrogen and phosphorus) and drought stress treatments. Methods of root phenotyping include evaluations in controlled conditions using hydroponics, pots and paper roll; and evaluations in field experiments. In the field, traits as vertical root pulling resistance and root capacitance or number of crown/brace roots were mainly measured at reproductive stage. On the contrary, QTL analysis based on finer root phenotyping (mainly targeting the embryonic root system), originated from experiments carried out in controlled conditions at early growth stages.

4.3.2 QTL clustering

Results of QTL projection and meta-analysis are summarized in Table 10. A total of 255 root QTLS were projected on the consensus map. Meta-analysis resulted in 56 MQTLs and 44 remaining individual QTLs. The number of mQTLs identified on each chromosome varied from four (chromosomes 4, 7, 8, 9) to ten (Chromosome 1), with an average of 5.6 mQTL per chromosome. The maximum number of QTLs grouped together in a mQTL was nine (chromosome 4- MQTL26). The mean value of 'explained phenotypic variance' of single QTLs considered in a mQTL was c. 4 % with a maximum of 48.5 % corresponding to MQTL38 that includes only one QTL. In general, the confidence intervals at most of the mQTLs were narrower than their respective original QTL, with the exception of MQTL24 on chromosome 4 (coefficient of reduction < 1). The confidence intervals of the mQTLs varied from 1.8 cM to 22.1 cM and the most accurate mQTLs were located on chromosome 1, 6 and 8 with CI values of 2.4, 2.4 and 1.8 cM, respectively. The physical intervals of the mQTLs varied from 0.26 Mb to 111.48 Mb. Four mQTLs were less than 600 Kb.

Several mQTL regions with small genetic and physical intervals were detected in the present analysis. Some of them, however, correspond to single QTLs representing a mQTL region (i.e. Chromosome9- MQTL51, chromosome 6- MQTL38). It is important to notice that physical/genetic proportion is not the same along chromosomes because of differences in frequency recombination between telomeric and pericentromeric regions (Farkhari *et al.*, 2011). For instance, on

chromosome 1, MQTL8 an MQTL10 have the same values of CI in cM (3,1), however, physical lengths in Mb are 2.51 and 0.5, respectively. Figure 19 shows how QTL and mQTL distributions vary on the consensus map when the map is expressed in physical rather than genetic units.

Chromosome regions previously identified to be important for root traits (Hund *et al.*, 2011) were confirmed in this study. These regions were bin 1.07, mainly controlling the root number per whorl; 2.04, controlling number and length of seminal roots, and number of crown roots; and 7.03, including total root length and root capacitance, which corresponded to MQTL7, MQTL14, MQTL20, and MQTL41, respectively. With the exception of MQTL14 that includes *qRoot-ABA-1*, other MQTLs resulting interesting, as well. MQTL21 on bin 3.06-3.07 is one with the smallest CI and physical length, and grouped QTLs for total and lateral length and number of seminal roots. In addition, MQTL42 on bin 7.04 grouped six different traits related mainly to root length and with a mean phenotypic variance of the QTL of 22.6%.

Table 10. Summary of QTL meta analysis for root traits.

MQTL	Chr.	No. initial QTLs[1]	Mean phenotypic variance of the QTL	Mean Initial CI (cM)	Position (cM)[2]	MQTL CI (95%) (cM)[3]	Physical length of MQTL (Mb)	Coefficient of reduction in length from mean initial QTL to MQTL
MQTL1	1	3	23,8	12,3	24,9	2,9	2,01	4,2
MQTL2	1	6	10,6	26,0	46,1	8,0	7,53	3,3
MQTL3	1	8	13,4	23,2	73,3	5,3	4,52	4,4
MQTL4	1	4	17,1	20,9	116,0	5,5	13,06	3,8
MQTL5	1	5	18,4	17,0	124,4	5,8	5,02	2,9
MQTL6	1	3	16,3	14,7	142,0	6,3	3,52	2,4
MQTL7	1	2	14,0	10,0	156,9	5,6	2,01	1,8
MQTL8	1	7	15,4	12,9	181,3	3,1	2,51	4,2
MQTL9	1	5	18,3	16,0	207,4	2,4	1,51	6,5
MQTL10	1	5	9,9	29,1	249,5	3,1	0,50	9,3
MQTL11	2	7	6,4	23,1	16,5	5,7	1,19	4,1
MQTL12	2	1	8,4	8,0	41,3	7,9	3,95	1,0
MQTL13	2	5	8,4	22,6	63,0	5,6	4,35	4,0
MQTL14	2	6	13,7	12,3	75,3	4,4	6,72	2,8
MQTL15	2	3	8,9	17,9	91,3	8,2	44,65	2,2
MQTL16	2	3	13,7	9,3	107,7	4,7	3,95	2,0
MQTL17	2	4	13,2	32,1	129,2	8,4	4,74	3,8
MQTL18	3	2	16,6	16,4	52,3	8,0	13,93	2,1
MQTL19	3	3	5,7	13,8	84,5	8,0	16,64	1,7
MQTL20	3	2	6,6	21,0	100,2	9,3	7,74	2,3
MQTL21	3	3	18,6	8,4	129,8	2,4	1,16	3,4
MQTL22	3	2	10,8	14,3	156,1	9,0	4,64	1,6
MQTL23	3	3	16,9	17,9	189,6	5,6	4,26	3,2
MQTL24	4	1	8,6	11,2	27,5	11,6	6,04	1,0

MQTL	Chr.	No. initial QTLs[1]	Mean phenotypic variance of the QTL	Mean Initial CI (cM)	Position (cM)[2]	MQTL CI (95%) (cM)[3]	Physical length of MQTL (Mb)	Coefficient of reduction in length from mean initial QTL to MQTL
MQTL25	4	3	7,0	40,7	65,5	22,1	111,48	1,8
MQTL26	4	9	9,4	35,1	110,2	12,0	7,65	2,9
MQTL27	4	2	7,1	22,0	146,5	12,9	22,54	1,7
MQTL28	5	3	10,6	25,4	18,1	6,3	1,82	4,0
MQTL29	5	2	6,7	20,8	38,6	12,1	4,00	1,7
MQTL30	5	2	11,9	17,0	76,0	10,2	84,97	1,7
MQTL31	5	7	7,1	28,1	96,9	10,4	9,08	2,7
MQTL32	5	7	10,6	28,9	122,9	8,6	9,08	3,4
MQTL33	5	3	8,6	28,8	161,1	11,2	2,91	2,6
MQTL34	6	4	11,7	16,4	11.75	4.91	1,97	3,3
MQTL35	6	6	10,4	24,7	35.41	6.02	6,49	4,1
MQTL36	6	3	13,3	5,9	63.23	3.33	4,51	1,8
MQTL37	6	5	8,3	33,0	78.85	10.72	10,72	3,1
MQTL38	6	1	48,5	2,1	120.81	2.11	0,56	1,0
MQTL39	6	2	7,5	8,6	131.25	2.2	0,56	3,9
MQTL40	7	4	7,9	22,6	29,9	11,3	7,07	2,0
MQTL41	7	3	7,6	32,4	76,0	17,1	13,55	1,9
MQTL42	7	6	9,4	27,8	112,1	7,8	4,13	3,6
MQTL43	7	4	10,5	25,8	145,6	6,2	0,88	4,2
MQTL44	8	2	4,5	18,2	3,0	11,9	3,22	1,5
MQTL45	8	3	4,7	20,4	33,8	8,8	5,57	2,3
MQTL46	8	4	22,6	14,2	62,2	1,8	2,64	7,7
MQTL47	8	4	9,1	25,3	118,2	5,5	2,05	4,7
MQTL48	9	2	8,8	22,1	4,5	10,6	2,87	2,1
MQTL49	9	4	7,9	32,9	49,9	6,4	5,23	5,1
MQTL50	9	2	4,1	20,2	106,6	9,8	4,44	2,1
MQTL51	9	1	10,4	9,3	127,4	2,8	0,26	3,3
MQTL52	10	2	5,9	23,1	9,6	16,1	3,50	1,4
MQTL53	10	5	10,4	31,3	46,9	8,8	49,81	3,5
MQTL54	10	5	10,8	23,7	63,6	4,6	18,77	5,2
MQTL55	10	5	16,2	20,8	91,8	4,8	3,00	4,3
MQTL56	10	3	14,2	25,3	124,0	10,9	3,00	2,3

[1] Each individual QTL was assigned to a given cluster based on membership probabilities given by BioMercator v4.1
[2] Most likely position on the consensus map in cM.
[3] Total length of the confidence interval (CI) centered on the most likely position in cM

4.3.3 Bin 1.06

In the work of Landi *et al.,* (2010) a QTL meta-analysis carried out with 15 QTLs for morpho-physiological traits previously identified in the Lo964xLo1016 background (Tuberosa *et al.,* 2002, Landi *et al.,* 2002), supported *root-yield-1.06* as a single segregating QTL. In the present study, we collected information on three additional populations and for traits such as plant height, stay green and grain yield QTLs overlapping to the *root-yield-1.06* region.

Nine mQTLs were detected along the chromosome with values of the CI between 2.4 and 6 cM. Two were located inside the original *qroot-yield-1.06* interval (118.4 to 147 cM) at positions on the consensus map of mQTL4 - 125.8 (95% CI: 123.5 – 128.1 cM) and mQTL5- 134.5 cM (95% CI: 131.5-137.5 cM). MQTL4 located at 125.8 cM is the one grouping more QTLs for roots and other agronomic traits as plant height and yield. The mQTL reported by Landi *et al.*, (2010) appears located between the two mQTLs at 130 cM (95% CI: 127-133) (Figure 17). Interestingly, the position corresponds to the new interval for the *qroot-yield-1.06* (124.9-133.6 cM) narrowed down with the latest mapping results (Figure 14).

Genes included in the mQTL4 interval (123.5-128.1 cM) were listed thanks to the option in BioMercator v4 that enable to connect genetic maps with genome annotation (Table 11). Figure 18 shows the genome area of the mQTL4 corresponding to an interval in the physical map of 2.5 Mb (177799-180310 Kb).

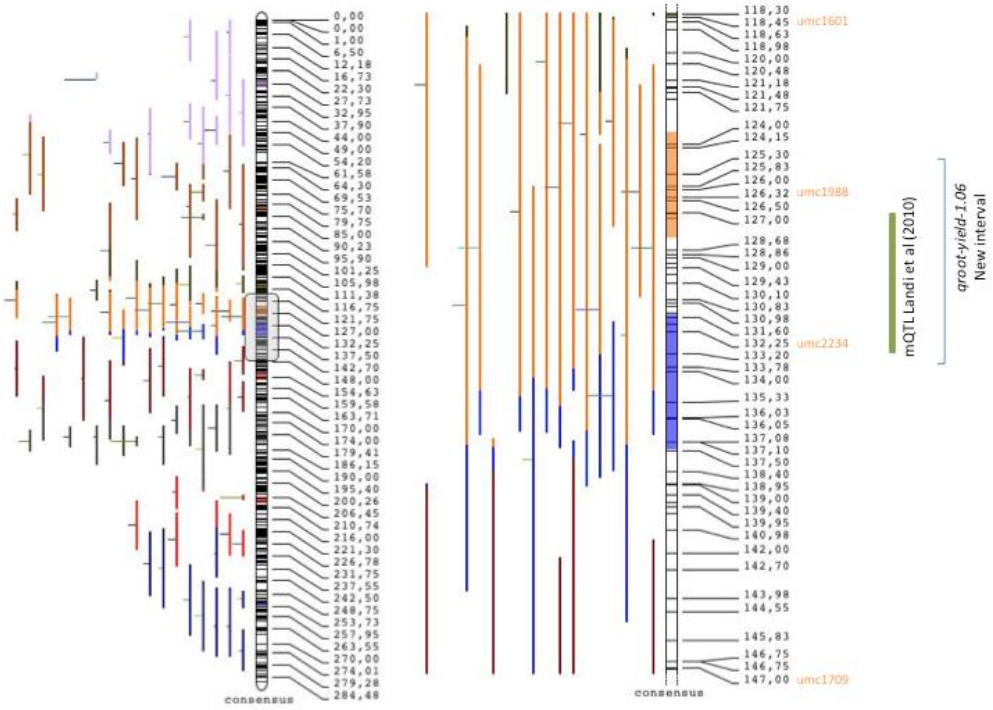

Figure 17. Meta-analysis for chromosome 1. On the left, BioMercator overview of meta-analysis results showing the position of mQTLs as colored bands along the consensus map. The rectangle is showing the region enlarged on the right, corresponding to the original QTL interval for *root-yield-1.06* flanking by SSR markers umc1601 and umc1709. Position of the first mQTL reported for the region (Landi *et al.*, 2010) and the new interval for *qroot-yield-1.06* are showed, as well.

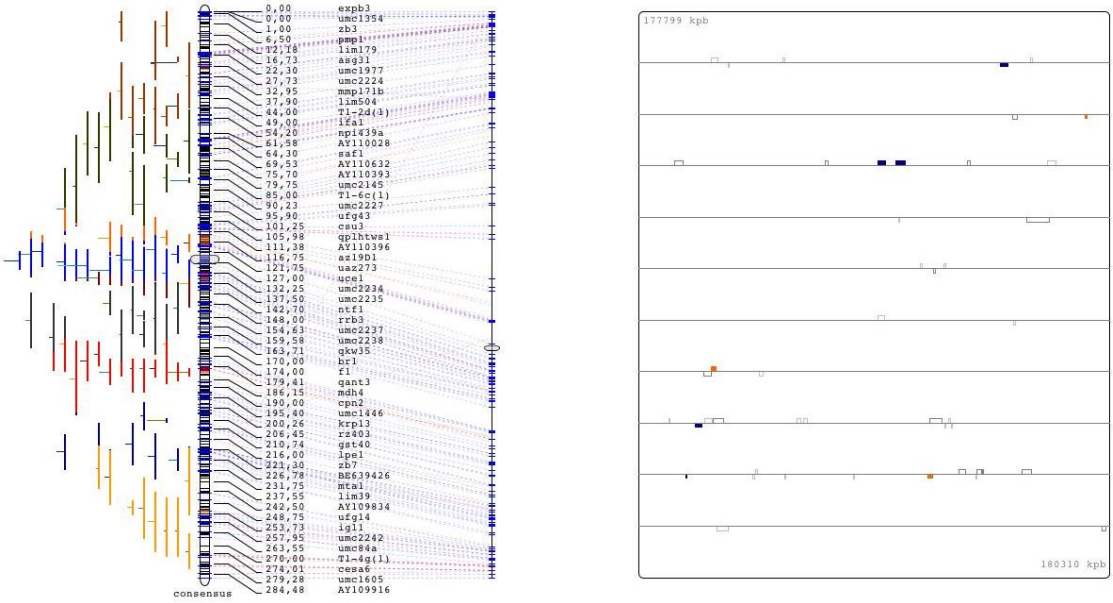

Figure 18. BioMercator display showing the genome area corresponding to the mQTL4 interval (123.5-128.1 cM) inside the *qroot-yield-1.06*. On the left genetic map of chromosome 1 with the small rectangle enclosing the mQTL; in the middle, the vertical line correspond to the physical map; and at the right the genome window (177799 - 180310 Kb), corresponding to the rectangle in both maps, showing the genes.

4.3.4 Graphical synthesis

Figure 18 shows the Circos representation of the different features of the QTL meta-analysis projected on the maize reference genetic map 'Genetic' (Lawrence et al, 2005). Position of single root QTLs (GY and PH also for chromosome 1) with a CI of 95%, the statistic 'overview' (Chardon *et al.,* 2004), positions with a CI of 95% of the mQTLs detected in the present study and those reported previously by Hund *et al.,* (2011), and positions of the known root mutants were plotted.

No notable feature in the distribution of the QTLs along the chromosomes was observed. Three regions (on chromosomes 1, 3 and 8), in particular, displayed high 'overview' statistic values, 4 to 10 times higher than the average value of the index. Accordingly, QTL meta-analysis confirmed mQTLs in these positions, with confidence intervals smaller than the corresponding smallest initial confidence interval. However, the genetic and molecular nature of these mQTLs remains unexplained.

For the QTL meta-analysis, 2.3 times more mQTLs were found in the present study as compared to those reported by Hund *et al.,* (2011), with more accurate positions (mean 95% CI: 7.9 cM). As mentioned above, it is evident the co-location of some mQTLs, and the lack of co-location in other cases, (e.g. on chr. 9).

On Figure 19, Circos representation was obtained using the physical map B73RefGen_v2 as reference. Gene and SNP density heatmaps easily allow to identify centromeric regions as characterized by a lower number of markers per Mb (Ganal *et al.*, 2011). Differences in recombination frequency along chromosomes is also reported, with much higher average frequency on telomeric regions than in pericentromeric regions (data not plotted) (Farkhari *et al.*, 2011). This fact is reflected when positions of single QTLs, with a CI of 95%, are projected on the physical map. QTLs located in the pericentromeric region became larger that those located in the telomeric region, and the same for mQTLS. Again, no particular QTL or mQTL distribution trend along the chromosomes was detected based on this representation.

Table 11. Genes included in the mQTL4 interval (123.5-128.1 cM), inside the *qroot-yield-1.06*, resulted of the QTL meta-analysis for root and other agronomical traits on chromosome 1 (Figure 18). Canonical positions and genes names are reported according to MaizeGDB (http://maizegdb.org)

Gene	Canonical position	Gene name
AC189052.3_FG003	177,865,165 - 177,868,243	protein_coding
GRMZM2G006853	177,873,835 - 177,874,727	protein_coding
GRMZM2G136372	177,903,254 - 177,904,176	protein_coding
GRMZM2G108859	178,019,268 -178,023,712	protein_coding
GRMZM2G402631	178,035,095 - 178,036,072	protein_coding
GRMZM2G396477	178,276,985 - 178,279,410	protein_coding
GRMZM2G073764	178,315,525 - 178,316,775	protein_coding
GRMZM2G027331	178,347,753 - 178,352,009	protein_coding
GRMZM2G475014	178,427,919 - 178,429,404	NAC-transcription factor 50 (nactf50)
GRMZM2G068604	178,455,867 - 178,460,697	bHLH-transcription factor 115 (bhlh115)
GRMZM2G049686	178,465,632 - 178,471,112	bhlh78 - bHLH-transcription factor 78
GRMZM2G080603	178,503,667 - 178,505,233	glycine-rich protein1 (grp1)
GRMZM2G356653	178,546,582 - 178,551,203	protein_coding
GRMZM2G499601	178,718,295 - 178,719,013	protein_coding
GRMZM2G428201	178,786,394 - 178,798,667	protein_coding
GRMZM2G384592	178,981,070 - 178,981,717	protein_coding
GRMZM2G136277	178,988,086 - 178,988,921	protein_coding
GRMZM5G820643	178,993,612 - 178,994,363	protein_coding
GRMZM2G026976	179,209,612 - 179,213,208	protein_coding
GRMZM2G165082	179,281,920 - 179,282,978	protein_coding
GRMZM2G131245	179,367,645 - 179,371,815	protein_coding
GRMZM2G131254	179,371,866 - 179,374,965	protein_coding
GRMZM2G478599	179,397,346-179,399,333	protein_coding
AC194452.3_FG001	179,600,415 - 179,600,879	protein_coding
GRMZM2G099319	179,614,336 - 179,618,197	Homeobox-transcription factor 84 (hb84)
GRMZM2G099366	179,619,542 - 179,623,388	protein_coding
GRMZM2G067028	179,668,752 - 179,670,667	protein_coding
GRMZM2G067162	179,672,176 - 179,674,258	protein_coding
GRMZM5G839017	179,739,475-179,745,846	protein_coding

Gene	Canonical position	Gene name
GRMZM2G059064	179,747,288 - 179,747,944	protein_coding
GRMZM2G059029	179,749,211 - 179,750,453	protein_coding
GRMZM2G358924	179,751,146-179,751,567	protein_coding
GRMZM2G370026	179,860,588 - 179,861,190	bZIP-transcription factor 31 (bzip31)
AC212323.4_FG007	179,895,949 - 179,896,878	protein_coding
AC212323.4_FG005	179,912,977 - 179,913,393	protein_coding
GRMZM2G051168	179,949,801 - 179,950,512	protein_coding
GRMZM2G093828	179,989,536 - 179,992,713	protein_coding
GRMZM2G093809	180,006,011 - 180,009,342	protein_coding
AC212323.4_FG010	180,015,325 - 180,015,840	protein_coding
GRMZM2G093755	180,018,458 - 180,019,178	protein_coding
GRMZM2G392791	180,015,529 - 180,017,868	protein_coding
GRMZM2G007381	180,039,864 - 180,044,548	protein_coding
GRMZM2G352915	180,127,900 - 180,133,950	protein_coding
GRMZM2G161335	180,333,582 - 180,335,486	bx9 - benzoxazinone synthesis9

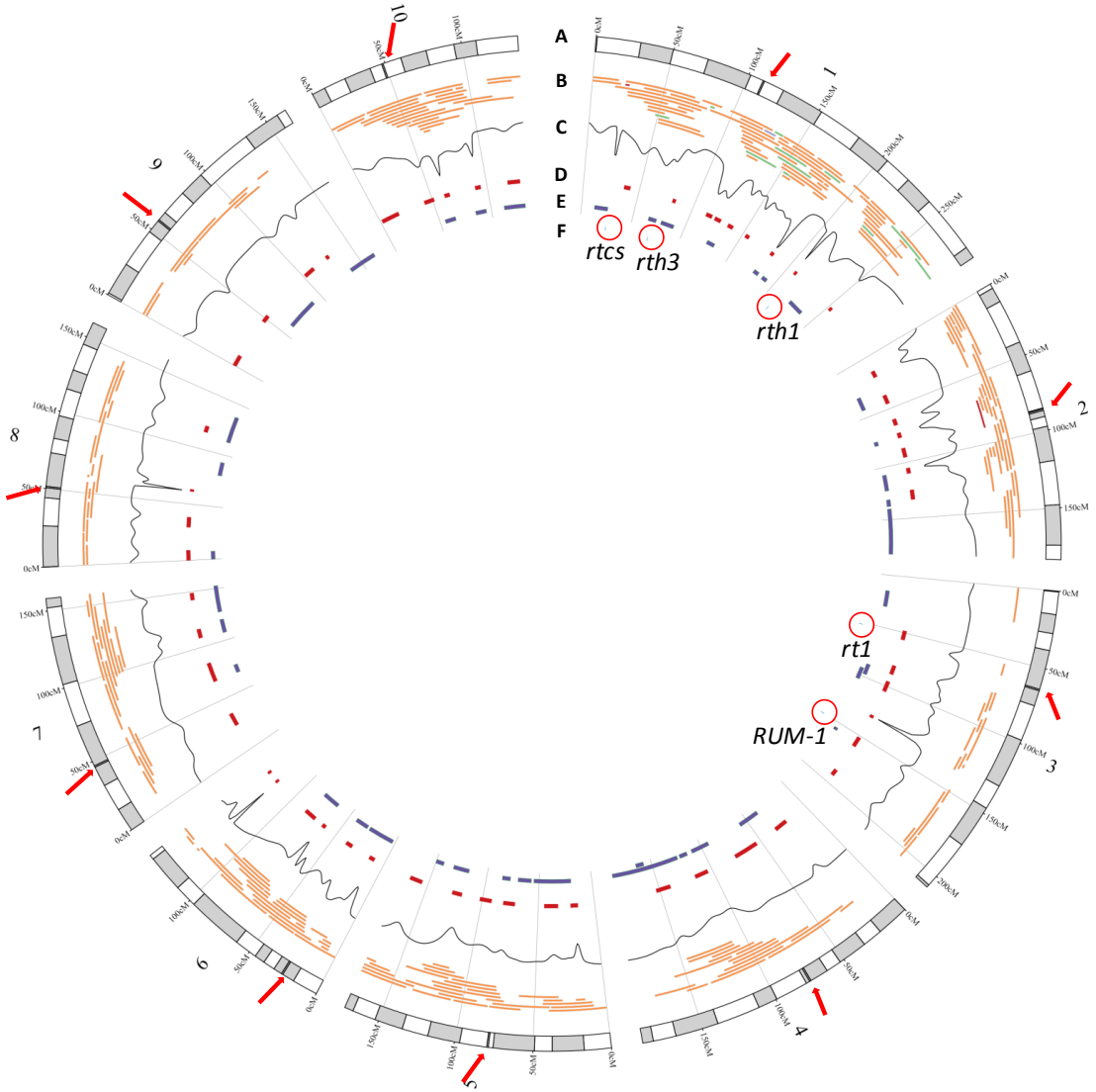

A. Reference chromosomes with genetic positions of bins as alternating gray and white bands, according with the maize reference map 'Genetic' (Lawrence et al, 2005) Approx. centromeric positions are indicated by red arrows.

B. Single QTLs. Bars indicate QTL position with a CI of 95%. (In Orange, QTLs for root traits, in pale blue, QTLS for yield, yield related traits and plant height on chr. 1, in red *sr1* and *qRoot-ABA-1*; in purple, the narrowed *qRoot-yield-1.06.*

C. Frequency of QTLs computed as **QTL-overview index** (Chardon *et al*. 2004).

D. MQTLs. Bars indicate the MQTL position with a CI of 95%.

E. MQTLs reported by Hund *et al.* 2011.

F. Root mutants.

Figure 19. Concentric circles summarizing the meta-QTL analysis results. Rtcs- rootless concerning crown and seminal roots, *rt1*-rootless1, *rum1*-rootless with undetectable meristems1 and *rth*- root hair defective 1 and 3.

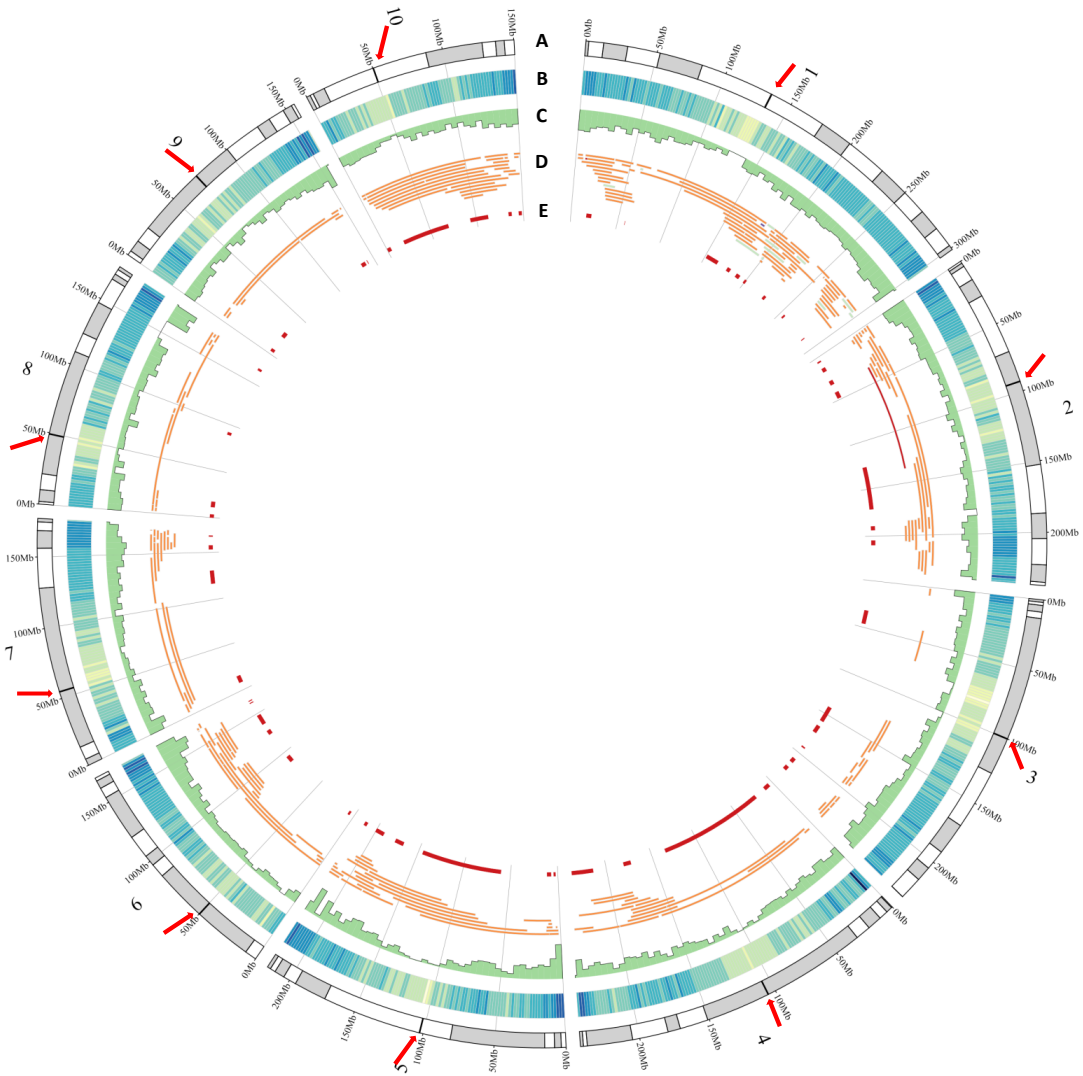

A. Reference chromosomes with physical position of bins as alternating gray and white bands. Approx. centromeric positions are indicated by red arrows.

B. Gene density (genes/2Mb). Based on B73RefGen_v2 (Lawrence et al, 2005) Scale: min= yellow; max=dark blue.

C. SNP density. No of polymorphic SNPS/Mb (Bin size is 5 Mb along the physical coordinates of the B73 sequence) (Ganal et al, 2011)

D. Single QTLs. Bars indicate QTL position with a CI of 95%. (In Orange, QTLs for root traits, in pale blue, QTLS for yield, yield related traits and plant height on chr. 1; in red *sr1* and *qRoot-ABA-1*; in purple, the narrowed *qRoot-yield-1.06.*

E. MQTLS. Bars indicate the MQTL position with a CI of 95%.

Figure 20. Concentric circles showing root QTL distribution on the maize genome.

4.4 Discussion and conclusions

In maize, two main studies (Tuberosa *et al.,* 2003 and Hund *et al.,* 2011) have been conducted to synthetize information on root QTLs. In the present study, a database for root QTLs in maize was done assembling a large collection of information on each QTL. The consensus map constructed with QTLs projected allows easily visualizing and highlighting regions of QTL clustering. Previous QTL meta-analysis reported by Hund *et al.,* (2011) was focus on traits related to root length, 'for the sake of clarity'. In this study, QTLs for all other traits describing root architecture in maize were included and pooled in a single analysis. Software constraints, about the minimum QTL number to run the analysis, don't allow analyzing single traits. Thus, the assumption was that several of the traits studied could be pleiotropically related.

One of the main limitations of the QTL meta-analysis is that the QTL dataset used for the analysis is not as accurate as each of the individual QTL mapping studies compiled. This is due to the heterogeneity of the source data and the necessity of meta-analysis tools of homogenous data (Courtois *et al.,* 2009). For instance, in some studies precise QTL positions or CI were not reported and only information in flanking markers was available. Despite this weakness, meta-analysis allowed to confirm previous highlighted regions (Tuberosa *et al.,* 2003 and Hund *et al.,* 2011) reporting root major QTLS with smaller CI, and additional interesting mQTL regions on chromosome 3 (bin 3.06-3.07-MQTL21) and on chromosome 7 (bin 7.04-MQTL42) clustering QTLs from several populations and traits.

Bin 1.06 has been highlighted as an important region of QTL clustering (Tuberosa *et al.,* 2007). Other than the major root QTL *root-yield-1.06* (Landi *et al.,* 2010), several others QTLs have been mapped in this region for other agronomical traits as grain yield, plant height and stay green, in different genetic backgrounds (Landi *et al.,* 2002, Tuberosa *et al.,* 2002, Lebreton *et al.,* 1995, Kaeppler *et al.,* 2000, Hirel *et al.,* 2001). In the present study, unlike what was reported by Landi *et al.,* 2010, two mQTLs instead of one were located along the region. Fine mapping advances on *qroot-yield-1.06* showed than the new interval of the QTL correspond to the position of the mQTL reported by Landi *et al.,* (2010) but at the same time co-localizes in some extent with both mQTLs. Courtois *et al.,* (2009), applying meta-analysis to QTLs surrounding cloned genes in rice, reported that the method was not always efficient to improve original QTL position. For some mQTLs the method improved the precision with resulting CIs, co-localizing with genes cloned, smaller than each original QTL. On the contrary, other mQTLs even not covered the gene or meta-analysis identified several mQTLs under a QTL cluster.

Two mQTLs inside the *q-root-yield-1.06* interval could also suggest the possibility that two linked loci are responsible to the positive association among root traits and other agronomical traits investigated by Landi *et al.*, (2010). Even the mQTL upstream (mQTL4, 123.5-128.1 cM) of *qroot-yield-1.06* grouped most of the QTLs of the QTL cluster, the mQTL downstream (mQTL5, 131.5-137.5cM) also group a QTL for RPF (Landi *et al.*, 2002) and one for GY (Tuberosa *et al.*, 2002). Then, distinguishing between pleiotropy and close linkage is not obvious, as suggested by Khowaja *et al.*, (2009), and results should be carefully analyzed.

4.5 References

Andorf, C. M., Lawrence, C. J., Harper, L. C., Schaeffer, M. L., Campbell, D. A., & Sen, T. Z. (2010). The Locus Lookup tool at MaizeGDB: identification of genomic regions in maize by integrating sequence information with physical and genetic maps. *Bioinformatics, 26*(3), 434-436.

Arcade, A., Labourdette, A., Falque, M., Mangin, B., Chardon, F., Charcosset, A., & Joets, J. (2004). BioMercator: integrating genetic maps and QTL towards discovery of candidate genes. *Bioinformatics, 20*(14), 2324-2326.

Barriere, Y., Gibelin, C., Argillier, O., & Mechin, V. (2001). Genetic analysis in recombinant inbred lines of early dent forage maize. I: QTL mapping for yield, earliness, starch and crude protein contents from per se value and top cross experiments. *Maydica, 46*(4), 253-266.

Bucksch, A., Burridge, J., York, L. M., Das, A., Nord, E., Weitz, J. S., & Lynch, J. P. (2014). Image-based high-throughput field phenotyping of crop roots. *Plant Physiol, 166*(2), 470-486.

Cai, H., Chen, F., Mi, G., Zhang, F., Maurer, H. P., Liu, W., . . . Yuan, L. (2012). Mapping QTLs for root system architecture of maize (Zea mays L.) in the field at different developmental stages. *Theoretical and Applied Genetics, 125*(6).

Chardon, F., Virlon, B., Moreau, L., Falque, M., Joets, J., Decousset, L., ... & Charcosset, A. (2004). Genetic architecture of flowering time in maize as inferred from quantitative trait loci meta-analysis and synteny conservation with the rice genome. *Genetics*, *168*(4), 2169-2185.

Courtois, B., Ahmadi, N., Khowaja, F., Price, A. H., Rami, J. F., Frouin, J., ... & Ruiz, M. (2009). Rice root genetic architecture: meta-analysis from a drought QTL database. *Rice*, *2*(2-3), 115-128.

Darvasi, A., & Soller, M. (1997). A simple method to calculate resolving power and confidence interval of QTL map location. *Behavior Genetics*, *27*(2), 125-132. doi: 10.1023/a:1025685324830

Farkhari, M., Lu, Y., Shah, T., Zhang, S., Naghavi, M. R., Rong, T., & Xu, Y. (2011). Recombination frequency variation in maize as revealed by genomewide single-nucleotide polymorphisms. *Plant Breeding, 130*(5), 533-539.

Galkovskyi, T., Mileyko, Y., Bucksch, A., Moore, B., Symonova, O., Price, C. A., . . . Weitz, J. S. (2012). GiA Roots: software for the high throughput analysis of plant root system architecture. *Bmc Plant Biology, 12*. doi: 10.1186/1471-2229-12-116

Ganal, M. W., Durstewitz, G., Polley, A., Bérard, A., Buckler, E. S., Charcosset, A., . . . Falque, M. (2011). A large maize (Zea mays L.) SNP genotyping array: development and germplasm genotyping, and genetic mapping to compare with the B73 reference genome. *PLoS One, 6*(12).

Giuliani, S., Bellotti, M., Landi, P., Sanguineti, M. C., Salvi, S., & Tuberosa, R. (2005). Root-ABA1: A QTL influencing L-ABA concentration and root traits in maize. *Comparative Biochemistry and Physiology a-Molecular & Integrative Physiology, 141*(3), S369-S370.

Giuliani, S., Busatto, C., Salvi, S., Ricciolini, C., Carraro, N., Presterl, T., . . . Tuberosa, R. (2009). *Genetic dissection of root characteristics at theseminal and seedling level in maize.* Paper presented at the EUCARPIA Maize and Sorghum Section, Bergamo, Italy.

Goffinet, B., & Gerber, S. (2000). Quantitative trait loci: a meta-analysis. *Genetics, 155*(1), 463-473.

Guingo, E., Hébert, Y., & Charcosset, A. (1998). Genetic analysis of root traits in maize. *Agronomie, 18*(3), 225-235.

Hao, Z., Li, X., Liu, X., Xie, C., Li, M., Zhang, D., & Zhang, S. (2010). Meta-analysis of constitutive and adaptive QTL for drought tolerance in maize. *Euphytica, 174*(2), 165-177.

Hetz, W., Hochholdinger, F., Schwall, M., & Feix, G. (1996). Isolation and characterization of rtcs, a maize mutant deficient in the formation of nodal roots. *Plant Journal, 10*(5), 845-857.

Hirel, B., Bertin, P., Quilleré, I., Bourdoncle, W., Attagnant, C., Dellay, C., ... & Gallais, A. (2001). Towards a better understanding of the genetic and physiological basis for nitrogen use efficiency in maize. *Plant Physiology, 125*(3), 1258-1270.

Hund, A., Fracheboud, Y., Soldati, A., Frascaroli, E., Salvi, S., & Stamp, P. (2004). QTL controlling root and shoot traits of maize seedlings under cold stress. *Theoretical and applied genetics, 109*(3), 618-629.

Hund, A., Reimer, R., & Messmer, R. (2011). A consensus map of QTLs controlling the root length of maize. *Plant and Soil, 344*(1-2).

Jenkins, M. (1930). Heritable characters of maize. XXXIV. Rootless. . *J Hered, 21*, 79-80.

Kaeppler, S. M., Parke, J. L., Mueller, S. M., Senior, L., Stuber, C., & Tracy, W. F. (2000). Variation among maize inbred lines and detection of quantitative trait loci for growth at low phosphorus and responsiveness to arbuscular mycorrhizal fungi. *Crop Science, 40*(2), 358-364.

Khowaja, F. S., Norton, G. J., Courtois, B., & Price, A. H. (2009). Improved resolution in the position of drought-related QTLs in a single mapping population of rice by meta-analysis. *Bmc Genomics, 10*.

Krzywinski, M., Schein, J., Birol, I., Connors, J., Gascoyne, R., Horsman, D., . . . Marra, M. A. (2009). Circos: An information aesthetic for comparative genomics. *Genome Research, 19*(9), 1639-1645.

Ku, L., Wei, X., Zhang, S., Zhang, J., Guo, S., & Chen, Y. (2011). Cloning and Characterization of a Putative TAC1 Ortholog Associated with Leaf Angle in Maize (Zea mays L.). *Plos One, 6*(6).

Landi, P., Sanguineti, M. C., Darrah, L. L., Giuliani, M. M., Salvi, S., Conti, S., & Tuberosa, R. (2002). Detection of QTLs for vertical root pulling resistance in maize and overlap with QTLs for root traits in hydroponics and for grain yield under different water regimes. *Maydica, 47*(3-4).

Landi, P., Sanguineti, M. C., Liu, C., Li, Y., Wang, T. Y., Giuliani, S., . . . Tuberosa, R. (2007). Root-ABA1 QTL affects root lodging, grain yield, and other agronomic traits in maize grown under well-watered and water-stressed conditions. *Journal of Experimental Botany, 58*(2). doi: 10.1093/jxb/erl161

Landi, P., Giuliani, S., Salvi, S., Ferri, M., Tuberosa, R., & Sanguineti, M. C. (2010). Characterization of root-yield-1.06, a major constitutive QTL for root and agronomic traits in maize across water regimes. *Journal of Experimental Botany, 61*(13), 3553-3562.

Lawrence, C. J., Seigfried, T. E., & Brendel, V. (2005). The maize genetics and genomics database. The community resource for access to diverse maize data. *Plant physiology, 138*(1), 55-58.

Lebreton, C., Lazić-Jančić, V., Steed, A., Pekić, S., & Quarrie, S. A. (1995). Identification of QTL for drought responses in maize and their use in testing causal relationships between traits. *Journal of Experimental Botany, 46*(7), 853-865.

Li, J. Z., Zhang, Z. W., Li, Y. L., Wang, Q. L., & Zhou, Y. G. (2011). QTL consistency and meta-analysis for grain yield components in three generations in maize. *Theoretical and Applied Genetics, 122*(4), 771-782.

Li, W. T., Liu, C., Liu, Y. X., Pu, Z. E., Dai, S. F., Wang, J. R., ... & Wei, Y. M. (2013). Meta-analysis of QTL associated with tolerance to abiotic stresses in barley. *Euphytica*, *189*(1), 31-49.

Liu, J., Li, J., Chen, F., Zhang, F., Ren, T., Zhuang, Z., & Mi, G. (2008). Mapping QTLs for root traits under different nitrate levels at the seedling stage in maize (Zea mays L.). *Plant and Soil*, *305*(1-2), 253-265.

Liu, J., Cai, H., Chu, Q., Chen, X., Chen, F., Yuan, L., ... & Zhang, F. (2011). Genetic analysis of vertical root pulling resistance (VRPR) in maize using two genetic populations. *Molecular breeding*, *28*(4), 463-474.

Mano, Y., & Omori, F. (2008). Verification of QTL controlling root aerenchyma formation in a maize* teosinte" Zea nicaraguensis" advanced backcross population. *Breeding Science*, *58*(3), 217-223.

Messmer, R., Fracheboud, Y., Baenziger, M., Stamp, P., & Ribaut, J.-M. (2011). Drought stress and tropical maize: QTLs for leaf greenness, plant senescence, and root capacitance. *Field Crops Research*, *124*(1).

Osman, K. A., Tang, B., Wang, Y., Chen, J., Yu, F., Li, L., ... & Qiu, F. (2013). Dynamic QTL analysis and candidate gene mapping for waterlogging tolerance at maize seedling stage. *PloS one*, *8*(11).

Ruta, N., Stamp, P., Liedgens, M., Fracheboud, Y., & Hund, A. (2010a). Collocations of QTLs for seedling traits and yield components of tropical maize under water stress conditions. *Crop science*, *50*(4), 1385-1392.

Ruta, N., Liedgens, M., Fracheboud, Y., Stamp, P., & Hund, A. (2010b). QTLs for the elongation of axile and lateral roots of maize in response to low water potential. *Theoretical and Applied Genetics*, *120*(3), 621-631.

Sala, R. G., Andrade, F. H., & Cerono, J. C. (2012). Quantitative trait loci associated with grain moisture at harvest for line per se and testcross performance in maize: a meta-analysis. *Euphytica*, *185*(3), 429-440. doi: 10.1007/s10681-011-0614-8

Salvi, S., & Tuberosa, R. (2005). To clone or not to clone plant QTLs: present and future challenges. *Trends in Plant Science*, *10*(6), 297-304. doi: 10.1016/j.tplants.2005.04.008

Salvi, S., & Tuberosa, R. (2015). The crop QTLome comes of age. Curr Opin Biotechnol, 32C, 179-185.

Salvi, S., Tuberosa, R., Chiapparino, E., Maccaferri, M., Veillet, S., van Beuningen, L., . . . Phillips, R. L. (2002). Toward positional cloning of Vgt1, a QTL controlling the transition from the vegetative to the reproductive phase in maize. *Plant Molecular Biology*, *48*(5), 601-613. doi: 10.1023/a:1014838024509

Semagn, K., Beyene, Y., Warburton, M. L., Tarekegne, A., Mugo, S., Meisel, B., . . . Prasanna, B. M. (2013). Meta-analyses of QTL for grain yield and anthesis silking interval in 18 maize populations evaluated under water-stressed and well-watered environments. *BMC Genomics*, *14*, 313.

Sosnowski, O., Charcosset, A., & Joets, J. (2012). BioMercator V3: an upgrade of genetic map compilation and quantitative trait loci meta-analysis algorithms. *Bioinformatics*, *28*(15), 2082-2083.

Trachsel, S., Messmer, R., Stamp, P., & Hund, A. (2009). Mapping of QTLs for lateral and axile root growth of tropical maize. *Theoretical and Applied Genetics*, *119*(8), 1413-1424.

Tuberosa, R., Sanguineti, M. C., Landi, P., Michela Giuliani, M., Salvi, S., & Conti, S. (2002). Identification of QTLs for root characteristics in maize grown in hydroponics and analysis of their overlap with QTLs for grain yield in the field at two water regimes. *Plant Molecular Biology*, *48*(5).

Tuberosa, R., Salvi, S., Sanguineti, M. C., Maccaferri, M., Giuliani, S., & Landi, P. (2003). Searching for quantitative trait loci controlling root traits in maize: a critical appraisal. In *Roots: The Dynamic Interface between Plants and the Earth* (pp. 35-54). Springer Netherlands.

Uga, Y., Sugimoto, K., Ogawa, S., Rane, J., Ishitani, M., Hara, N., . . . Yano, M. (2013). Control of root system architecture by DEEPER ROOTING 1 increases rice yield under drought conditions. *Nat Genet, 45*(9), 1097-1102. doi: 10.1038/ng.2725

Utz, H. F. (2001). PLABSTAT: a computer program for statistical analysis of plant breeding experiments. *Institute for Plant Breeding, Seed Science and Population Genetics, University of Hohenheim, Stuttgart*.

van Beem, J., Smith, M. E., & Zobel, R. W. (1998). Estimating root mass in maize using a portable capacitance meter. *Agronomy Journal, 90*(4).

Veyrieras, J. B., Goffinet, B., & Charcosset, A. (2007). MetaQTL: a package of new computational methods for the meta-analysis of QTL mapping experiments. *BMC bioinformatics*, *8*(1), 49.

Wang, Y., Huang, Z., Deng, D., Ding, H., Zhang, R., Wang, S., ... & Xu, X. (2013). Meta-analysis combined with syntenic metaQTL mining dissects candidate loci for maize yield. *Molecular breeding*, *31*(3), 601-614.

Wen, T. J., & Schnable, P. S. (1994). Analyses of mutants of 3 genes that influence root hair development in zea-mays (gramineae) suggest that root hairs are dispensable. *American Journal of Botany, 81*(7), 833-842. doi: 10.2307/2445764

Woll, K., Borsuk, L. A., Stransky, H., Nettleton, D., Schnable, P. S., & Hochholdinger, F. (2005). Isolation, characterization, and pericycle-specific transcriptome analyses of the novel maize lateral and seminal root initiation mutant rum1. *Plant Physiology*, *139*(3), 1255-1267. doi: 10.1104/pp.105.067330

Xiang, K., Reid, L. M., Zhang, Z.-M., Zhu, X.-Y., & Pan, G.-T. (2012). Characterization of correlation between grain moisture and ear rot resistance in maize by QTL meta-analysis. *Euphytica*, *183*(2), 185-195. doi: 10.1007/s10681-011-0440-z

Zhang, X., Tang, B., Yu, F., Li, L., Wang, M., Xue, Y., ... & Qiu, F. (2013). Identification of major QTL for waterlogging tolerance using genome-wide association and linkage mapping of maize seedlings. *Plant Molecular Biology Reporter*, *31*(3), 594-606.

Zhu, J., Kaeppler, S. M., & Lynch, J. P. (2005a). Mapping of QTLs for lateral root branching and length in maize (Zea mays L.) under differential phosphorus supply. *Theoretical and Applied Genetics*, *111*(4), 688-695.

Zhu, J., Kaeppler, S. M., & Lynch, J. P. (2005). Mapping of QTL controlling root hair length in maize (Zea mays L.) under phosphorus deficiency. *Plant and Soil*, *270*(1), 299-310.

5 Comparative transcriptomics of *qroot-yield-1.06* NILs

5.1 Introduction

Drought is the most devastating abiotic stress limiting global food production (Tuberosa and Salvi 2006), since water availability is critical for plant development. Consequently, food security depends on the release of cultivars with improved resistance to drought conditions and with high yield stability (Tuberosa 2012). Drought resistance is shaped by two main strategies: dehydration avoidance and dehydration tolerance (Blum 2011). The first pathway implies the capacity to avoid plant components dehydration under drought stress, and traits mainly responsible are related to plant development and size, roots, plant surface, osmotic adjustments and "stay green" (Blum 2011).

Root traits are an interesting target for programs in crop breeding for drought resistance. Roots play essential functions in water acquisition and are a key element of plant adaptation in water-limited environments (Lynch *et al.,* 2012). Root architecture and size have a fundamental role in the water balance of the plant considering that roots are the principal mechanism for meeting transpiration demand (Blum, 2011). However, a greater comprehension of how functional root traits are connected with the general plant strategies under drought conditions is needed (Comas *et al.,* 2013). Progress in genomics platforms, sequencing and bioinformatics has allowed evaluating drought tolerance as a whole based on the study of the combined expression of thousands of genes and their products controlling drought tolerance (Shinozaki *et al.,* 2007; Xu *et al.,* 2014).

In maize, gene expression profile experiments using microarray hybridization (Meyers *et al.,* 2004) have been done in the past to interpret transcriptional changes upon water deficit, on seedlings (Zheng *et al.,* 2004), the developing ear and tassel (Zhuang *et al.,* 2007) and roots (Poroyko *et al.,* 2007; Yamaguchi and Sharp 2010; Spollen *et al.,* 2008). Currently, high-throughput sequencing methods have been extended to transcriptome analysis by what is known as RNA-seq (RNA sequencing) (Wang *et al.,* 2009). RNA-seq is becoming the standard method for quantifying RNA expression levels and for identifying the differentially expressed genes in two o more conditions (Rapaport *et al.,* 2013) due to the clear advantages of the method respect to microarray technology (Malone and Oliver, 2011). RNA-Seq studies have been conducted in maize to identify the differentially expressed genes (DEGs) in response to water deficits comparing the transcriptomes of meristems (Kakumanu *et al.,* 2012) and primary roots (Opitz *et al.,* 2014) of stressed and control

plants. Both studies reported the complex transcriptional regulation to water deficit response depended on duration and intensity of the treatment.

In the present work we used RNA-seq approach to analyze transcript profiles of the *qroot-yield-1.06* NILs, how profiles changed at different developmental stages and drought stress treatments. We expect that RNA-seq experiments should shed light on the genetic basis of the observed differences between NILs and thus *qroot-yield-1.06* QTL alleles.

5.2 Material and methods

5.2.1 Plant material and stress treatment

Experiment was conducted with the *root-yield-1.06* pair of NILs 157(--) and NIL158 (++). Seeds were surface-sterilized and pre-germinated in Petri dishes for 48 h at 25 ^{0}C in the dark. Homogeneous seedlings were transferred into pots containing peat and sand (3:1) and were grown under greenhouse conditions (day: 16 h, 26–28 °C, with supplemental light 500 μE m^{-2} s^{-1} photosynthetic photon flux density; night: 16 °C). At the four-leaf stage plants were subjected to a 'drought stress treatment'.

The experiment included two replications, each one consisting of four pots for each treatment. Each pot contained six plants (three plants/genotype). Pots were distributed according to a completely randomized design and their positions were changed daily. Pots were weighed and watered daily until the four-leaf stage, when water stress (WS) treatment was started by withholding water. Leaf samples (third leaf) were collected at mid-day of day 7 (7d) and day 22 (22d) of the beginning of WS treatment, from both treated and control plants. At day 23 after starting the WS treatment, plants were irrigated again (rehydration), and leaf tissue was collected one day later at mid-day (RH). Samples were frozen in liquid nitrogen and stored at -80 C.

5.2.2 RNA extraction and sequencing

RNA was extracted using the RNeasy Plus Mini Kit (QIAGEN) for a total of 48 samples corresponding to: 2 genotypes x 2 treatments x 2 tissues x 3 samplings x 2 replications. RNA quality and quantification were checked running an agarose gel 1% and confirmed using Infinite® 200 PRO (TECAN, Mannedorf, Switzerland). Only samples with a 260/280 ratio >1.8 were used for downstream analyses. RNA samples were submitted to 'IGA technology services' (Udine, Italy)

for RNA-seq using a Illumina platform, according to conditions required. 100pb paired-end RNA sequencing was carried out in a 24x multiplexing level, for a total of 10 million of reads per sample.

5.2.3 Processing and mapping of Illumina sequencing reads

Raw sequencing reads were processed and quality trimmed with the tool FastqMcf of ea-utils (Aronesty, 2011). Read mapping was performed with the free open source software STAR_2.4.0 (http://code.google.com/ p/rna-star/) (Dobin *et al.,* 2013). The sub-command *multicov* of Bedtools 2.19.0 was used to count the alignments from position-sorted and indexed BAM files (Quinlan and Hall 2010). Next, functional annotation was carried out using the PEDANT genome database (Frishman *et al.,* 2003) with the gene set MA 5b.

5.2.4 Statistical analysis for evaluating differential gene expression

Statistical analysis was carried out with Voom, a Limma-based method that works with "log-counts normalized for sequence depth, specifically with log-counts per million" (Law *et al.,* 2014). Counts per million (cpm) results of the division of each read count by the corresponding library size in millions.

The experimental setup allowed several comparisons of control groups against different water stress levels (7d, 22d and rehydration) and comparisons between the minus (NIL157) and plus (NIL158) NILs. After computing these contrasts, resulting *p*-values of each contrast were corrected for multiplicity using the false discovery rate (FDR)-approach (Benjamini and Yekutieli, 2001). In addition, a two-way analysis of variance (ANOVA) was accomplished with genotype main effect, treatment main effect and genotype by treatment interaction using RStudio (Version 0.98.1103). Computed *p*-values were corrected for multiplicity using FDR. A transcript was differentially expressed using a fold change (FC) cut-off of -1>FC>1 and significance *p*-values of < 0.001.

5.2.5 Gene Ontology (GO)

GO and KEGG function enrichment analysis to the differentially expressed genes (DEGs) was performed using Blast2GO (Conesa *et al.,* 2005). GO term was assigned to each transcript based on the GO annotations for biological process, molecular function and cellular component.

5.3 Results

5.3.1 Exploration of differentially expressed genes

General comparisons between transcripts of the two genotypes subjected to the two treatments (Control and WS) at different times (7d, 22d and RH) were carried out using the value of NIL157 (--), control sample, at 7d (157_7d_c) as reference. A general FDR (*p*-value correction) for a comparison over all samples in respect to 157_7d_c was computed. Log2 FC values of every single comparison with 157_7d_c were plotted vs –log10 (FDR) to evaluate the general behavior of the two NILs during the time of the experiment for the two treatments (Figure 20).

Figure 20 shows that the number of differentially regulated genes increased from 7d to 22d and RH in both genotypes and treatments, and they are predominantly down-regulated in comparison with the reference. In the specific comparison between allele NIL157 (i.e. '-' allele) and allele NIL158 (ie. '+' allele) in not stressed plants at the 7d time of sampling, a group of genes was expressed only in the NIL158. The count of the DEGs up and down-regulated, selected with the criteria of |FC|≥1 and FDR < 0.01%, supported these previous observations (Figure 21). 2,510 out of the 39,422 genes detected in the RNA-seq experiment were DEGs (i.e. 6%), with 891 (35.4%) and 1,619 (64.5%) up and down-regulated, respectively. The 24% of DEGs mapped to chromosome 1.

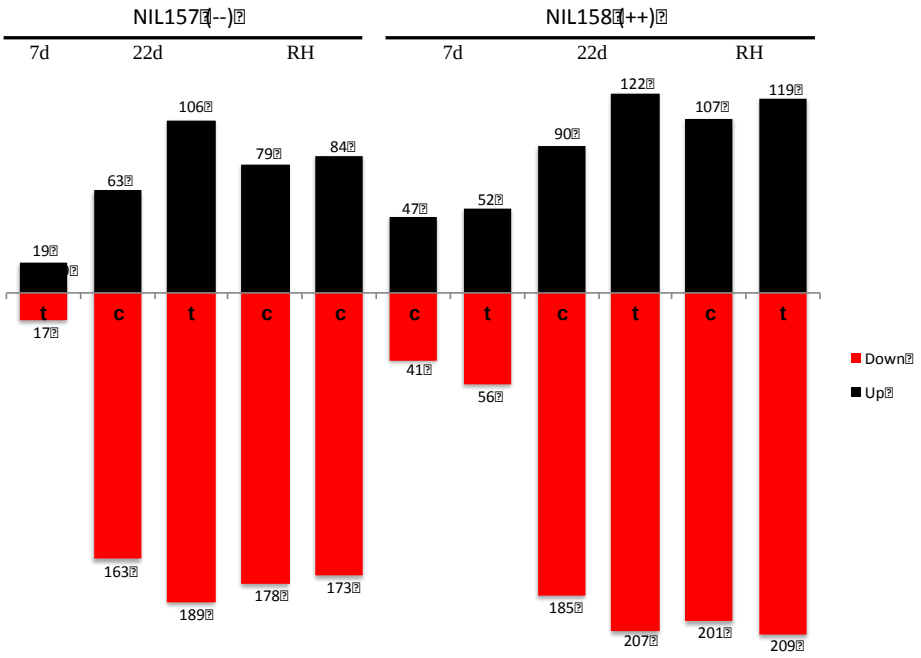

Figure 21. Number of differentially expressed genes. Bars represent up and down-regulated genes in the 11 pairwise comparisons with 157_7d_c. |FC|≥ 1 and FDR < 0.1%. c- control, t – WS treatment.

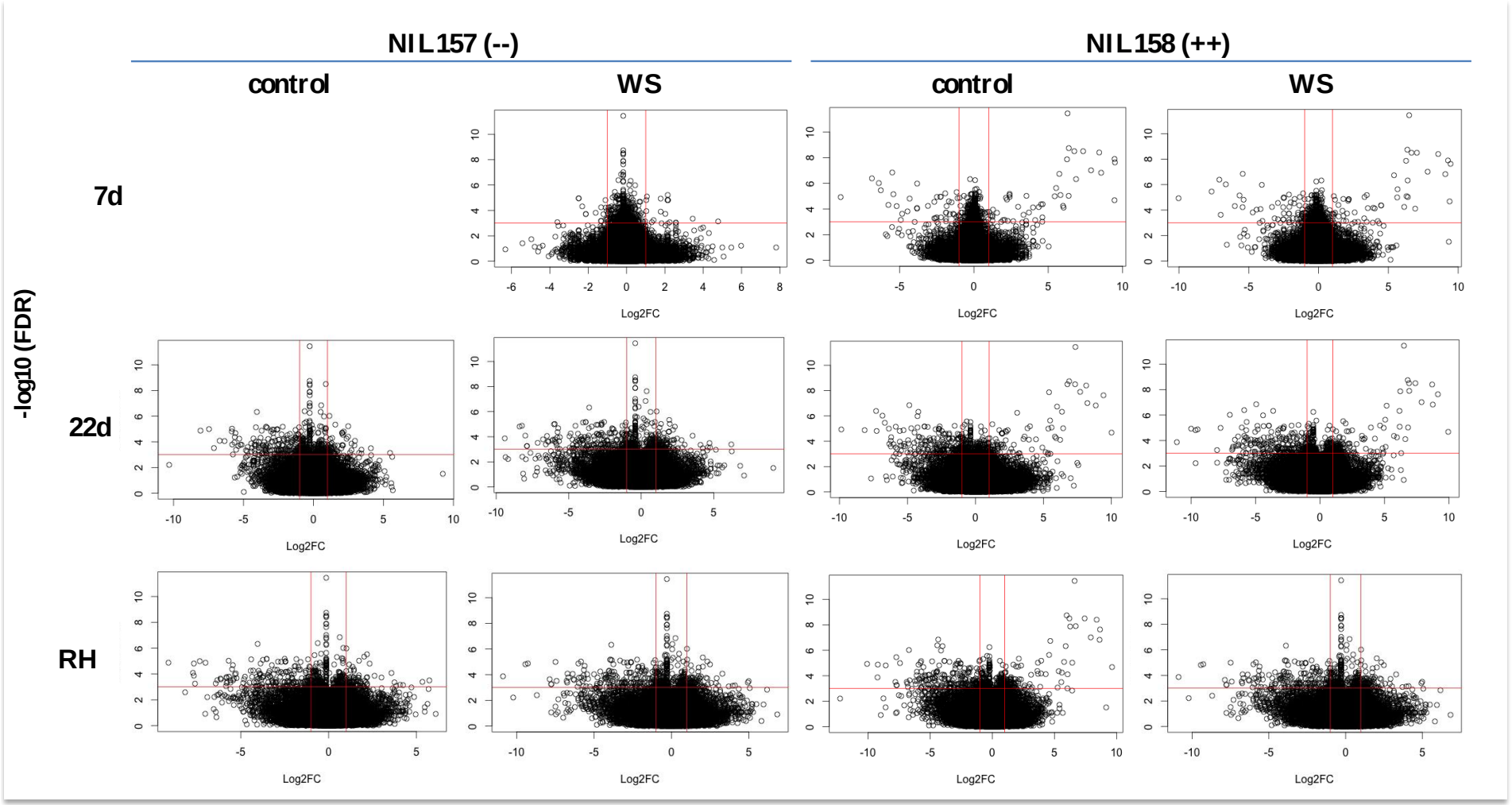

Figure 22. Volcano plot analysis of differentially expressed transcripts. Log FC, calculated for each of the 11 possible comparisons with 157_7d_c, was plotted on the x-axis and the negative log10 FDR was plotted on the y-axis. Red lines show threshold values of $|FC| \geq 1$ and FDR $\leq 0.1\%$ used to select the differentially expressed transcripts. WS- water stress treatment; 7d – 7 days after WS; 22d – 22 days after WS; RH – Rehydration.

For more specific comparisons the FDR value, as computed with the AOV with genotype as main effect, was used to discriminate differential expression between general means of the contrasting NILs. As expected, the stringency increased with the *p*-value recalculated for genotypes (Figure 22). However, for additional specific comparisons between genotypes, treatments and/or time levels, current *p*-value cannot be utilized and will have to be recalculated for the correct discrimination of statistically significant DEGs.

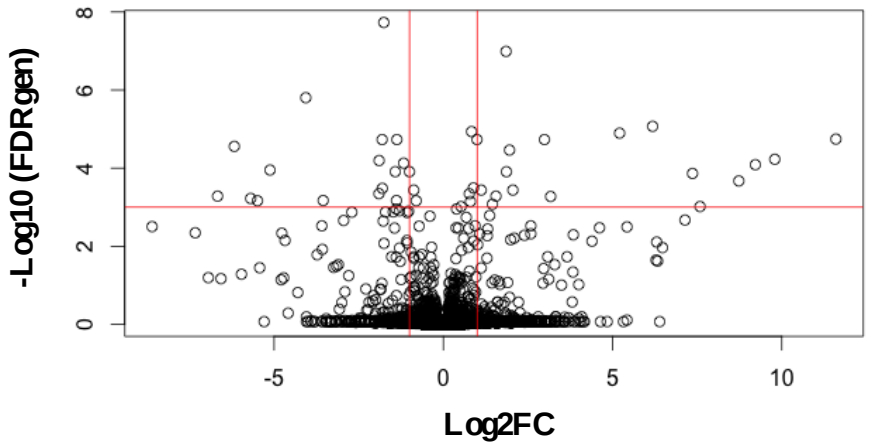

Figure 23. Volcano plot analysis. Log FC was calculated with means comparisons between NIL57 (--) and NIL 158 (++). FDR value was obtained of the AOV with genotype as main effect. Red lines show threshold values of $|FC| \geq 1$ and FDR $\leq 0.1\%$ used to select the differentially expressed transcripts.

5.3.2 Differential expressed genes in the *qroot-yield-1.06*

NILs for the *qroot-yield-1.06* were confirmed to have alternative haplotypes at chromosome bin 1.06, while the rest of their genomes resulted identical and homozygous (Chapter 3). A considerable portion of the total number of DEGs (67%) map to our target QTL interval (i.e. 166.8 to 195.6 Mb in the maize reference map B73RefGen_v02. http://www.maizegdb.org; Andorra *et al.*, 2010), as illustrated by plotting DEGs map physical positions along chromosome 1 (Figure 23).

Table 12 reports the list of DEGs selected on *qroot-yield-1.06* chromosome region. Figure 24 shows DEGs expression calculates as counts per million. Interestingly, genes located in the upper part of the QTL region (i.e. 166.9 Mb to 182.1 Mb) were mainly higher expressed in the NIL 158 (++).

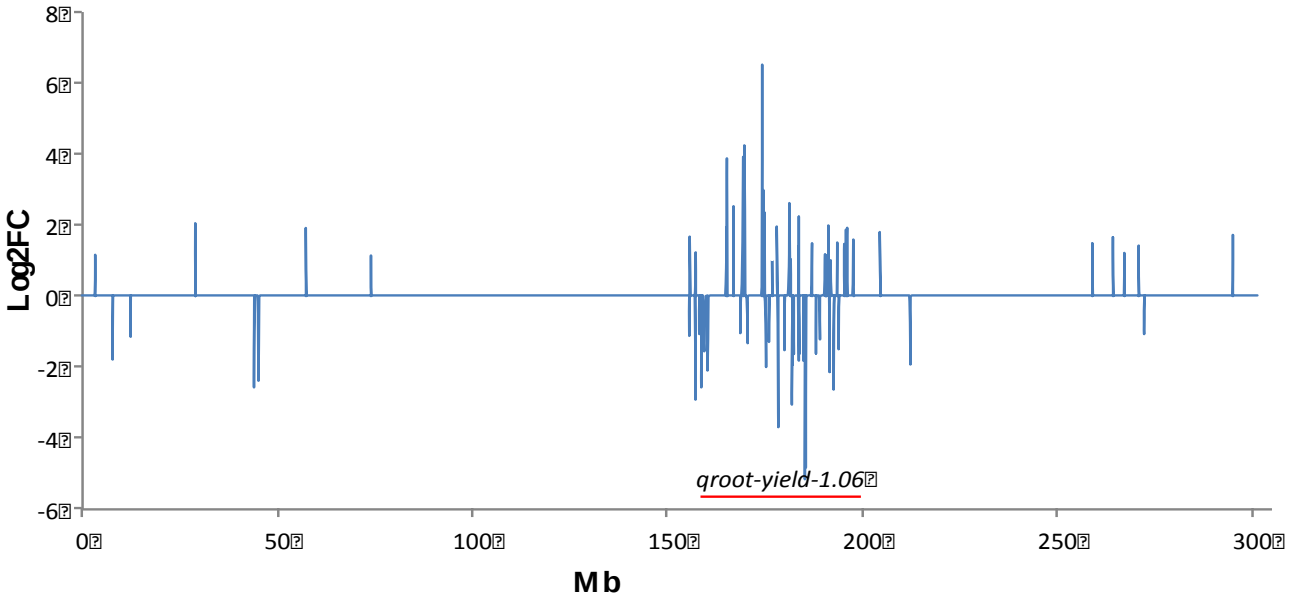

Figure 24. Physical position on the B73_RefGen_v2 reference map (http://www.maizegdb.org) of DEGs detected on chromosome 1. Bars represent the fold change value from the comparison between general means of NIL157 (--) and NIL158 (++) expression.

Table 12. List of DEGs in the *qroot-yield*-1.06 chromosome region. Start and end physical position of transcript model on B73_RefGen_v02 map, strand where the transcript was positioned, the mean of count per million (cpm) values for each NIL, and the FDR value are reported.

GeneID	start	end	strand	157_cpm	158_cpm	FDR
GRMZM2G017405	166927438	166963157	-	1,85	14,67	9,E-06
GRMZM2G069317	169431421	169432980	+	0,00	12,72	1,E-08
GRMZM2G350793	169737427	169740876	+	0,00	19,28	2,E-07
GRMZM2G088375	174300890	174307328	+	0,19	114,23	2,E-05
GRMZM2G164672	174565242	174567097	+	0,01	7,39	3,E-09
GRMZM2G090379	174932178	174933091	+	0,00	3,90	2,E-09
GRMZM2G090411	174934003	174934941	+	0,00	4,23	3,E-09
GRMZM2G023068	176053059	176054692	+	4,23	0,65	6,E-03
GRMZM2G300788	181241954	181245076	-	2,05	0,18	1,E-02
GRMZM2G357455	182098597	182100186	-	0,08	6,06	6,E-05
GRMZM2G023791	182391232	182393687	+	24,98	7,17	4,E-04
GRMZM2G048616	183563865	183564765	+	39,17	11,58	2,E-05
GRMZM2G037615	183592281	183593251	+	0,01	1,60	2,E-06
GRMZM2G037639	183680001	183680573	+	0,02	1,34	1,E-05
GRMZM2G050273	183801615	183805298	-	0,01	3,54	5,E-07
GRMZM2G113726	184911635	184915752	-	26,09	7,45	4,E-04
GRMZM2G137861	185225795	185226599	+	656,03	175,46	6,E-06
GRMZM2G533147	185469108	185472525	+	38,95	0,10	1,E-05

GeneID	start	end	strand	157_cpm	158_cpm	FDR
GRMZM2G134205	188060402	188062129	+	106,96	3,08	1,E-07
AC234203.1	190600745	190603189	+	17,79	5,20	3,E-04
GRMZM2G329750	191263450	191264705	-	3,59	8,84	7,E-03
GRMZM2G006293	175291509	175293495	+	6,81	28,28	1,E-05
GRMZM2G124797	192613104	192614115	-	5,94	0,06	3,E-06
GRMZM2G114841	193873303	193877807	+	12,25	3,63	4,E-03

The specific DEGs for the *qroot-yield-1.06* interval were analyzed for GO category enrichment using Blast2GO. The most significant GO term was "ATP binding" (GO:0005524) for molecular function.

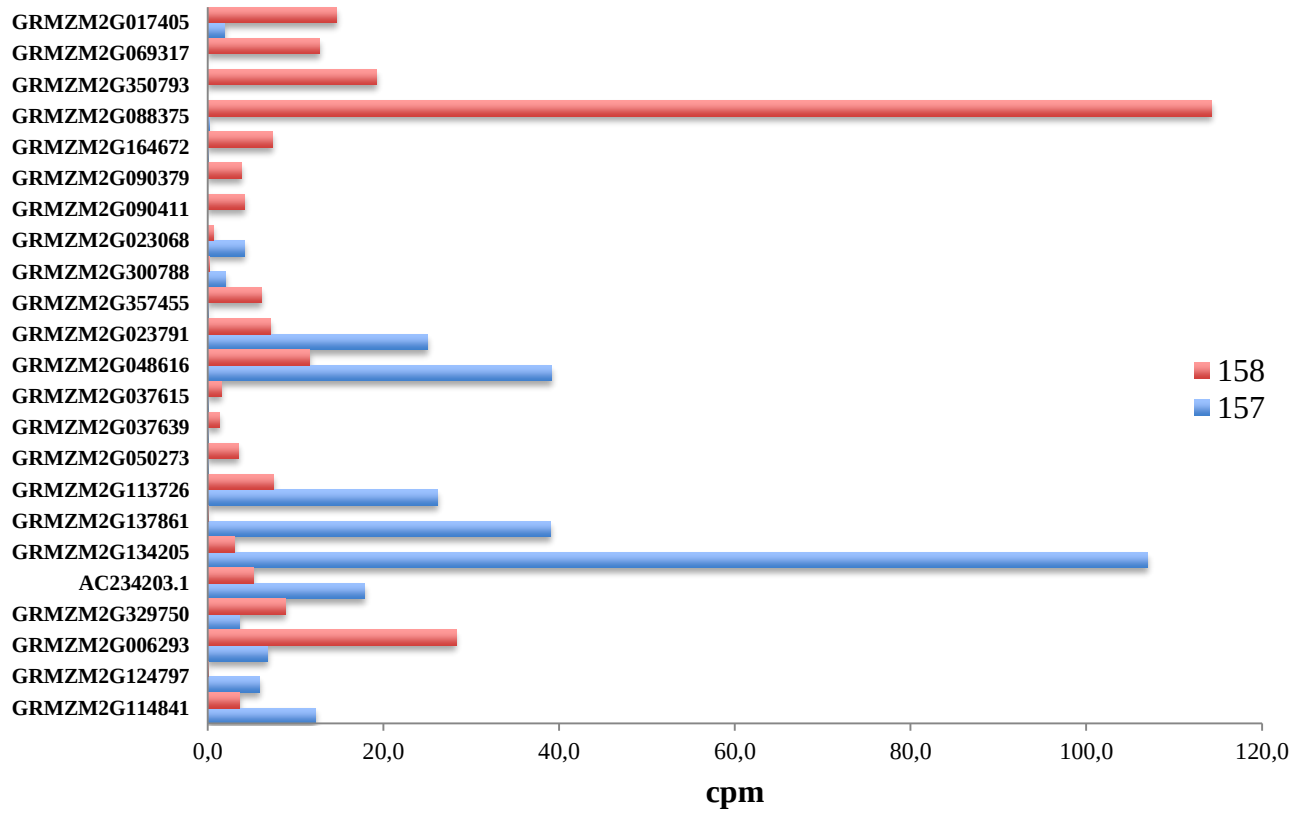

Figure 25. Gene expression quantified as counts per million of the transcripts mapped in the *qroot-yield-1.06* chromosome region.

5.4 Discussion and conclusions

In the present study, RNA-seq was used to compare transcriptomes of NILs with contrasting alleles at *qroot-yield-1.06* in drought-stressed and control conditions (i.e. not stressed). In total, 2510 genes were expressed under at least one of the genotype/time/treatment combinations. For the NIL 157 (--), 36, 295 and 257 DEGs were identified with expression changes at 7d to 22d and RH of the WS treatment,

respectively. For the NIL 158 (++) 108, 329 and 328 were differentially expressed at 7d, 22d and RH, respectively. For both NILs, an overrepresentation of down-regulated genes was observed. Similar patterns of altered gene expression in response to intense stress treatment has been reported by Opitz *et al.,* (2014) evaluating the transcriptome responses of primay roots to low water potentials. In addition, it has been reported that responsive genes at an earlier stage of the treatment are a subset of the responsive genes at later stages (Ozturk *et al.,* 2002; Humbert *et al.,* 2013; Opitz *et al.,* 2014). In the evaluation of root transcriptomes in NILs subjected to drought stress in rice, Moumeni *et al.,* (2011) reported that even in a common genetic background, NILs seemed to carry different mechanisms for tolerance to drought. In our case, the group of DEGs for each combination genotype/time treatment will be identified by further statistical analysis. This will enable to better understand if *qroot-yield-1.06* is water-stress responsive or acts mainly constitutively as previously reported (Landi *et al.,* 2002; Tuberosa *et al.,* 2002; Landi *et al.,* 2010).

The presence of genetically alternative haplotypes at chromosome bin 1.06 between NILs for *qroot-yield-1.06* were well evident based on RNA-seq transcript profiles. As expected, we observed a considerable accumulation (67%) of DEGs in our target QTL interval (by considering the physical position of the gene model originating the transcript, based on current genome annotation) of total DEGs found in chromosome 1. The individuation and the analysis of the 24 DEGs in the QTLregion should help to understand the molecular mechanisms underpinning the genetic effects of the two *qroot-yield-1.06* alleles. One interesting observation is that most DEGs located in the upper part of the QTL region (i.e. 166.9 Mb to 182.1 Mb) showed higher expression in NIL 158 (++). Indeed, accordingly with our results reported in Chapter 2 and 3, and to what previously reported (Landi *et al.,* 2010), the allele provided by Lo1016 (i.e. '+' allele) is the QTL allele increasing the value of the traits. Interestingly, the currently most likely *qroot-yield-1.06* map position after the fine-mapping approach (Chapter 3) is within this region.

Very distinct responses to stress, at molecular level, have been reported by evaluating transcript profiles of different organs in the plant (Humbert *et al.,* 2013). In the experiment here described, roots were also collected along with the leaf samples utilized for RNA-seq analysis. RNA-seq is planned on these root samples with the aim to confirm the expression patterns of the *qroot-yield-1.06* candidate genes identified based on the leaf transcriptome.

5.5 References

Alba, R., Fei, Z., Payton, P., Liu, Y., Moore, S. L., Debbie, P., ... & Giovannoni, J. (2004). ESTs, cDNA microarrays, and gene expression profiling: tools for dissecting plant physiology and development. *The Plant Journal*, *39*(5), 697-714.

Andorf, C. M., Lawrence, C. J., Harper, L. C., Schaeffer, M. L., Campbell, D. A., & Sen, T. Z. (2010). The Locus Lookup tool at MaizeGDB: identification of genomic regions in maize by integrating sequence information with physical and genetic maps. *Bioinformatic*s, 26(3), 434-436.

Aronesty, E. (2011). ea-utils : "Command-line tools for processing biological sequencing data"; Expression Analysis, Durham, NC http://code.google.com/p/ea-utils

Benjamini, Y., & Yekutieli, D. (2001). The control of the false discovery rate in multiple testing under dependency. *Annals of statistics*, 1165-1188.

Blum, A. (2011). *Plant water relations, plant stress and plant production* (pp. 11-52). Springer New York.

Comas, L. H., Becker, S. R., Von Mark, V. C., Byrne, P. F., & Dierig, D. A. (2013). Root traits contributing to plant productivity under drought. *Frontiers in plant science*, *4*.

Conesa, A., Götz, S., García-Gómez, J. M., Terol, J., Talón, M., & Robles, M. (2005). Blast2GO: a universal tool for annotation, visualization and analysis in functional genomics research. *Bioinformatics*, *21*(18), 3674-3676.

Dobin, A., Davis, C. A., Schlesinger, F., Drenkow, J., Zaleski, C., Jha, S., ... & Gingeras, T. R. (2013). STAR: ultrafast universal RNA-seq aligner. *Bioinformatics*, *29*(1), 15-21.

Frishman, D., Mokrejs, M., Kosykh, D., Kastenmüller, G., Kolesov, G., Zubrzycki, I., ... & Mewes, H. W. (2003). The PEDANT genome database. *Nucleic acids research*, *31*(1), 207-211.Jansen, L., Hollunder, J., Roberts, I., Forestan, C., Fonteyne, P., Quickenborne, C., ... & Beeckman, T. (2013). Comparative transcriptomics as a tool for the identification of root branching genes in maize. *Plant biotechnology journal*, *11*(9), 1092-1102.

Humbert, S., Subedi, S., Cohn, J., Zeng, B., Bi, Y. M., Chen, X., ... & Rothstein, S. J. (2013). Genome-wide expression profiling of maize in response to individual and combined water and nitrogen stresses. *BMC genomics*, *14*(1), 3.

Kakumanu, A., Ambavaram, M. M., Klumas, C., Krishnan, A., Batlang, U., Myers, E., ... & Pereira, A. (2012). Effects of drought on gene expression in maize reproductive and leaf meristem tissue revealed by RNA-Seq. *Plant physiology*, *160*(2), 846-867.

Landi, P., Sanguineti, M. C., Darrah, L. L., Giuliani, M. M., Salvi, S., Conti, S., & Tuberosa, R. (2002). Detection of QTLs for vertical root pulling resistance in maize and overlap with QTLs for root traits in hydroponics and for grain yield under different water regimes. *Maydica*, *47*(3-4).

Landi, P., Giuliani, S., Salvi, S., Ferri, M., Tuberosa, R., & Sanguineti, M. C. (2010). Characterization of root-yield-1.06, a major constitutive QTL for root and agronomic traits in maize across water regimes. *Journal of Experimental Botany*, *61*(13), 3553-3562.

Law, C. W., Chen, Y., Shi, W., & Smyth, G. K. (2014). Voom: precision weights unlock linear model analysis tools for RNA-seq read counts. *Genome Biol*, *15*(2), R29.

Lynch, J. P., & Brown, K. M. (2012). New roots for agriculture: exploiting the root phenome. *Philosophical Transactions of the Royal Society B: Biological Sciences*, *367*(1595), 1598-1604.

Malone, J. H., & Oliver, B. (2011). Microarrays, deep sequencing and the true measure of the transcriptome. *BMC biology*, *9*(1), 34.

Meyers, B. C., Galbraith, D. W., Nelson, T., & Agrawal, V. (2004). Methods for Transcriptional Profiling in Plants. Be Fruitful and Replicate. *Plant Physiology*,*135*(2), 637–652.

Opitz, N., Paschold, A., Marcon, C., Malik, W. A., Lanz, C., Piepho, H. P., & Hochholdinger, F. (2014). Transcriptomic complexity in young maize primary roots in response to low water potentials. *BMC genomics*, *15*(1), 741.

Ozturk, Z. N., Talamé, V., Deyholos, M., Michalowski, C. B., Galbraith, D. W., Gozukirmizi, N., ... & Bohnert, H. J. (2002). Monitoring large-scale changes in transcript abundance in drought-and salt-stressed barley. *Plant molecular biology*, *48*(5-6), 551-573.

Poroyko, V., Spollen, W. G., Hejlek, L. G., Hernandez, A. G., LeNoble, M. E., Davis, G., ... & Bohnert, H. J. (2007). Comparing regional transcript profiles from maize primary roots under well-watered and low water potential conditions. *Journal of experimental botany*, *58*(2), 279-289.

Quinlan, A. R., & Hall, I. M. (2010). BEDTools: a flexible suite of utilities for comparing genomic features. *Bioinformatics*, *26*(6), 841-842.

Rapaport, F., Khanin, R., Liang, Y., Pirun, M., Krek, A., Zumbo, P., ... & Betel, D. (2013). Comprehensive evaluation of differential gene expression analysis methods for RNA-seq data. *Genome Biol*, *14*(9), R95.

Shinozaki K, Yamaguchi-Shinozaki K: Gene networks involved in drought stress response and tolerance. *J Exper Botany* 2007, 58(2):221–227.

Spollen, W. G., Tao, W., Valliyodan, B., Chen, K., Hejlek, L. G., Kim, J. J., ... & Nguyen, H. T. (2008). Spatial distribution of transcript changes in the maize primary root elongation zone at low water potential. *BMC plant biology*, *8*(1), 32.

Tuberosa, R. (2012). Phenotyping for drought tolerance of crops in the genomics era. *Frontiers in physiology*, *3*.

Tuberosa, R., Sanguineti, M. C., Landi, P., Michela Giuliani, M., Salvi, S., & Conti, S. (2002). Identification of QTLs for root characteristics in maize grown in hydroponics and analysis of their overlap with QTLs for grain yield in the field at two water regimes. Plant Molecular Biology, 48(5).

Tuberosa, R., & Salvi, S. (2006). Genomics-based approaches to improve drought tolerance of crops. *Trends in plant science*, *11*(8), 405-412.

Wang, Z., Gerstein, M., & Snyder, M. (2009). RNA-Seq: a revolutionary tool for transcriptomics. *Nature Reviews Genetics*, *10*(1), 57-63.

Xu, J., Yuan, Y., Xu, Y., Zhang, G., Guo, X., Wu, F., ... & Lu, Y. (2014). Identification of candidate genes for drought tolerance by whole-genome resequencing in maize. *BMC plant biology*, *14*(1), 83.

Yamaguchi, M., & Sharp, R. E. (2010). Complexity and coordination of root growth at low water potentials: recent advances from transcriptomic and proteomic analyses. Plant, cell & environment, 33(4), 590-603.

Zheng, J., Zhao, J., Tao, Y., Wang, J., Liu, Y., Fu, J., ... & Wang, G. (2004). Isolation and analysis of water stress induced genes in maize seedlings by subtractive PCR and cDNA macroarray. *Plant molecular biology*, *55*(6), 807-823.

Zhuang, Y., Ren, G., Yue, G., Li, Z., Qu, X., Hou, G., ... & Zhang, J. (2007). Effects of water-deficit stress on the transcriptomes of developing immature ear and tassel in maize. *Plant cell reports*, *26*(12), 2137-2147.

6 General discussion

Even with the recent advances in genomic technologies and the availability of the maize genome sequence (Schnable *et al.,* 2009), none of the hundreds of maize root QTLs so far reported has been cloned. Phenotyping for root traits in large populations remains a bottleneck in root genetic analysis including investigations aimed at QTL cloning (Zhu *et al* 2011). Many protocols have been developed for root analysis in controlled conditions (Iyer-Pascuzzi *et al.,* 2010, Grift *et al.,* 2011, Nagel *et al.,* 2012, Lobet and Draye, 2013) but, the main concern with these artificial systems is usually weak or at the best-unknown correlation with field conditions (Lynch and Brown 2012). Field grown plants are controlled by very large interactions between root and soil, extremely variable among experiments, that imply that the observed effect of a given QTL in one experiment may not be repeatable in a different one (Mai *et al.,* 2014). This is a general problem of QTL studies, and of breeding practices trying to capitalize on QTL information. As already recognized, a quantitative trait phenotype in one individual is typically the result of non-linear responses to a large number of factors, of genetic and environmental origin (Salvi and Tuberosa 2015). Consequently, one of the main purposes of our work was to improve a field root phenotyping protocol to enable a collection of quantity and quality data suitable for selection in breeding programs and for mapping and cloning purposes, in our case for *qroot-yield-1.06*.

The results presented in this study show that shovelomics (Trachsel *et al* 2011) combined with image-based analysis with specialized software (Bucksch *et al.,* 2014, Galkovskyi *et al.,* 2012, Colombi *et al.,* 2015) can be adopted to enable a level of phenotypic investigation suitable for genetic mapping and physiological studies. Shovelomics, even if labor intense, allowed a rapid visualization of excavated and washed root crowns giving visual scores to traits determining root architecture. However, limitations were noticed in terms on objectivity and throughput of the method. The combination with image-based analyses enables to the automatic testing of many root architectural traits in a high-throughput way. Nevertheless, the analysis was strongly dependent upon the quality of the root images collected and a new imaging set has to be adopted.

Improved phenotyping protocol and marker saturation, allowed to identify recombinants lines at the *qroot-yield-1.06* region. A new interval of 4.1 Mb was correlated with the target QTL phenotypic expression. On the contrary, even *qroot-yield-1.06* was initially described collecting several easily measurable traits at an early growth stage of plants grown in hydroponics (Tuberosa *et al.,* 2002), the

segregation at *qroot-yield-1.06* could not be associated with any seedling-based traits, according with our results in the greenhouse experiment.

Complementary approaches, which could help in QTL cloning as QTL meta-analysis and expression analysis of genes within the candidate region (Norton *et al.,* 2008), were evaluated in the present study. Meta-analysis, conducted with the software packages BioMercator (Arcade *et al.,* 2004, Sosnowski *et al.,* 2012), enabled large set of previously generated root QTL data to be grouped in meta QTLs (mQTLs). Particularly, on bin 1.06 that has been highlighted as an important region of QTL clustering (Tuberosa *et al.,* 2007), two mQTLs were located unlike a single mQTL reported by Landi *et al.,* (2010). Interestingly, fine mapping advances on *qroot-yield-1.06* showed than the new interval of the QTL correspond to the position of the mQTL reported by Landi *et al.,* (2010) but at the same time co-localizes in some extent with both mQTLs. Confidence intervals (CI) of the resulting mQTLs (4.6 and 6 cM) were shorter than CI of corresponding QTLs in the cluster. This reduction of the CI was used to prioritize candidate genes inside the target QTL and additional reduction of the number of candidate genes was expected from the comparative study of transcriptional profiles of *qroot-yield-1.06* contrasting NILs. However, none of the genes listed inside the mQTL were differentially expressed.

Even though the limitations of meta-analysis, the presence of two mQTLs inside the *q-root-yield-1.06* interval could also suggest the possibility that two linked loci are responsible to the positive association among root traits and other agronomical traits. Landi *et al.,* (2010) suggested that the consistent association among traits was concurrently controlled by the same gene/s. However, in the present study, only a mild phenotypic effect for PH was associated to *qroot-yield-1.06.* The fine mapping and cloning of the *qroot-yield-1.06* will resolve if QTL cluster results from a pleiotropic gene or from multiple linked genes.

The mapping resolution obtained so far is still too limited for identifying the gene or even to shortlist a small number of candidate genes. However, the reduction of the *qroot-yield-1.06* interval and the availability of 83 NILs carrying recombinants events in this region, will provide a potential map resolution around the QTL of ca. 49 kb, which corresponds to the average gene density per kilobase in maize (i.e. one gene every 43.5 kb) (Haberer *et al.,* 2005). Such resolution seems sufficient to identify at least one marker tightly linked to and physically placed on the same BAC/YAC clone. In addition, comparative transcriptomics of NILs revealed a differential response of genes inside the *qroot-yield-1.06* interval that will enable us to select the candidate genes responsible for our target QTL.

Table S1. Genotypes of F4 families that will be evaluated in the summer 2015. In yellow minus allele provided by Lo964; in green plus allele provided by Lo1016. The enclosed part in the rectangle shows the 4.1 Mb interval, most likely carrying *qroot-yield-1.06*. Families carrying recombinant events in this region are highlighted in blue.

	PZE-101129304	SYN10174	PZE-101133216	PZE-101133651	PZE-101134093	PZE-101134142	PZE-101135508	SYN2406	PZE-101136791	SYN9635	PZE-101138198	SYN13130	PZE-101140981	SYN8998	0192831_0351	SYN1741	PZE-101143985	PUT-163a-13178383-177	SYN37120
Lines	**3,8**	**5,4**	**6,2**	**6,7**	**7,1**	**7,3**	**8,6**	**9,0**	**9,4**	**9,6**	**10,2**	**14,8**	**15,7**	**17,4**	**17,7**	**18,4**	**18,8**	**20,7**	**21,4**
15	ade	ade	ade	gua	gua	ade	ade	ade	ade	gua	gua	gua	ade	cyt	gua	ade	ade	gua	gua
16	ade	gua	-	ade	ade	gua	gua	gua	gua	ade	ade	ade	gua	ade	ade	cyt	gua	gua	gua
18	gua	ade	ade	gua	gua	ade	ade	ade	ade	gua	ade	ade	gua	ade	ade	cyt	gua	ade	ade
20	ade	gua	gua	ade	ade	gua	gua	gua	gua	ade	ade	ade	gua	ade	ade	cyt	gua	ade	gua
24	gua	ade	ade	gua	gua	ade	gua	gua	gua	ade	ade	ade	gua	ade	ade	cyt	gua	ade	ade
31	gua	ade	ade	gua	gua	ade	ade	ade	ade	gua	gua	gua	ade	ade	ade	cyt	gua	ade	ade
35	gua	ade	ade	gua	gua	ade	ade	ade	ade	gua	gua	gua	ade	ade	ade	cyt	gua	ade	ade
37	ade	ade	ade	gua	gua	ade	ade	ade	ade	gua	gua	gua	ade	cyt	gua	ade	ade	gua	gua
50	gua	ade	ade	gua	gua	ade	ade	ade	ade	gua	gua	ade	gua	ade	ade	cyt	gua	ade	ade
51	ade	gua	gua	ade	ade	gua	gua	gua	gua	ade	ade	gua	ade	cyt	gua	ade	ade	gua	gua
55	gua	ade	ade	gua	gua	ade	ade	ade	ade	gua	gua	ade	gua	ade	ade	cyt	gua	ade	ade
56	ade	gua	gua	ade	ade	gua	gua	gua	gua	ade	gua	gua	ade	cyt	gua	ade	ade	gua	gua
57	ade	gua	gua	ade	ade	gua	gua	gua	gua	ade	ade	ade	ade	cyt	gua	ade	ade	gua	gua
58	gua	ade	ade	gua	gua	ade	ade	ade	ade	gua	gua	ade	gua	ade	ade	cyt	gua	ade	ade
59	ade	gua	gua	ade	ade	gua	gua	gua	gua	ade	ade	ade	gua	ade	ade	ade	ade	gua	gua
60	gua	ade	ade	gua	gua	ade	ade	ade	ade	gua	gua	gua	ade	cyt	gua	ade	ade	ade	ade
61	gua	ade	ade	gua	gua	ade	ade	ade	ade	gua	gua	gua	ade	ade	ade	cyt	gua	ade	ade
62	gua	ade	ade	gua	gua	ade	ade	ade	ade	gua	gua	gua	ade	cyt	gua	ade	ade	ade	ade
63	gua	ade	ade	gua	gua	ade	ade	ade	ade	gua	gua	gua	gua	ade	ade	cyt	gua	ade	ade
64	gua	ade	ade	gua	gua	ade	ade	ade	ade	gua	gua	gua	gua	ade	ade	cyt	gua	ade	ade
65	gua	ade	ade	gua	gua	ade	gua	gua	gua	ade	ade	ade	gua	ade	ade	cyt	gua	ade	ade
66	gua	ade	gua	ade	ade	gua	gua	gua	gua	ade	ade	ade	gua	ade	ade	cyt	gua	ade	ade
67	gua	ade	ade	gua	gua	ade	ade	ade	ade	gua	gua	gua	-	ade	ade	cyt	gua	ade	ade
68	gua	ade	ade	gua	gua	ade	ade	ade	ade	gua	gua	ade	gua	ade	ade	cyt	gua	ade	ade
69	ade	gua	gua	ade	ade	gua	gua	gua	gua	ade	ade	ade	gua	ade	ade	cyt	gua	gua	gua
70	ade	gua	gua	ade	ade	gua	gua	gua	gua	gua	gua	gua	ade	cyt	gua	ade	ade	gua	gua
71	gua	ade	ade	gua	gua	ade	ade	ade	ade	gua	gua	gua	ade	cyt	gua	cyt	gua	ade	ade
72	gua	ade	ade	gua	gua	ade	ade	ade	gua	ade	ade	ade	gua	ade	ade	cyt	gua	ade	ade
73	ade	gua	gua	ade	ade	gua	gua	gua	gua	ade	ade	ade	gua	ade	ade	cyt	gua	gua	gua
74	-	gua	gua	ade	ade	gua	gua	gua	gua	ade	ade	ade	gua	cyt	gua	ade	-	gua	gua
75	ade	gua	ade	gua	gua	ade	ade	ade	ade	gua	gua	gua	ade	cyt	gua	ade	ade	gua	gua
76	gua	ade	-	gua	gua	ade	ade	ade	ade	gua	gua	gua	ade	cyt	gua	ade	gua	ade	ade
77	ade	gua	gua	ade	ade	gua	ade	ade	ade	gua	gua	gua	ade	cyt	gua	ade	ade	gua	gua

Lines	PZE-101129304	SYN10174	PZE-101133216	PZE-101133651	PZE-101134093	PZE-101134142	PZE-101135508	SYN2406	PZE-101136791	SYN9635	PZE-101138198	SYN13130	PZE-101140981	SYN8998	0192831_0351	SYN1741	PZE-101143985	PUT-163a-13178383-177	SYN37120
	3,8	5,4	6,2	6,7	7,1	7,3	8,6	9,0	9,4	9,6	10,2	14,8	15,7	17,4	17,7	18,4	18,8	20,7	21,4
78	gua	ade	ade	gua	gua	ade	ade	ade	-	gua	gua	ade	gua	ade	ade	cyt	gua	ade	ade
79	ade	gua	gua	ade	ade	gua	gua	gua	gua	ade	ade	ade	gua	ade	ade	cyt	gua	gua	gua
80	gua	ade	ade	gua	gua	ade	ade	ade	ade	gua	gua	ade	gua	ade	ade	cyt	gua	ade	ade
81	gua	ade	ade	gua	gua	ade	ade	ade	ade	gua	gua	ade	gua	ade	ade	cyt	gua	ade	ade
82	ade	gua	gua	ade	ade	gua	gua	gua	gua	ade	ade	ade	gua	cyt	gua	ade	ade	gua	gua
83	ade	gua	ade	gua	gua	ade	ade	ade	ade	gua	gua	gua	ade	cyt	gua	ade	ade	gua	gua
84	ade	gua	-	ade	ade	gua	gua	gua	gua	ade	ade	ade	gua	ade	ade	cyt	gua	gua	gua
85	gua	ade	ade	gua	gua	ade	ade	ade	ade	gua	gua	gua	ade	cyt	gua	cyt	gua	ade	ade
86	gua	ade	ade	gua	gua	ade	ade	ade	gua	ade	ade	ade	gua	ade	ade	cyt	gua	ade	ade
87	gua	ade	ade	gua	gua	ade	ade	ade	ade	gua	gua	gua	ade	cyt	gua	ade	ade	ade	ade
88	ade	gua	gua	ade	ade	gua	gua	gua	gua	ade	ade	gua	ade	cyt	gua	ade	ade	gua	gua
89	gua	ade	ade	gua	gua	ade	gua	gua	gua	ade	ade	ade	gua	ade	ade	cyt	gua	ade	ade
90	ade	gua	gua	ade	ade	gua	gua	gua	gua	ade	ade	ade	gua	ade	ade	cyt	gua	gua	gua
91	ade	gua	ade	gua	gua	ade	ade	ade	ade	gua	gua	gua	ade	cyt	gua	ade	ade	gua	gua
92	ade	gua	gua	ade	ade	gua	gua	gua	gua	ade	ade	ade	gua	ade	ade	ade	ade	gua	gua
93	ade	gua	gua	ade	ade	gua	ade	ade	ade	gua	gua	gua	ade	cyt	gua	ade	ade	gua	gua
94	ade	gua	gua	ade	ade	gua	gua	gua	gua	ade	ade	gua	ade	cyt	gua	ade	ade	gua	gua
95	ade	gua	gua	ade	ade	gua	gua	gua	gua	ade	ade	ade	gua	ade	ade	cyt	gua	gua	gua
96	gua	ade	ade	gua	gua	ade	gua	gua	gua	ade	ade	ade	gua	ade	ade	cyt	gua	ade	ade
97	ade	gua	gua	ade	ade	gua	ade	ade	ade	gua	gua	gua	ade	cyt	gua	ade	ade	gua	gua
98	ade	gua	gua	ade	gua	ade	ade	ade	ade	gua	gua	gua	ade	cyt	gua	ade	ade	gua	gua
99	gua	ade	ade	gua	gua	ade	ade	ade	ade	gua	gua	ade	gua	ade	ade	cyt	gua	ade	ade
100	gua	ade	ade	gua	gua	ade	ade	ade	ade	gua	gua	ade	gua	ade	ade	cyt	gua	ade	ade
101	ade	gua	gua	ade	ade	gua	gua	gua	gua	ade	ade	gua	ade	cyt	gua	ade	ade	gua	gua
102	ade	gua	gua	ade	ade	gua	gua	gua	gua	ade	ade	ade	gua	ade	ade	cyt	gua	gua	gua
103	gua	ade	ade	gua	gua	ade	ade	ade	ade	gua	gua	gua	ade	ade	ade	cyt	gua	ade	ade
104	gua	ade	ade	gua	gua	ade	ade	ade	ade	gua	gua	gua	ade	cyt	gua	ade	ade	ade	ade
105	ade	gua	gua	ade	ade	gua	gua	gua	gua	ade	ade	ade	gua	ade	ade	ade	ade	gua	gua
106	gua	ade	ade	gua	gua	ade	ade	ade	ade	gua	gua	gua	ade	ade	ade	cyt	gua	ade	ade
107	ade	gua	gua	ade	ade	gua	gua	gua	ade	gua	gua	gua	ade	cyt	gua	ade	ade	gua	gua
108	gua	ade	ade	gua	gua	ade	ade	ade	ade	gua	gua	gua	ade	ade	ade	cyt	gua	ade	ade
109	gua	ade	ade	gua	gua	ade	ade	ade	ade	gua	gua	ade	gua	ade	ade	cyt	gua	ade	ade
110	ade	gua	gua	ade	ade	gua	ade	ade	ade	gua	gua	gua	ade	cyt	gua	ade	ade	gua	gua
111	gua	ade	ade	gua	ade	gua	gua	gua	gua	ade	ade	ade	gua	ade	ade	cyt	gua	ade	ade
112	ade	gua	-	ade	ade	gua	gua	gua	gua	ade	ade	ade	ade	cyt	gua	ade	ade	gua	gua
113	gua	ade	ade	gua	gua	ade	gua	gua	gua	ade	ade	ade	gua	ade	ade	cyt	gua	ade	ade
114	ade	gua	gua	ade	ade	-	gua	gua	gua	ade	ade	gua	ade	cyt	gua	ade	ade	gua	gua
115	ade	gua	gua	ade	ade	gua	gua	gua	gua	ade	ade	ade	gua	ade	ade	cyt	gua	gua	gua
116	gua	ade	ade	gua	gua	ade	ade	ade	ade	gua	gua	gua	ade	cyt	gua	cyt	gua	ade	ade
117	gua	ade	ade	gua	gua	ade	ade	ade	ade	gua	gua	ade	gua	ade	ade	cyt	gua	ade	ade

	PZE-101129304	SYN10174	PZE-101133216	PZE-101133651	PZE-101134093	PZE-101134142	PZE-101135508	SYN2406	PZE-101136791	SYN9635	PZE-101138198	SYN13130	PZE-101140981	SYN8998	0192831_0351	SYN1741	PZE-101143985	PUT-163a-13178383-177	SYN37120
Lines	**3,8**	**5,4**	**6,2**	**6,7**	**7,1**	**7,3**	**8,6**	**9,0**	**9,4**	**9,6**	**10,2**	**14,8**	**15,7**	**17,4**	**17,7**	**18,4**	**18,8**	**20,7**	**21,4**
118	ade	gua	gua	ade	ade	gua	gua	gua	gua	ade	ade	ade	gua	cyt	gua	ade	ade	gua	gua
119	ade	gua	gua	ade	ade	gua	gua	gua	gua	ade	ade	ade	gua	ade	ade	cyt	gua	gua	gua
120	ade	gua	gua	ade	ade	-	gua	ade	ade	gua	gua	gua	ade	cyt	gua	ade	ade	gua	gua
121	gua	ade	ade	gua	gua	ade	ade	ade	ade	gua	gua	gua	ade	cyt	gua	ade	ade	ade	ade
122	ade	gua	gua	ade	ade	gua	gua	ade	ade	gua	gua	gua	ade	cyt	gua	ade	ade	gua	gua
123	ade	gua	gua	ade	ade	gua	gua	gua	gua	ade	ade	ade	gua	cyt	gua	ade	ade	gua	gua
124	gua	ade	ade	gua	ade	gua	gua	gua	gua	ade	ade	ade	gua	ade	ade	cyt	gua	ade	ade
125	gua	ade	ade	gua	gua	ade	ade	ade	gua	ade	ade	ade	gua	ade	ade	cyt	gua	ade	ade
126	gua	ade	ade	gua	gua	ade	ade	ade	ade	gua	gua	ade	gua	ade	ade	cyt	gua	ade	ade
127	gua	ade	ade	gua	gua	ade	-	ade	ade	gua	gua	gua	ade	cyt	gua	ade	ade	ade	ade
128	gua	ade	ade	gua	gua	ade	gua	gua	gua	ade	ade	ade	gua	ade	ade	cyt	gua	ade	ade
129	ade	gua	gua	ade	ade	gua	gua	gua	gua	ade	ade	ade	gua	ade	ade	cyt	gua	gua	gua
130	gua	ade	ade	gua	gua	ade	ade	ade	ade	gua	gua	gua	gua	ade	ade	cyt	gua	ade	ade
131	ade	gua	gua	ade	ade	gua	ade	ade	-	gua	gua	gua	ade	cyt	gua	ade	ade	gua	gua
132	gua	ade	ade	gua	gua	ade	gua	gua	gua	ade	ade	ade	gua	ade	ade	cyt	gua	ade	ade
133	ade	gua	gua	ade	ade	gua	ade	ade	ade	gua	gua	gua	ade	cyt	gua	ade	ade	gua	gua
134	gua	ade	ade	gua	gua	ade	ade	ade	ade	gua	gua	gua	ade	cyt	gua	ade	ade	ade	ade
135	ade	gua	gua	ade	gua	ade	ade	ade	ade	gua	gua	gua	ade	cyt	gua	ade	ade	gua	gua
136	gua	ade	ade	gua	gua	ade	ade	ade	ade	gua	ade	ade	gua	ade	ade	cyt	gua	ade	ade
137	ade	gua	gua	ade	ade	gua	ade	ade	ade	gua	gua	gua	ade	cyt	gua	ade	ade	gua	gua
138	ade	gua	gua	ade	ade	gua	gua	gua	gua	ade	ade	ade	gua	cyt	gua	ade	ade	gua	gua
139	gua	ade	ade	gua	gua	ade	ade	ade	ade	gua	gua	gua	ade	cyt	gua	ade	ade	ade	ade
140	ade	gua	gua	ade	ade	gua	gua	gua	gua	ade	ade	ade	gua	ade	ade	cyt	gua	gua	gua
141	gua	ade	ade	gua	gua	ade	gua	gua	gua	ade	ade	ade	gua	ade	ade	cyt	gua	ade	ade
142	gua	ade	ade	gua	gua	ade	ade	ade	ade	gua	gua	gua	ade	cyt	gua	cyt	gua	ade	ade
143	ade	gua	gua	ade	ade	gua	gua	gua	gua	ade	ade	ade	gua	ade	ade	cyt	ade	gua	gua
144	ade	gua	gua	ade	ade	gua	ade	-	ade	gua	gua	gua	-	cyt	gua	ade	ade	gua	gua
145	gua	ade	ade	gua	gua	ade	ade	ade	ade	gua	gua	ade	gua	ade	ade	cyt	gua	ade	ade
146	gua	ade	ade	-	gua	ade	ade	ade	ade	gua	gua	ade	gua	ade	ade	cyt	gua	ade	ade
147	gua	ade	ade	gua	gua	ade	ade	ade	ade	gua	gua	gua	gua	ade	ade	cyt	gua	ade	ade
148	ade	gua	gua	ade	ade	gua	ade	ade	ade	gua	gua	gua	ade	cyt	gua	ade	ade	gua	gua
149	ade	gua	gua	ade	ade	gua	gua	gua	gua	ade	ade	gua	ade	cyt	gua	ade	ade	gua	gua
150	ade	gua	gua	ade	ade	gua	gua	gua	gua	ade	ade	gua	ade	cyt	gua	ade	ade	gua	gua
151	gua	ade	ade	gua	gua	ade	ade	ade	gua	ade	ade	ade	gua	ade	ade	cyt	gua	ade	ade
152	ade	gua	gua	ade	gua	ade	ade	ade	ade	gua	gua	gua	ade	cyt	gua	ade	ade	gua	gua
153	ade	gua	gua	ade	ade	gua	gua	gua	gua	ade	ade	ade	gua	ade	ade	cyt	gua	gua	gua
154	gua	ade	ade	gua	gua	ade	ade	ade	ade	gua	gua	ade	gua	ade	ade	cyt	gua	ade	ade
155	gua	ade	ade	gua	ade	gua	gua	gua	gua	ade	ade	ade	gua	ade	ade	cyt	gua	ade	ade
156	gua	ade	ade	gua	gua	ade	ade	ade	ade	gua	gua	ade	gua	ade	ade	cyt	gua	ade	ade
157	ade	gua	gua	gua	gua	ade	ade	ade	ade	gua	gua	gua	ade	cyt	gua	ade	ade	gua	gua

	PZE-101129304	SYN10174	PZE-101133216	PZE-101133651	PZE-101134093	PZE-101134142	PZE-101135508	SYN2406	PZE-101136791	SYN9635	PZE-101138198	SYN13130	PZE-101140981	SYN8998	0192831_0351	SYN1741	PZE-101143985	PUT-163a-13178383-177	SYN37120
Lines	**3,8**	**5,4**	**6,2**	**6,7**	**7,1**	**7,3**	**8,6**	**9,0**	**9,4**	**9,6**	**10,2**	**14,8**	**15,7**	**17,4**	**17,7**	**18,4**	**18,8**	**20,7**	**21,4**
158	gua	ade	ade	gua	gua	ade	ade	ade	ade	gua	gua	ade	gua	ade	ade	cyt	gua	ade	ade
159	ade	gua	gua	ade	ade	gua	gua	gua	gua	ade	ade	ade	gua	cyt	gua	ade	ade	gua	gua
160	gua	ade	ade	gua	gua	ade	ade	ade	ade	gua	gua	gua	ade	cyt	gua	ade	ade	ade	ade
161	ade	gua	gua	ade	ade	gua	gua	gua	gua	ade	ade	ade	gua	cyt	gua	ade	ade	gua	gua
162	gua	ade	ade	gua	gua	-	ade	ade	ade	gua	gua	gua	ade	cyt	gua	cyt	gua	ade	ade
163	ade	-	gua	ade	ade	gua	gua	gua	gua	ade	ade	ade	gua	ade	ade	ade	ade	gua	gua
164	gua	ade	ade	gua	gua	ade	ade	ade	ade	gua	gua	gua	ade	cyt	gua	ade	ade	ade	ade
165	gua	ade	ade	gua	gua	ade	ade	ade	ade	gua	gua	gua	ade	cyt	ade	cyt	gua	ade	ade
166	gua	ade	ade	gua	gua	ade	ade	ade	ade	gua	gua	ade	gua	ade	ade	cyt	gua	ade	ade
167	gua	ade	ade	gua	gua	ade	ade	ade	-	gua	gua	ade	gua	ade	ade	cyt	gua	-	ade
168	ade	gua	gua	ade	ade	gua	gua	gua	gua	ade	ade	-	gua	ade	ade	ade	ade	gua	gua
169	ade	gua	gua	ade	ade	gua	gua	gua	gua	ade	ade	ade	gua	ade	ade	cyt	gua	gua	gua
170	gua	ade	ade	gua	gua	ade	ade	ade	ade	gua	gua	ade	gua	ade	ade	cyt	gua	ade	ade
171	gua	ade	ade	gua	ade	gua	gua	gua	gua	ade	ade	ade	gua	ade	ade	cyt	gua	ade	ade
172	gua	ade	ade	gua	gua	ade	ade	ade	ade	gua	gua	gua	ade	cyt	gua	ade	ade	ade	ade
173	ade	gua	ade	gua	gua	ade	ade	ade	ade	gua	gua	gua	ade	cyt	gua	ade	ade	gua	gua
174	ade	gua	gua	ade	ade	gua	gua	gua	gua	ade	ade	gua	ade	cyt	gua	ade	ade	gua	gua
175	gua	ade	ade	gua	gua	ade	ade	ade	ade	gua	gua	ade	gua	ade	ade	cyt	gua	ade	ade
176	gua	ade	ade	gua	gua	ade	ade	ade	ade	gua	gua	gua	ade	cyt	gua	cyt	gua	ade	ade
177	ade	gua	gua	ade	ade	gua	gua	gua	gua	ade	ade	ade	gua	ade	ade	cyt	gua	gua	gua
178	gua	ade	ade	gua	gua	ade	ade	ade	ade	gua	gua	gua	ade	cyt	gua	cyt	gua	ade	ade
179	ade	gua	gua	ade	ade	gua	gua	gua	ade	gua	gua	gua	ade	cyt	gua	ade	ade	gua	gua
180	gua	ade	ade	gua	gua	ade	ade	ade	ade	gua	gua	ade	gua	ade	ade	cyt	gua	ade	ade
181	gua	ade	ade	gua	gua	ade	ade	ade	ade	gua	gua	gua	ade	cyt	gua	ade	ade	ade	ade
182	ade	gua	gua	ade	ade	gua	gua	gua	gua	ade	ade	gua	ade	cyt	gua	ade	ade	gua	gua
183	ade	gua	gua	ade	ade	gua	ade	ade	ade	gua	gua	gua	ade	cyt	gua	ade	ade	gua	gua
184	ade	gua	gua	ade	ade	gua	gua	ade	ade	gua	gua	gua	ade	cyt	gua	ade	ade	gua	gua
185	ade	gua	gua	ade	ade	gua	ade	ade	ade	gua	gua	gua	ade	cyt	-	ade	ade	gua	gua
186	gua	ade	ade	gua	gua	ade	ade	ade	ade	gua	gua	gua	ade	cyt	gua	cyt	gua	ade	ade
187	ade	gua	gua	ade	ade	gua	gua	gua	gua	ade	ade	gua	ade	cyt	gua	ade	ade	gua	gua
188	ade	gua	gua	ade	ade	gua	gua	gua	gua	ade	gua	gua	ade	cyt	gua	ade	ade	gua	gua
189	ade	gua	gua	ade	ade	gua	gua	gua	gua	ade	ade	gua	ade	cyt	gua	ade	ade	gua	gua
190	gua	ade	ade	gua	gua	ade	ade	ade	ade	gua	gua	ade	gua	ade	ade	cyt	gua	ade	ade
191	gua	ade	ade	gua	gua	ade	ade	ade	ade	gua	gua	gua	ade	ade	ade	cyt	gua	ade	ade
192	gua	ade	ade	gua	gua	ade	ade	ade	ade	gua	gua	gua	ade	cyt	gua	ade	ade	gua	ade
193	gua	ade	ade	gua	gua	ade	ade	ade	ade	gua	gua	ade	gua	ade	ade	cyt	gua	ade	ade
194	ade	gua	gua	ade	ade	gua	ade	ade	ade	gua	gua	gua	ade	cyt	gua	ade	ade	gua	gua
195	gua	ade	ade	gua	gua	gua	gua	gua	gua	ade	ade	ade	gua	ade	ade	cyt	gua	ade	ade
196	ade	gua	gua	ade	ade	gua	ade	ade	ade	gua	gua	gua	ade	cyt	gua	ade	ade	gua	gua
197	gua	ade	ade	gua	ade	gua	gua	gua	gua	ade	ade	ade	gua	ade	ade	cyt	gua	ade	ade

	PZE-101129304	SYN10174	PZE-101133216	PZE-101133651	PZE-101134093	PZE-101134142	PZE-101135508	SYN2406	PZE-101136791	SYN9635	PZE-101138198	SYN13130	PZE-101140981	SYN8998	0192831_0351	SYN1741	PZE-101143985	PUT-163a-13178383-177	SYN37120
Lines	**3,8**	**5,4**	**6,2**	**6,7**	**7,1**	**7,3**	**8,6**	**9,0**	**9,4**	**9,6**	**10,2**	**14,8**	**15,7**	**17,4**	**17,7**	**18,4**	**18,8**	**20,7**	**21,4**
198	gua	ade	ade	gua	gua	ade	ade	ade	ade	gua	gua	gua	ade	cyt	gua	ade	ade	ade	ade
199	ade	gua	gua	ade	ade	gua	gua	gua	gua	ade	ade	ade	gua	ade	ade	ade	ade	gua	gua
200	gua	ade	ade	gua	gua	ade	ade	ade	ade	gua	gua	gua	ade	cyt	-	ade	ade	ade	ade
201	gua	ade	ade	gua	gua	ade	ade	ade	ade	gua	ade	ade	gua	ade	ade	cyt	gua	ade	ade
202	ade	gua	gua	ade	ade	gua	gua	gua	gua	ade	ade	gua	ade	cyt	gua	ade	ade	gua	gua
203	gua	ade	ade	gua	gua	gua	gua	gua	gua	ade	ade	ade	gua	ade	ade	cyt	gua	ade	ade
204	gua	ade	ade	gua	gua	ade	ade	ade	ade	gua	gua	gua	gua	ade	ade	cyt	gua	ade	ade
205	gua	ade	ade	gua	gua	ade	ade	ade	ade	gua	gua	gua	ade	cyt	gua	ade	gua	ade	ade
206	gua	ade	ade	gua	gua	ade	ade	ade	ade	gua	gua	gua	ade	cyt	gua	ade	gua	ade	ade
207	gua	ade	ade	gua	gua	ade	gua	gua	gua	ade	ade	ade	gua	ade	ade	cyt	gua	ade	ade
208	gua	ade	ade	gua	gua	ade	ade	ade	ade	gua	gua	gua	ade	cyt	gua	cyt	gua	ade	ade
209	ade	gua	gua	ade	ade	gua	gua	gua	gua	ade	ade	gua	ade	cyt	gua	ade	ade	gua	gua
210	gua	ade	ade	gua	gua	ade	ade	ade	ade	gua	gua	gua	ade	cyt	gua	cyt	gua	ade	ade
211	ade	gua	gua	ade	ade	gua	gua	gua	gua	ade	ade	ade	gua	cyt	gua	ade	ade	gua	gua
212	gua	ade	ade	gua	-	ade	gua	gua	gua	ade	ade	ade	gua	ade	ade	cyt	gua	ade	ade
213	ade	gua	gua	ade	ade	gua	gua	gua	gua	ade	ade	ade	gua	cyt	gua	ade	ade	gua	gua
214	gua	ade	ade	gua	gua	ade	ade	ade	ade	gua	gua	ade	gua	ade	ade	cyt	gua	ade	ade
215	gua	ade	ade	gua	gua	ade	gua	gua	gua	ade	ade	ade	gua	ade	ade	cyt	gua	ade	ade
216	ade	gua	gua	ade	ade	gua	gua	gua	gua	ade	ade	ade	gua	ade	ade	cyt	gua	ade	gua
217	gua	ade	ade	gua	gua	ade	ade	ade	ade	gua	gua	gua	ade	cyt	gua	cyt	gua	ade	ade
218	gua	ade	ade	gua	gua	ade	ade	ade	gua	ade	ade	ade	gua	ade	ade	cyt	gua	ade	ade
219	ade	gua	gua	ade	ade	gua	gua	gua	gua	ade	ade	gua	ade	cyt	gua	ade	ade	gua	gua
220	ade	gua	gua	ade	ade	gua	gua	gua	gua	ade	ade	ade	gua	ade	ade	cyt	gua	ade	gua
221	gua	ade	ade	gua	gua	ade	ade	ade	ade	gua	gua	gua	ade	cyt	gua	cyt	gua	ade	ade
222	ade	gua	gua	ade	ade	gua	gua	gua	gua	ade	ade	ade	gua	ade	ade	cyt	gua	gua	gua
223	gua	ade	ade	gua	gua	ade	ade	ade	ade	gua	gua	gua	ade	cyt	gua	cyt	gua	ade	ade
224	gua	ade	ade	gua	gua	ade	ade	ade	ade	gua	gua	gua	ade	cyt	gua	ade	ade	ade	ade
225	ade	gua	gua	ade	ade	gua	gua	gua	ade	gua	gua	gua	ade	cyt	gua	ade	ade	gua	gua
226	ade	gua	-	ade	ade	gua	gua	gua	gua	ade	ade	gua	ade	cyt	gua	ade	ade	gua	gua
227	gua	ade	ade	gua	gua	ade	ade	ade	ade	gua	gua	gua	gua	ade	ade	cyt	gua	ade	ade
228	gua	ade	ade	gua	gua	ade	ade	ade	ade	gua	gua	gua	ade	ade	ade	cyt	gua	ade	ade
229	gua	ade	ade	gua	gua	ade	ade	ade	ade	gua	gua	gua	ade	ade	ade	cyt	gua	ade	ade
230	gua	ade	ade	gua	gua	ade	ade	ade	ade	gua	gua	ade	gua	ade	ade	cyt	gua	ade	ade
231	ade	gua	gua	ade	ade	gua	ade	ade	ade	gua	gua	gua	ade	cyt	gua	ade	ade	gua	gua
232	ade	gua	gua	ade	ade	gua	gua	gua	gua	ade	ade	ade	gua	ade	ade	cyt	ade	gua	gua
233	gua	ade	ade	gua	gua	ade	ade	ade	ade	gua	gua	gua	ade	cyt	gua	cyt	gua	ade	ade
234	ade	gua	gua	ade	ade	gua	gua	gua	gua	ade	ade	ade	gua	ade	ade	ade	ade	gua	gua
235	ade	gua	gua	ade	ade	gua	gua	gua	gua	ade	ade	gua	ade	cyt	gua	ade	ade	gua	gua
236	gua	ade	ade	gua	gua	ade	ade	ade	ade	gua	gua	gua	ade	cyt	gua	ade	ade	ade	ade
237	ade	gua	gua	ade	ade	gua	gua	gua	gua	ade	ade	ade	gua	cyt	gua	ade	ade	gua	gua

	PZE-101129304		SYN10174		PZE-101133216		PZE-101133651		PZE-101134093		PZE-101134142		PZE-101135508		SYN2406		PZE-101136791		SYN9635		PZE-101138198		SYN13130		PZE-101140981		SYN8998		0192831_0351		SYN1741		PZE-101143985		PUT-163a-13178383-177		SYN37120	
Lines	**3,8**		**5,4**		**6,2**		**6,7**		**7,1**		**7,3**		**8,6**		**9,0**		**9,4**		**9,6**		**10,2**		**14,8**		**15,7**		**17,4**		**17,7**		**18,4**		**18,8**		**20,7**		**21,4**	
238	gua	gua	ade	ade	ade	ade	gua	gua	gua	gua	ade	ade	ade	ade	ade	ade	ade	ade	gua	gua	ade	ade	gua	gua	ade	ade	ade	ade	cyt	cyt	gua	gua	ade	ade	ade	ade
239	gua	gua	ade	ade	ade	ade	gua	gua	gua	gua	ade	ade	ade	ade	ade	ade	ade	ade	gua	gua	gua	gua	ade	ade	cyt	cyt	gua	gua	ade	ade	ade	ade	ade	ade	ade	ade
240	ade	ade	gua	gua	gua	gua	ade	ade	ade	ade	gua	gua	gua	gua	gua	gua	gua	gua	ade	ade	gua	gua	ade	ade	cyt	cyt	gua	gua	ade	ade	ade	ade	gua	gua	gua	gua
241	gua	gua	ade	ade	ade	ade	gua	gua	gua	gua	ade	ade	ade	ade	ade	ade	ade	ade	gua	gua	ade	ade	gua	gua	ade	ade	ade	ade	cyt	cyt	gua	gua	ade	ade	ade	ade
242	gua	gua	ade	ade	-	-	gua	gua	ade	ade	gua	gua	gua	gua	gua	gua	gua	gua	ade	ade	ade	ade	ade	ade	gua	gua	ade	ade	cyt	cyt	gua	gua	ade	ade	ade	ade
243	gua	gua	ade	ade	ade	ade	gua	gua	gua	gua	ade	ade	ade	ade	ade	ade	ade	ade	gua	gua	gua	gua	ade	ade	gua	gua	ade	ade	cyt	cyt	gua	gua	ade	ade	ade	ade
244	ade	ade	gua	gua	gua	gua	ade	ade	ade	ade	gua	gua	gua	gua	gua	gua	gua	gua	ade	ade	ade	ade	gua	gua	ade	ade	cyt	cyt	gua	gua	ade	ade	ade	ade	gua	gua
245	ade	ade	gua	gua	gua	gua	ade	ade	ade	ade	gua	gua	gua	gua	gua	gua	gua	gua	ade	ade	ade	ade	ade	ade	gua	gua	ade	ade	cyt	cyt	ade	ade	gua	gua	gua	gua
246	gua	gua	ade	ade	ade	ade	gua	gua	gua	gua	ade	ade	ade	ade	ade	ade	ade	ade	gua	gua	gua	gua	gua	gua	gua	gua	ade	ade	cyt	cyt	gua	gua	ade	ade	ade	ade
247	ade	ade	gua	gua	gua	gua	ade	ade	ade	ade	gua	gua	ade	ade	ade	ade	ade	ade	gua	gua	gua	gua	ade	ade	cyt	cyt	gua	gua	ade	ade	ade	ade	gua	gua	gua	gua
248	ade	ade	gua	gua	-	-	ade	ade	ade	ade	gua	gua	gua	gua	gua	gua	gua	gua	ade	ade	gua	gua	ade	ade	cyt	cyt	gua	gua	ade	ade	ade	ade	gua	gua	gua	gua
249	gua	gua	ade	ade	ade	ade	gua	gua	gua	gua	ade	ade	-	-	ade	ade	ade	ade	gua	gua	gua	gua	ade	ade	cyt	cyt	gua	gua	ade	ade	ade	ade	ade	ade	ade	ade
250	gua	gua	ade	ade	ade	ade	gua	gua	gua	gua	ade	ade	ade	ade	ade	ade	ade	ade	gua	gua	ade	ade	gua	gua	ade	ade	ade	ade	cyt	cyt	gua	gua	ade	ade	ade	ade
251	ade	ade	gua	gua	gua	gua	-	-	ade	ade	gua	gua	gua	gua	gua	gua	ade	ade	-	-	gua	gua	gua	gua	-	-	cyt	cyt	gua	gua	ade	ade	-	-	gua	gua
252	gua	gua	ade	ade	ade	ade	gua	gua	gua	gua	ade	ade	gua	gua	gua	gua	gua	gua	ade	ade	ade	ade	ade	ade	gua	gua	ade	ade	cyt	cyt	gua	gua	ade	ade	ade	ade
253	gua	gua	ade	ade	ade	ade	gua	gua	gua	gua	ade	ade	ade	ade	ade	ade	ade	ade	gua	gua	gua	gua	gua	gua	ade	ade	cyt	cyt	gua	gua	ade	ade	ade	ade	gua	ade
254	ade	ade	gua	gua	gua	gua	ade	ade	ade	ade	gua	gua	gua	gua	gua	gua	gua	gua	ade	ade	ade	ade	gua	gua	ade	ade	ade	ade	ade	ade	ade	ade	gua	gua	gua	gua
255	ade	ade	gua	gua	gua	gua	ade	ade	ade	ade	gua	gua	-	-	gua	gua	gua	gua	ade	ade	gua	gua	ade	ade	cyt	cyt	gua	gua	ade	ade	ade	ade	gua	gua	gua	gua
256	ade	ade	gua	gua	gua	gua	ade	ade	ade	ade	gua	gua	gua	gua	ade	ade	ade	ade	gua	gua	gua	gua	ade	ade	cyt	cyt	gua	gua	ade	ade	ade	ade	gua	gua	gua	gua
257	ade	ade	gua	gua	gua	gua	ade	ade	ade	ade	gua	gua	ade	ade	ade	ade	ade	ade	gua	gua	gua	gua	ade	ade	cyt	cyt	gua	gua	ade	ade	ade	ade	gua	gua	gua	gua
258	gua	gua	ade	ade	ade	ade	gua	gua	gua	gua	ade	ade	ade	ade	ade	ade	ade	ade	gua	gua	gua	gua	gua	gua	gua	gua	ade	ade	cyt	cyt	gua	gua	ade	ade	ade	ade
259	gua	gua	ade	ade	ade	ade	gua	gua	gua	gua	ade	ade	ade	ade	ade	ade	ade	ade	gua	gua	gua	gua	ade	ade	cyt	cyt	gua	gua	ade	ade	ade	ade	gua	gua	ade	ade
260	ade	ade	gua	gua	gua	gua	ade	ade	ade	ade	gua	gua	gua	gua	gua	gua	gua	gua	ade	ade	ade	ade	gua	gua	ade	ade	ade	ade	cyt	cyt	gua	gua	gua	gua	gua	gua
261	gua	gua	ade	ade	ade	ade	gua	gua	gua	gua	ade	ade	ade	ade	ade	ade	ade	ade	gua	gua	gua	gua	-	-	cyt	cyt	gua	gua	ade	ade	ade	ade	gua	gua	ade	ade
262	gua	gua	ade	ade	ade	ade	gua	gua	gua	gua	ade	ade	ade	ade	ade	ade	ade	ade	gua	gua	gua	gua	ade	ade	cyt	cyt	gua	gua	ade	ade	ade	ade	ade	ade	ade	ade
263	ade	ade	gua	gua	-	-	ade	ade	ade	ade	gua	gua	ade	ade	ade	ade	ade	ade	gua	gua	gua	gua	ade	ade	cyt	cyt	gua	gua	ade	ade	ade	ade	gua	gua	gua	gua
264	gua	gua	gua	gua	gua	gua	ade	ade	ade	ade	gua	gua	ade	ade	ade	ade	ade	ade	gua	gua	gua	gua	ade	ade	cyt	cyt	gua	gua	ade	ade	ade	ade	gua	gua	gua	gua
265	gua	gua	ade	ade	ade	ade	gua	gua	gua	gua	ade	ade	ade	ade	ade	ade	ade	ade	gua	gua	gua	gua	gua	gua	ade	ade	ade	ade	cyt	cyt	gua	gua	ade	ade	ade	ade
F4-21																																				
F4-22																																				
F4-13.3																																				
F4-27																																				
F4-14.8																																				
F4-39																																				
F4-23																																				
F4-49																																				
F4-3.2																																				
F4-29																																				
F4-38																																				
F4-47																																				

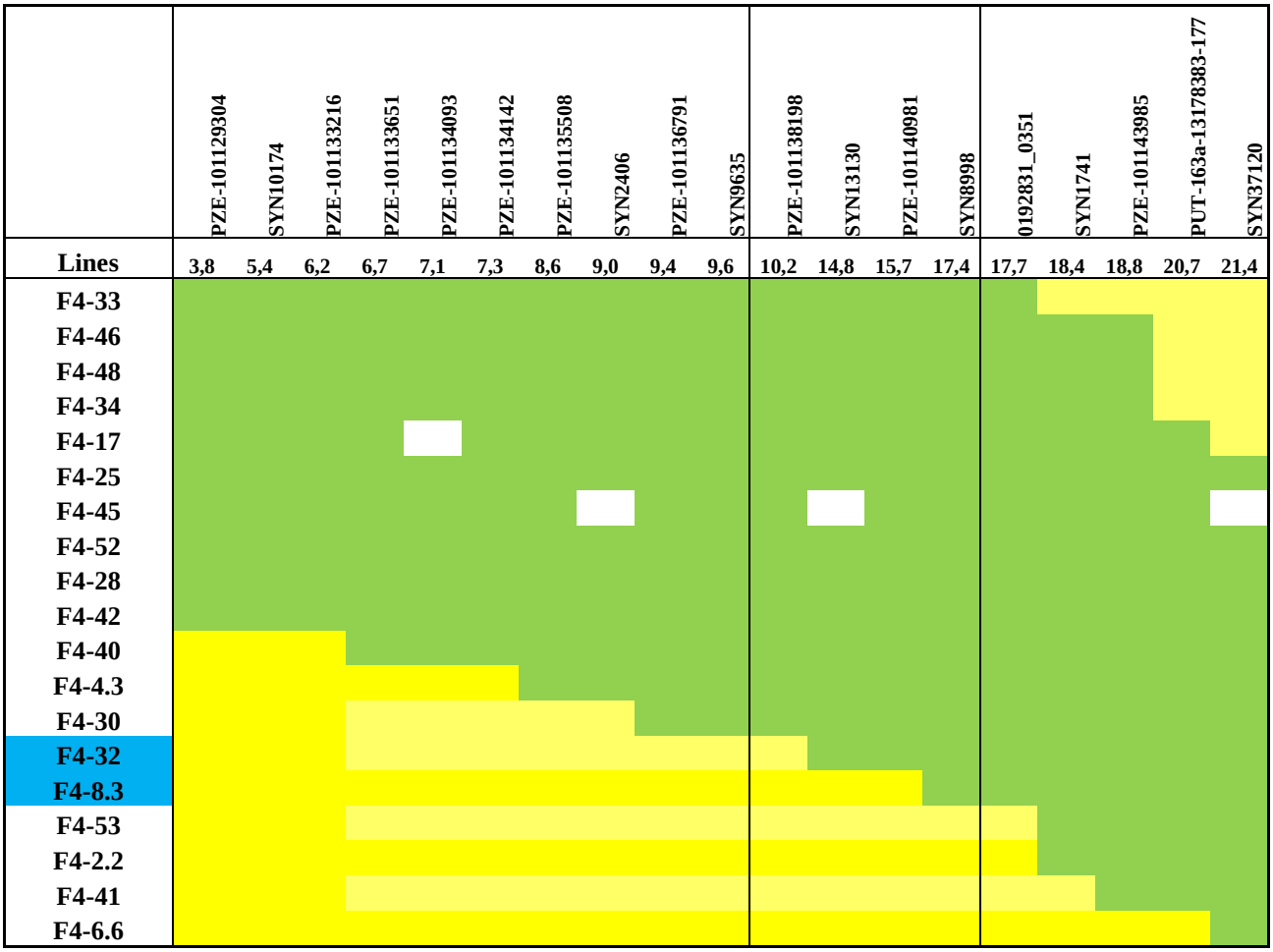
PZE-101129304
SYN10174
PZE-101133216
PZE-101133651
PZE-101134093
PZE-101134142
PZE-101135508
SYN2406
PZE-101136791
SYN9635
PZE-101138198
SYN13130
PZE-101140981
SYN8998
0192831_0351
SYN1741
PZE-101143985
PUT-163a-13178383-177
SYN37120
Lines
3,8 5,4 6,2 6,7 7,1 7,3 8,6 9,0 9,4 9,6 10,2 14,8 15,7 17,4 17,7 18,4 18,8 20,7 21,4
F4-33
F4-46
F4-48
F4-34
F4-17
F4-25
F4-45
F4-52
F4-28
F4-42
F4-40
F4-4.3
F4-30
F4-32
F4-8.3
F4-53
F4-2.2
F4-41
F4-6.6

Acknowledgments

We gratefully acknowledge KWS SAAT AG for the financial and technical support. Special thanks go to Milena Ouzunova, Thomas Prestel, Daniela Scheuermann, Fabio Monguzzi and Vincenzo Giovannelli.

I wish to express my sincere gratitude to Claude Urbany and the bioinformatics group from KWS SAAT AG for all the support with the transcriptomics analysis.

I also would like to thank to Alexander Bucksch from the Georgia Institute of Technology for enabling us to use the software DIRT, and for his recommendations in root image acquisition.

I would like to thank to my supervisor Prof. Roberto Tuberosa for the opportunity to do my research in his group and Prof. Silvio Salvi for his scientific guidance and final correction of the document.

I also thank to Prof. Pierangelo Landi for his useful comments during lab meetings.

Many thanks to Sandra Stefanelli and Simona Cornetti, quite hard workers who were always willing to give me a hand.

I am very grateful to all people who were or are being part of the DipSA genetics group, for their continuous support during this three years: Irma Terraciano, Andrea Ricci, Marta Graziani, Sara Castelletti, Chiara Colalungo, Maria Angela Cané, Sara Milner, Fabio Valli, Facundo Tabita, Valentina Talamè, Silvia Guiliani, Carlos Busanello and Danara Ormanbekova. A special thanks to Giuseppe Sciara for the fast course in R.

Special thanks to my friends Jose and Ricardo, because of their help and for the funny time we lived, no matters if we were at summer time in the middle of a cornfield.

I take this opportunity to record my sincere thanks to the group of field workers of the Unibo's experimental station for their excellent job and disposition even the hard work.

Finally, the deepest gratitude to my beloved parents and brothers: Jesús, Mireya, Jesús Alejandro and Melisa, for their unconditional support and love in spite of the thousands of miles away.